Applications of photoacoustic sensing techniques

Andrew C. Tam

IBM Almaden Research Center, San Jose, California 95120-6099

This paper reviews the theory and applications of photoacoustic (also called optoacoustic) methods belonging to the more general area of photothermal measurement techniques. The theory covers excitation of gaseous or condensed samples with modulated continuous light beams or pulsed light beams. The applications of photoacoustic methods include spectroscopy, monitoring deexcitation processes, probing physical properties of materials, and generating mechanical motions. Several other related photothermal methods, as well as particle-acoustics and wave-acoustics methods are also described. This review complements an earlier and narrower review [Rev. Mod. Phys. **53**, 517 (1981)] that is mainly concerned with sensitive detection by pulsed photoacoustic spectroscopy in condensed matter.

CONTENTS

I. INTRODUCTION

The term "photoacoustics" (PA) or "optoacoustics" (OA) usually refers to the generation of acoustic waves by modulated optical radiation. Both terms are in common usage and have the same meaning. In its broader sense, photoacoustics can mean the generation of acoustic waves or other thermoelastic effects by any type of energetic radiation, including electromagnetic radiation from radio frequency to x ray, electrons, protons, ions, and other particles. The PA effect was discovered by A. G. Bell (1880), who observed that audible sound is produced when chopped sunlight is incident on optically absorbing materials. The current renewed interest in PA appears to have started with the work of Kruezer (1971), who reported that ultra-trace gas constituents (at the sub-part-per-billion level) could be detected by laser-induced PA generation. Subsequently, much experimental and theoretical work has been reported in the literature to demonstrate not only spectroscopic applications, but also many other PA applications in various fields of physics, chemistry, biology, engineering, and medicine.

There are four general classes of applications of PA methods.

(1) PA spectroscopy: in this class of application, the PA signal amplitude is measured for a range of optical excitation wavelength, producing a PA spectrum; other

factors (e.g., efficiency in thermal deexcitation and in acoustic wave generation) are usually kept or assumed fixed while the PA spectrum is obtained. This is actually an "excitation spectrum" based on acoustic detection.

(2) PA monitoring of deexcitation processes: here, the thermal decay branch is monitored to provide information on a competing decay branch. After optical excitation, four decay branches are generally possible: luminescence, photochemistry, photoelectricity, and heat that may be generated directly or through energy-transfer processes. For example, if luminescence and heat are the only two competing branchings, PA monitoring of the heat branch can provide the quantum efficiency of luminescence under suitable circumstances.

(3) PA probing of thermoelastic and other physical properties of materials: various information can be obtained conveniently with the help of the optical generation of thermal waves or acoustic waves. Such information includes sound velocity, elasticity, temperature, flow velocity, specific heat, thermal diffusivity, thickness of a thin film, subsurface defects, and so on.

(4) PA generation of mechanical motions: this is a small area of application now. PA effects can produce motions like liquid droplet ejection or structural vibrations.

In a previous article, Patel and Tam (1981) reviewed the spectroscopic studies of condensed matter by pulsed-laser-induced PA generation. This article is intended to complement that previous review, since the many applications of PA generation are not limited to spectroscopy nor to pulsed lasers. The general scope of the present article is the review of important practical examples of PA sensing, with minimum repetition of the materials already covered in Patel and Tam (1981).

Most PA generation is due to the deposition of heat by light, the so-called "photothermal" (PT) effect. Thus, to put PA sensing techniques in perspective, we first summarize other types of PT sensing methods. We then discuss some important modern theories and applications of PA methods, including spectroscopy, deexcitation studies, materials testing, and imaging. Both "contact methods" (involving the use of microphones or other transducers in contact with or in proximity to the sample) and "noncontact methods" (involving the use of optical beams to probe the acoustic wave in the sample) are discussed. PA applications involving the use of particle beams for excitation are also included. We do not intend to cover all the applications that have been reported in the literature; instead, we shall describe representative examples of various kinds. Emphasis will be given to the more recent results. Other reviews have been given, e.g., by Pao (1977), Somoano (1978), Rosencwaig (1978,1980a), Colles *et al.* (1979), Kirkbright and Castleden (1980), Lyamshev and Sedov (1981), Kinney and Staley (1982), Tam (1983), and West *et al.* (1983).

While extensive applications of PA generation and detection have been developed as described in this report, there are two related effects that are less well known. These are briefly mentioned here, since they may find new important applications in the future. The first is the effect of "sonoluminescence" (see, for example, Crum and Reynolds, 1985), which is the *reverse* PA effect, namely, the generation of optical radiation by acoustic waves. One mechanism for sonoluminescence is acoustic cavitations followed by bubble collapse, which drives the interior gases to high temperature, resulting in production of free radicals and subsequent radiative recombinations. The second is the *inverse* PA effect (see, for example, Didascalou *et al.*, 1985,1986; Royce and Benziger, 1986), which is the generation of sound due to optical radiation energy's being *lost* from a sample, instead of being deposited in a sample as in the usual PA effect. Here, optical radiation loss can be achieved by exposing the sample to a surface at a lower temperature (e.g., exposing a room-temperature sample to a liquid-nitrogen-cooled surface); by modulating such an exposure, sound is generated in the sample

II. PHOTOTHERMAL EFFECTS AND DETECTIONS

"Photothermal effects" are caused by the heating of a sample after the absorption of optical energy (or, in general, the absorption of an energetic beam). After optical absorption, other deexcitation channels besides heating can also occur, as indicated in Fig. 1. These other "deexcitation branches" complement the heating branch in the sense that all branching ratios must add up to one. Photothermal heating of a sample is frequently produced with the use of laser beams, Xe arcs, or other intense light sources. Generally, these PT sources are not simply used as "very expensive Bunsen burners," but are needed for some of the following reasons: (1) PT heating can provide convenient and sensitive methods for detecting optical absorptions in matter; (2) information concerning deexcitation mechanisms can be obtained; (3) very localized or very rapid photothermal heating can be achieved to provide novel measurements or produce new effects.

PT heating can result in many different effects, which, in turn, provide the detection mechanisms. Some of the

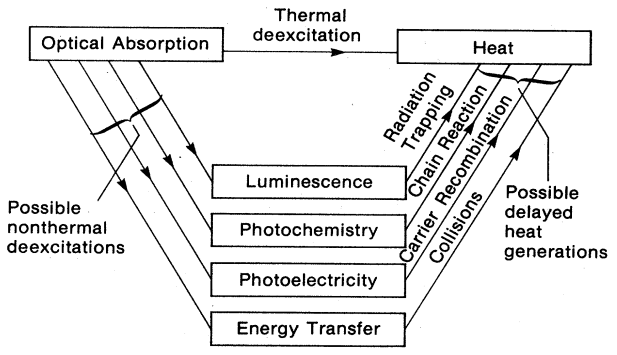

FIG. 1. Possible consequences of optical absorption. The possible nonthermal deexcitation channels reduce the "prompt" heat production, but may contribute to delayed heat generation by some possible mechanisms indicated.

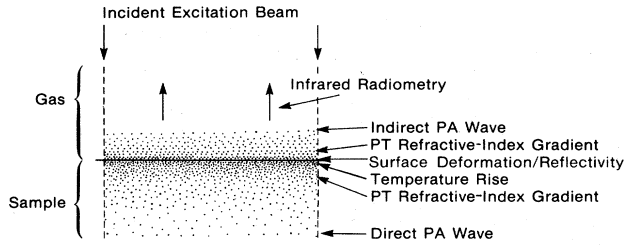

FIG. 2. Some common photothermal heating effects that can be used to detect the optical energy absorbed with thermal deexcitation.

more common PT heating effects are indicated in Fig. 2 and discussed below.

A. Temperature rise

The most direct method for measuring PT heating is the monitoring of the rise in temperature; this is sometimes called "optical calorimetry" or "laser calorimetry," since a laser beam is frequently used for excitation. To detect the laser-induced temperature rise, thermocouples or thermisters have been used (Brilmyer *et al.*, 1977; Bass *et al.*, 1979; Bass and Liou, 1984), and pyroelectric detectors with higher sensitivity have also been exploited (Baumann *et al.*, 1983; Coufal, 1984). Even absorption spectroscopy can be used to detect the rise in temperature if the corresponding Boltzmann molecular population change can be analyzed (Zapka and Tam, 1982a).

There are advantages and disadvantages of using a temperature sensor to detect PT temperature rise directly rather than using other detection methods described later. The main advantage is that absolute calibration is usually directly obtainable, i.e., the observed temperature rise can be directly related to physical parameters like absorption coefficients. The disadvantages are that response is usually slow, and sensitivity is typically low compared to other methods; furthermore, in what is basically a "dc method," heat leakage from the sample must be minimized by elaborate thermal isolation. However, Coufal (1984) has shown that fast risetime and high sensitivity for a thin-film sample is possible if it is directly coated onto a thin pyroelectric detector.

B. Thermal refractive-index gradients

A thermal refractive-index gradient is produced by the heat gradient due to the absorption of the excitation beam. An acoustic refractive-index gradient is also produced (propagating at acoustic speed), which will be treated later. The thermal refractive-index gradient generated by the excitation beam affects its own propagation, resulting in the well-known effect of "self-defocusing" or "thermal blooming." Self-defocusing generally occurs instead of self-focusing because the derivative of the refractive index with respect to temperature is usually negative, so that the temperature gradient results in a negative lens. On the other hand, the refractive-index gradient by the excitation beam also affects the propagation of another weak "probe" beam in the vicinity of the excitation beam. Thus the refractive-index gradient can be monitored either by self-defocusing or by probe-beam refraction (PBR). Leite *et al.* (1964) were the first to show that monitoring the self-defocusing of the excitation beam offers a sensitive spectroscopic tool, and Solimini (1966) later provided a quantitative theory. Swofford *et al.* (1976) have shown that the PBR method with an additional collinear probe beam provides higher sensitivity than the single-beam self-defocusing method; this is called "thermal lensing" spectroscopy using a probe beam [see Fig. 3(a)]. Bialkowski (1985) has analyzed aberration effects of the thermal lens.

The PBR technique for probing the refractive-index gradient need not employ collinear beams as in the thermal lens experiment. A probe beam that is parallel to, but displaced from, the excitation beam can also be used. Boccara *et al.* (1980) and Jackson *et al.* (1981a) have pointed out that the PBR method, using beams with appropriate displacements, should have higher sensitivity than thermal lens spectroscopy; this is because, in the

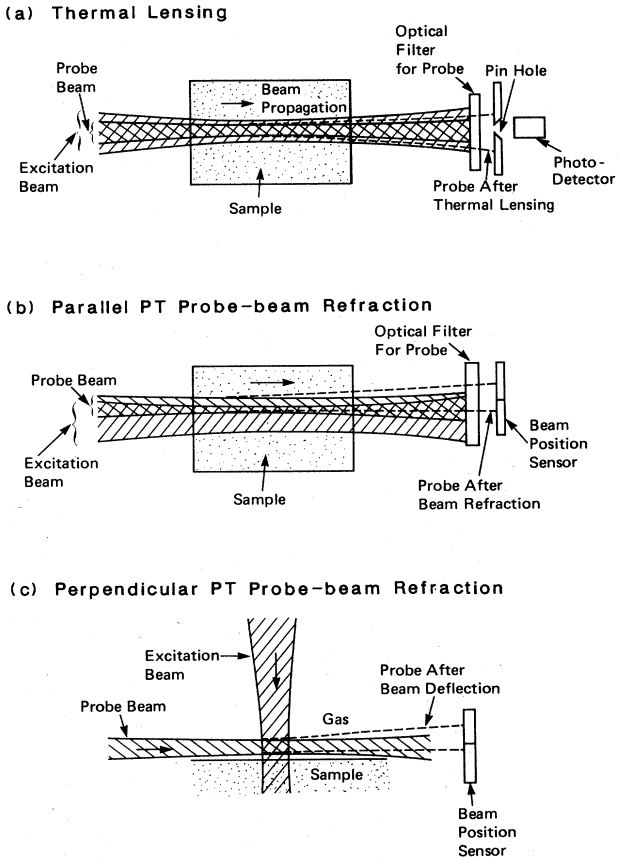

FIG. 3. Various methods that have been used to detect the PT refractive-index gradient.

thermal lens method, the probe is situated in the center, but not at the maximum refractive-index gradient produced by the excitation beam, while in the noncollinear PBR method, the probe can be positioned at the maximum refractive-index gradient, which is situated at approximately one beam radius from the axis of the excitation beam [see Fig. 3(b)].

For PBR methods in general, the probe beam need not even be parallel to the excitation beam. Although the parallel configuration with a displacement of one beam radius gives the largest probe deflection, this configuration may not always be possible. For example, transmission monitoring cannot be performed on opaque samples, for which orthogonal PBR detection is generally used [Fig. 3(c)]. Moreover, a nonparallel configuration is generally needed to obtain spatially resolved probing. Orthogonal photothermal PBR (or "mirage" probing) has been used for novel spectroscopic applications by Fournier *et al.* (1980), Murphy and Aamodt (1981), and Low *et al.* (1982). In addition, orthogonal PBR (with the probe intersecting the pump beam inside the sample) has been used by Dovichi *et al.* (1984) for photothermal microscopy applications.

Boccara *et al.* (1980) have reported that the PBR method is very sensitive for detecting weak absorption. For example, they indicated that for parallel but displaced beams [Fig. 3(b)], an absorption fraction αl as small as 10^{-8} can be measured. Here, α is the absorption coefficient and l is the path length. Boccara *et al.* (1980) have also derived theoretical formulas for the PBR deflection angle φ. We show here that φ for the case of Fig. 3(b) can be simply derived for negligible thermal diffusion and a narrow probe beam at a radial distance r from the axis of the excitation beam with a Gaussian profile given by

$$E(r)=\frac{E_{\text{in}}}{\pi a^2}\exp(-r^2/a^2)\ , \tag{1}$$

where E_{in} is the incident pulse energy of the excitation beam, a is the excitation beam radius, and $E(r)$ is the energy density at r. The corresponding temperature gradient at r

$$\frac{dT}{dr}\approx\frac{2E_{\text{in}}\alpha}{\rho C\pi a^2}\frac{r\exp(-r^2/a^2)}{a^2}\ , \tag{2}$$

where ρ=density, C=specific heat, and weak absorption of the excitation pulse is assumed. For small probe deflection φ, geometrical optics gives

$$\frac{\varphi}{l}\approx\frac{dn}{dr}=\frac{dn}{dT}\frac{dT}{dr}\ , \tag{3}$$

where l is the optical path length. Combining Eqs. (2) and (3), we have

$$\varphi(r)\approx\frac{dn}{dT}\frac{2E_{\text{in}}\alpha l}{\rho C\pi a^2}\frac{r\exp(-r^2/a^2)}{a^2}\ . \tag{4}$$

Equation (4) is basically the same as Eq. (1) of Boccara *et al.* (1980). We see from Eq. (4) that the probe-beam deflection $\varphi(r)$ depends linearly on the temperature derivative of the refractive index, and linearly on α (for weak absorption), and is maximum at $r=a/\sqrt{2}$.

Equation (4) deals only with the simplest PBR case, when the beams are parallel, the excitation beam is only weakly absorbed, and thermal diffusion is negligible. More general cases have been considered by Murphy and Aamodt (1980) and by Jackson *et al.* (1981a), who have calculated the probe-beam deflection for cases of cw or pulsed excitation with either perpendicular or parallel probe. Jackson *et al.* (1981a) have also experimentally verified some of the predictions of their theory. For example, they have used PBR spectroscopy to measure the optical absorption of benzene at 607 nm due to the sixth harmonic of the C-H stretch. From their experimental results for a 0.1% solution of benzene in CCl_4, they concluded that the PBR method can detect an absorption coefficient of 2×10^{-7} cm^{-1} for a 1-mJ pulsed-excitation laser with the detection limit being apparently due to the pointing instability and other noises of the HeNe probe laser.

Numerous applications of photothermal PBR techniques have been reported. Murphy and Aamodt (1980,1981) have demonstrated PT imaging using transverse PBR (called the "mirage effect"). Fournier *et al.* (1981) have reported PBR Fourier transform spectroscopy for absorption and dichroism measurements and obtained 3 orders of magnitude improvement in sensitivity over conventional PA spectroscopy. Jackson *et al.* (1981b) have reported the measurement of absorption spectra of crystalline and amorphous Si by photothermal PBR spectroscopy. Low *et al.* (1984) have combined the infrared Fourier-multiplexed excitation technique with photothermal PBR detection for spectroscopy of "difficult" samples like polymers, fabrics, paper, and bones. Nickolaisen and Bialkowski (1985) have used a pulsed infrared laser for thermal lens spectroscopy of a flowing gas sample, and Long and Bialkowski (1985) have shown its use for trace gas detection at the sub-part-per-billion level. Loulergue and Tam (1985) have used a pulsed-excitation CO_2 laser beam and a continuous HeNe probe beam that is parallel to but displaced from the excitation beam for thermal diffusivity measurements in an unconfined hot gas. Sontag and Tam (1985b) have demonstrated "traveling thermal lens" spectroscopy for monitoring flow velocity, temperature, and composition in a flowing fluid.

The use of time-resolved photothermal PBR techniques to detect delayed heat release due, for example, to energy transfers or photochemical reactions is also possible. This has been demonstrated by Tam *et al.* (1985) for the case of photochemical particulate production in a CS_2 vapor induced by a pulsed N_2 laser, where the delayed heat release is attributed to the nucleation and growth of particulates.

We have described only PBR techniques for detecting photothermal refractive-index gradients, which however can also be probed by other optical techniques, notably the phase-fluctuation heterodyne interferometry technique (Davis, 1980) and the Moire deflectometry technique (Glatt *et al.*, 1984).

C. Surface deformation

The PT heating of a surface causes distortions due to thermal expansion. The distortions can be very small, e.g., 10^{-3} Å. However, Amer and co-workers (Amer, 1983; Olmstead *et al.*, 1983; Olmstead and Amer, 1984) have observed that even such small surface deformations can be detected, providing new sensitive spectroscopic applications. This has been called PT displacement spectroscopy.

The technique of photothermal displacement spectroscopy can be understood from Fig. 4. Figure 4(a) indicates the case when a laser beam of power P and area A chopped at a frequency f is incident on a solid. Let us assume the simple case of weak absorption by a thin coating (of thickness l and absorption coefficient α) on a transparent substrate. The modulated heating is "spread" through a thermal diffusion length μ given by

$$\mu=\left[\frac{D}{\pi f}\right]^{1/2}, \tag{5}$$

where D is the thermal diffusivity of the solid. The temperature rise ΔT of the dotted region in Fig. 4(a) can be estimated as

$$\Delta T=\frac{\alpha l P}{2f\rho C\mu A}, \tag{6}$$

where $P/2f$ is approximately the incident energy in one cycle, αl is the fraction of light absorbed, ρ is the density, and C is the specific heat of the solid. The magnitude of the maximum surface displacement h_0 is estimated as

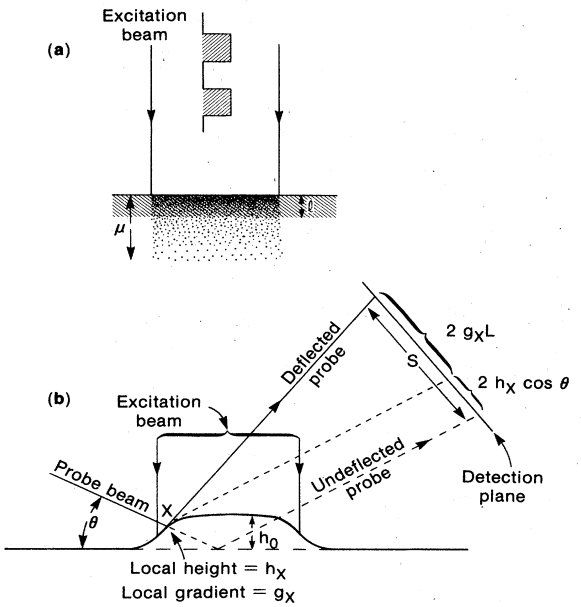

FIG. 4. Photothermal displacement spectroscopy exemplified for the case of an absorbing layer of thickness l on a transparent substrate. (a) Schematics. (b) The probe beam incident at position X of the displaced surface (exaggerated in the figure) is deflected, and the displacement at the detection plane is $2h_x\cos\theta+2g_xL$.

$$h_0=\beta\mu\Delta T=\frac{\beta\alpha l P}{2f\rho CA}, \tag{7}$$

where β is the linear thermal expansion coefficient of the solid. Equation (7) indicates that the surface displacement is proportional to the coating absorption coefficient α, and hence absorption spectroscopy of the coating can be performed by monitoring the distortion as a function of the excitation laser wavelength.

Amer and co-workers show that the surface displacement can be conveniently monitored by a probe-beam deflection method indicated in Fig. 4(b). The continuous probe is deflected by the deformation, and the displacement S at a detector plane (perpendicular to the probe beam) is given by [see Fig. 4(b)]

$$S=2h_x\cos\theta+2g_xL. \tag{8}$$

Here, the subscript x indicates the location where the probe beam meets the solid surface, h_x is the height of the distortion at x, g_x is the local gradient due to the distortion at x, L is the distance from x to the detector, and θ is the grazing angle of the probe beam. Both h_x and g_x are proportional to h_0 given by Eq. (7) for small distortion. The gradient deflection term $(2g_xL)$ can be made much larger than the height deflection term $(2h_x\cos\theta)$ by making the optical lever arm L sufficiently long.

The advantages of PT displacement spectroscopy for absorption measurements are that it is noncontact and compatible with a vacuum environment. The disadvantages are that it is applicable only to reflective and smooth surfaces, and careful aiming of the probe beam is required. Olmstead and Amer (1984) have used photothermal displacement spectroscopy for measuring absorption at silicon surfaces and have achieved a new understanding of the surface atomic structure.

Amer (1983) has described other methods for detecting PT surface deformation. These include the use of optical interferometry and attenuated total reflection, both of which have also been used for measuring surface displacements in other work. For example, optical interferometry was used by Hutchins and Nadeau (1983) for measuring surface deformation due to PA pulse generation, by Cielo *et al.* (1985) and Cielo (1985) for nondestructive testing of the degree of bonding in layered materials, and by Kino *et al.* (1980) for detecting surface acoustic waves. Attenuated total reflection has been used extensively in chemical analysis at a surface (see, for example, Cotten, 1980).

It is not always possible to totally separate surface deformation effects from the refractive-index gradient effects described in Sec. II.B. For example, Rosencwaig *et al.* (1983) and Opsal *et al.* (1983) have examined the case of a coated sample (SiO_2 on Si) in which the probe beam can be significantly affected by several PT effects, including deformations of the SiO_2 and of the Si surfaces, refractive-index gradients in the gas and in the SiO_2, optical interference effects in the SiO_2 film, and PT-induced reflectivity variations.

D. Photothermal radiometry

Photothermal radiometry (PTR) relies on the detection of variations in the infrared thermal radiation emitted from a sample that is excited by electromagnetic radiation (typically from a laser or from an arc lamp) of varying intensity or wavelength. A simple theory of PTR is given by Nordal and Kanstad (1979). The total radiant energy W emitted from a grey body of emissivity ε and absolute temperature T is given by the Stefan-Boltzmann law:

$$W=\varepsilon\sigma T^4 , \tag{9}$$

where σ is the Stefan-Boltzmann constant. Suppose the body is irradiated by an optical pulse of energy E at wavelength λ that is absorbed by the body with an absorption coefficient $\alpha(\lambda)$, resulting in a small temperature rise $\delta T(E,\alpha)$. By Eq. (9), the total radiant energy is increased by

$$\delta W(E,\alpha)=4\varepsilon\sigma T^3\delta T(E,\alpha) . \tag{10}$$

If $\delta T(E,\alpha)$ varies linearly with αE, spectroscopic applications are meaningful by defining the "normalized" PTR signal S as

$$S(\alpha)=\delta W(E,\alpha)/E . \tag{11}$$

An excitation spectrum called a PTR spectrum can be obtained by monitoring S for various excitation wavelengths λ.

In general photothermal radiometry measurements, the excitation beam (of photons, or more generally, of any form of energy) is usually either continuously modulated, with about 50% duty cycle, or pulse modulated, with very low duty cycle but high peak power. The observation spot can, in principle, be anywhere on the sample; however, the ir emission is usually detected from the excitation spot backwards (called "backscattering PTR" here), or from a spot that is "end-on" through the sample thickness with respect to the excitation spot (called "transmission PTR" here). Thus there are four common variations of PTR in the literature, as classified according to the excitation mode (continuously modulated or pulsed) and to the detection mode (transmission or backscattered). These are summarized in Fig. 5, and some applications published in the literature are listed in Table I as reviewed by Tam (1985). Examples of these applications are as follows. Using continuously modulated transmission PTR, Busse (1980), Busse and Eyerer (1983), and Busse and Renk (1983) have detected voids inside opaque solids. By continuously modulated backscattering PTR, Nordal and Kanstad (1979,1981) have demonstrated very sensitive spectroscopic absorption measurements, e.g., due to less than a monolayer of molecules on a surface. Moreover, such spectroscopic measurements can be performed on "difficult" samples like powders or materials at high temperature. Using pulsed transmission PTR, Deem and Wood (1962) have measured thermal diffusivity of "dangerous" materials like nuclear fuels. With pulsed

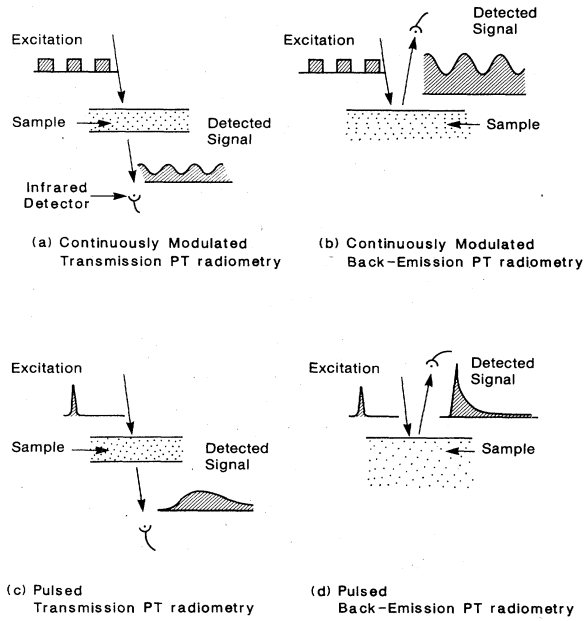

FIG. 5. Variations of the photothermal radiometry techniques.

TABLE I. Examples of work in various modes of photothermal radimetry.

Excitation	Detection: Transmission	Detection: Backscattering
Continuously modulated	Busse (1980) Busse and Eyerer (1983) Busse and Renk (1983)	Hendler *et al.* (1963) Nordal and Kanstad (1979,1981) Luukkala (1980) Vanzetti and Traub (1983)
Pulsed	Deem and Wood (1962) Taylor (1972)	Tam and Sullivan (1983) Leung and Tam (1984a,1984b) Tam (1985) Cielo (1984) Imhof *et al.* (1984)

backscattering PTR, Tam and Sullivan (1983) and Leung and Tam (1984a,1984b) have demonstrated several remote-sensing applications, including the measurement of absolute absorption coefficients, monitoring of layered structure and film thickness, and detection of the degree of aggregation in powdered materials. Using intense pulsed lasers for excitation and single-ended monitoring, such measurements can be extended to samples that are ~ 1 km away.

III. PA GENERATION

PA generation is generally due to PT heating effects, but other mechanisms are also possible. Some PA generation mechanisms are shown in Fig. 6, where the PA generation efficiency η (i.e., acoustic energy generated/light energy absorbed) generally increases downwards for the mechanisms listed. For electrostriction and for thermal expansion (also called thermoelastic) mechanisms, η is small, typically on the order of 10^{-12} to 10^{-8}, while for breakdown mechanisms, η can be as large as 30% (Teslenko, 1977). We shall limit our present discussion mainly to the most commonly used PT case, i.e., thermal expansion, where η is small.

PA generation can be classified as either direct or indirect. In direct PA generation, the acoustic wave is produced in the sample where the excitation beam is adsorbed. In indirect PA generation, the acoustic wave is generated in a coupling medium adjacent to the sample, usually due to heat leakage and to acoustic transmission from the sample. Here, the coupling medium is typically a gas or a liquid, and the sample is a solid or a liquid. We shall examine the case of direct PA generation in Sec. III.A and indirect generation in Sec. III.B.

PA generation can also be classified according to the two excitation modes: the continuous-wave (cw) modulation mode, whereby the excitation beam is modulated near 50% duty cycle, and the pulsed mode, whereby the excitation beam is of very low duty cycle but high peak power. In the cw case, the signal is typically analyzed in the frequency domain; amplitude and phase of one or several Fourier components are measured and narrow-band filters can be used to suppress noise. In the pulsed technique, however, the signal is acquired and analyzed in the time domain, making simple gating techniques for noise suppression possible. The features of the two PA techniques are indicated in Fig. 7 and compared in Table II. Discussions of these two PA generation techniques are given by Atalar (1980), Tam and Coufal (1983b), and in the Appendix.

In pulsed PA measurements, the excitation pulse is typically short ($\lesssim \mu$sec) and the acoustic propagation dis-

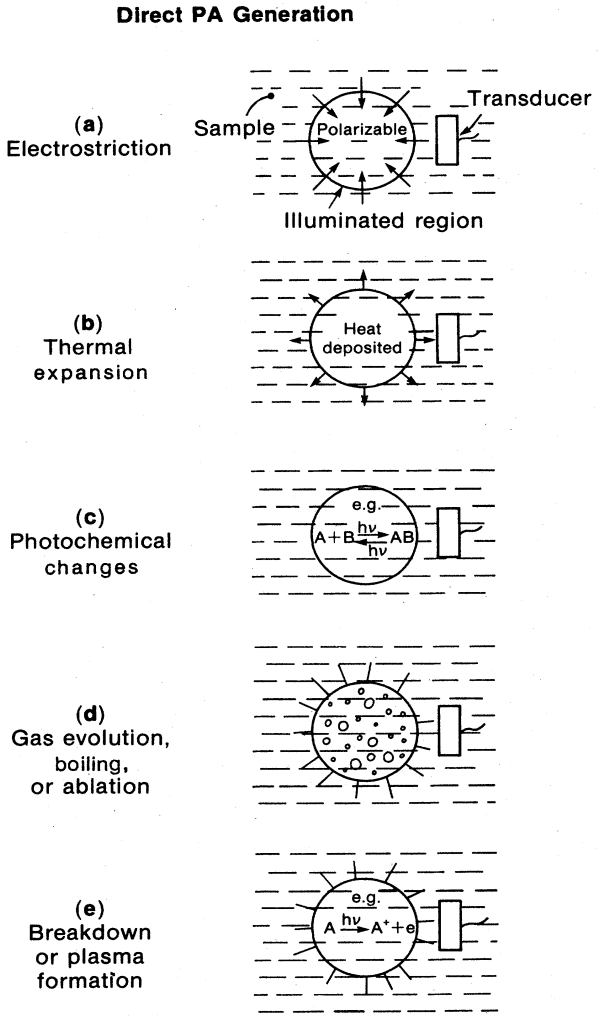

FIG. 6. Some common direct PA generation mechanisms, listed in typical order of efficiency, with the greatest generation efficiency given by method (e).

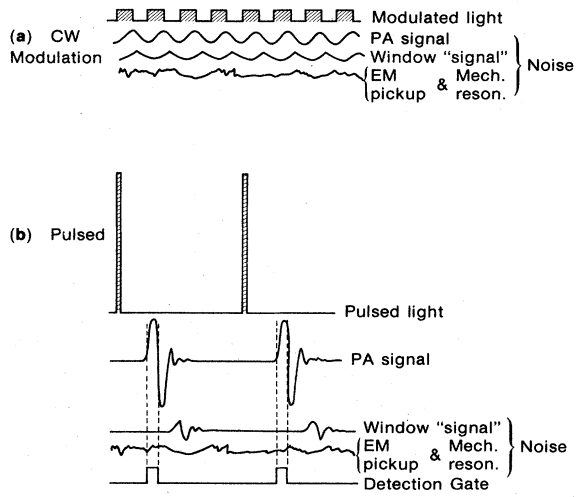

FIG. 7. Schematic comparison of the cw modulated PA detection method (a) and the pulsed PA detection method (b). Some typical noises due to absorptions at windows, electromagnetic interference, and mechanical resonances or background vibrations are also indicated.

TABLE II. Comparison of cw modulated and pulsed PA techniques.

	cw modulated	Pulsed
Modulated intensity	high duty cycle, low peak power	low duty cycle, high peak power
Acoustic detection	low frequency transducer and lock-in detector usually used	high frequency transducer and boxcar or transient recorder usually used
PA generation efficiency	low	high
Thermal diffusion effects	may be important	usually negligible
Acoustic boundary conditions	important	unimportant
Unmodulated background heating	usually substantial	usually small

tance during the excitation pulse is typically much smaller than the dimension of the sample; hence, in most cases, the PA pulse shape is independent of boundary reflections, and the sample can often be treated as infinite in extent. In cw modulated PA measurements, the modulation frequency is typically in the 10^0—10^3-Hz regime, and the acoustic propagation distance during a period is typically much larger than the sample cell. In such cases, we must first determine the acoustic eigenmodes of the sample cell, and the excitation beam will excite an eigenmode to an amplitude depending on the magnitude of the overlap integral of the thermal source with the eigenmode (see Tam, 1983).

Some important cases of PA generation that will be useful for later discussions are given in the following.

A. Direct PA generation

1. Semiquantitative theory for small laser radius and weak absorption

The theoretical treatment is illustrated by first considering a simplified case of pulsed PA generation. The excitation pulse is assumed short enough so that thermal diffusion is negligible (this usually means that the excitation pulse is much shorter than one millisecond). Consider a long cylindrical irradiated region with small radius R_s [see Fig. 8(a)], i.e., $R_s < v\tau_L$, where v is the sound velocity in the medium and τ_L is the laser pulse width. The initial expansion ΔR of the "source" radius R immediately after the laser pulse is given by

$$\pi(R+\Delta R)^2 l - \pi R^2 l = \beta V_1 \Delta T \ , \tag{12}$$

with the temperature rise just after the laser pulse being

$$\Delta T = \frac{E\alpha l}{\rho V_1 C_p} \ , \tag{13}$$

where l is the length of the PA source (assumed long), β is the expansion coefficient, $V_1 = R^2 l$ is the source volume, E is the laser pulse energy, α is the absorption coefficient (with $\alpha l \ll 1$), ρ is the density, and C_p is the specific heat at constant pressure. The question now is: What is the "source" radius R? In the previous work of Patel and Tam (1981), R was taken to be the illuminated radius R_s; this was actually incorrect, since Eqs. (12) and (13) are valid just after the laser pulse, when the active source volume has expanded to a larger radius $v\tau_L$ due to acoustic propagation. Thus we should put

$$R = v\tau_L \ . \tag{14}$$

Combining Eqs. (12)—(14) and assuming $\Delta R \ll R$ (true in all cases we are considering), we have

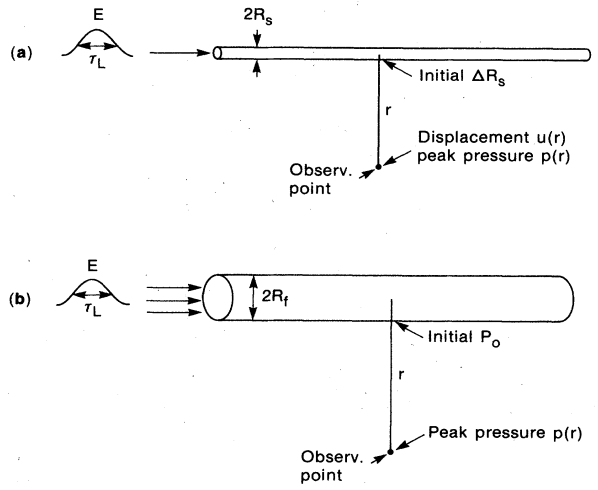

FIG. 8. Pulsed PA generation for weak absorption in an infinite medium; (a) laser beam radius R_s smaller than $v\tau_L$; (b) beam radius R_f larger than $v\tau_L$.

$$\Delta R = \frac{\beta E \alpha}{2\pi \rho C_p v \tau_L} . \tag{15}$$

The peak displacement $U_s(r)$ at the observation point, at distance r from the PA source (for $r \ll l$), varies as $r^{-1/2}$ because of conservation of acoustic energy, as described by Landau and Lifshitz (1959) for a cylindrical acoustic wave:

$$U_s(r) = \Delta R\,(R/r)^{1/2} = \frac{\beta E \alpha}{2\pi \rho C_p (v\tau_L r)^{1/2}} . \tag{16}$$

The peak acoustic pressure $P_s(r)$ at position r is related to the acoustic displacement $U_s(r)$ by

$$P_s(r) \approx v\rho U_s(r)/\tau_L . \tag{17}$$

Substituting Eq. (16) into (17), we obtain the peak PA pressure observed at r for small source radius,

$$P_s(r) \approx \frac{\beta E \alpha v^2}{2\pi C_p (v\tau_L)^{3/2} r^{1/2}} . \tag{18}$$

A more rigorous estimate of the peak acoustic pressure occurring at times $t_\pm$ for small beam radius has been given in Eq. (38) of Patel and Tam (1981) as

$$P(r, t_\pm) \approx \pm \frac{\beta E \alpha}{\pi C_p \tau_L^2} \left[\frac{v\tau_L}{2\pi r} \right]^{1/2} . \tag{19}$$

We see that Eqs. (18) and (19) are essentially identical.

2. Semiqualitative theory for large laser radius and weak absorption

The opposite case of a large laser radius, i.e., $R_f > v\tau_L$ [see Fig. 8(b)] is also simple. Here, a large radius means that the heated value does not have time to expand isobarically immediately after the laser pulse; instead a pressure increase P_0 is produced at the cylinder surface immediately after the laser pulse:

$$P_0 = \rho v^2 \beta \Delta T = \frac{\rho v^2 \beta E \alpha}{\pi R_f^2 \rho C_p} , \tag{20}$$

where ρv^2 is the bulk modulus of the medium and Eq. (20) is obtained from the consideration that the stress P_0 and the strain $\beta \Delta T$ are related by the bulk modulus. Again, the peak acoustic pressure $P_f(r)$ for the cylindrical wave scales as $r^{-1/2}$, so that

$$P_f(r) = P_0 (R_f/r)^{1/2} = \frac{\beta v^2 E \alpha}{\pi R_f^{3/2} C_p r^{1/2}} . \tag{21}$$

Equation (21) is seen to be basically the same as Eq. (18), except that the effective source radius $v\tau_L$ in the small-laser-radius case is replaced by the actual radius R_f in the large-laser-radius case. The acoustic amplitude $P_f(r)$ given in Eq. (21) resembles those given by Nelson and Patel (1981) and by Naugol'nykh (1977) in that all pressure amplitudes go as $\beta v^2 E \alpha / C_p$. While the different authors indicate different dependences on R_f and r, we believe that the form given in Eq. (21) is correct.

3. Comparison of the small and large radii cases

Comparing Eqs. (18) and (21), we see that

$$\frac{P_f(r)}{P_s(r)} \approx \left[\frac{v\tau_L}{R_f} \right]^{3/2} < 1 , \tag{22}$$

which shows that a large source radius produces a weaker PA pulse than a small source radius, all other conditions being identical. This is intuitively appealing, since for the large-radius case ($R_f > v\tau_L$), the contributions from different positions in the source do not add up coherently because of the long acoustic transit time across the diameter.

Both Eqs. (18) and (21) imply that the peak acoustic pressure P is linearly dependent on the laser pulse energy E, which means that the acoustic energy E_{ac} varies as E^2. Hence the PA generation efficiency η is

$$\eta = \frac{E_{ac}}{E} \propto E . \tag{23}$$

Thus higher PA efficiency occurs for higher laser energy, and this is true for all cases of PA generation by a thermal expansion mechanism with low generation efficiency. This, however, does not violate energy conservation principle.

4. Rigorous theory of PA generation by thermal expansion and electrostriction

Theories of PA generation by a thermal expansion mechanism have been developed by White (1963), Gournay (1966), Hu (1969), Liu (1982), and others. Theories of PA generation by thermal expansion and by electrostriction have been developed by Bebchuk *et al.* (1978), Brueck *et al.* (1980), Lai and Young (1982), and Heritier (1983). Here, we briefly outline Lai and Young's theory for the weak-absorption case (i.e., line PA source). The basic equations for the PA generation are the equation of motion

$$\rho \ddot{\mathbf{u}} = -\nabla p \tag{24}$$

and the equation of expansion

$$\nabla \cdot \mathbf{u} = -\frac{p}{\rho v^2} + \beta T - \frac{\gamma I}{2 n c_L \rho v^2} , \tag{25}$$

where $\mathbf{u}(r,t)$ is the acoustic displacement at distance r from the axis of the PA cylindrical source, $p(r,t)$ is the acoustic pressure, T is the temperature rise due to the laser pulse of intensity $I(r,t)$, γ is the electrostrictive coefficient, n is the refractive index of light, and c_L is the velocity of light in a vacuum. We use the notation that one and two dots above a quantity indicate a first and second time derivative, respectively. Taking the second time derivative of Eq. (25), we get

$$\frac{1}{\rho v^2} \frac{\partial^2 p}{\partial t^2} + \nabla \cdot \ddot{\mathbf{u}} = \beta \ddot{T} - \frac{\gamma}{2 n c_L \rho v^2} \frac{\partial^2 I}{\partial t^2} . \tag{26}$$

Substituting Eq. (24) into Eq. (26) and also using

$$\ddot{T}=\frac{\alpha \dot{I}}{\rho C_p} , \tag{27}$$

where thermal diffusion is neglected (when laser pulse duration is much shorter than thermal diffusion time), we get the following inhomogeneous wave equation for the acoustic pressure:

$$\left[\frac{1}{v^2}\frac{\partial^2}{\partial t^2}-\nabla^2\right]p=\left[\frac{\alpha\beta}{C_p}\frac{\partial}{\partial t}-\frac{\gamma}{2nc_L v^2}\frac{\partial^2}{\partial t^2}\right]I . \tag{28}$$

The solution of Eq. (28) may be simplified by introducing a potential function $\varphi(r,t)$ that satisfies the following reduced wave equation:

$$\left[\frac{1}{v^2}\frac{\partial^2}{\partial t^2}-\nabla^2\right]\varphi=I(r,t) . \tag{29}$$

Equations (28) and (29) imply the following: the acoustic pressure p can be written as the sum of a thermal expansion term $p_{\rm th}$ and an electrostriction term $p_{\rm el}$, given by

$$p_{\rm th}=\frac{\alpha\beta}{C_p}\frac{\partial\varphi}{\partial t} , \tag{30}$$

and

$$p_{\rm el}=-\frac{\gamma}{2nc_L v^2}\frac{\partial^2\varphi}{\partial t^2} , \tag{31}$$

with

$$p=p_{\rm th}+p_{\rm el} . \tag{32}$$

Equations (30) and (31) have the following two important implications. First, $p_{\rm el}$ is proportional to the time derivative of $p_{\rm th}$, i.e.,

$$p_{\rm el}\propto dp_{\rm th}/dt . \tag{33}$$

Hence, whenever $p_{\rm th}$ is at a peak, $p_{\rm el}$ passes through zero. Thus the effect of $p_{\rm el}$ can be minimized by using a boxcar integrator to detect the PA signal, with the boxcar gate set at t_1 with a suitable gate width. Second, the peak magnitudes $|p_{\rm el}|$ and $|p_{\rm th}|$ are related by

$$\frac{|p_{\rm el}|}{|p_{\rm th}|}\approx\frac{\gamma C_p}{2nc_L v^2\alpha\beta}\frac{1}{\tau_a} , \tag{34}$$

where τ_a is the width of the PA pulse. If we put $\tau_a=1$ μsec and substitute values for the other parameters in Eq. (34) for typical liquids like water or ethanol, we conclude that

$$\frac{|p_{\rm el}|}{|p_{\rm th}|}\lesssim\frac{10^{-5}}{\alpha} ,$$

where α is expressed in $\rm cm^{-1}$. Hence, for common liquids at room temperature the electrostrictive pressure is small compared to the thermal expansion pressure, unless α is smaller than $\sim 10^{-5}$ $\rm cm^{-1}$; however, even in this low-absorption case, the electrostrictive pressure effect can be suppressed (e.g., by a factor of 100) by suitably setting the boxcar gate for detection as discussed above (Lai and Young, 1982).

The solution of Eqs. (29) and (30) to obtain the pressure profile $p_{\rm th}(r,t)$ due to thermal expansion has been carried out by several authors. The simplest case is for an infinitely long and *narrow* pulsed PA source produced by a pulsed laser beam with instantaneous energy $E(t)$ given by

$$E(t)=\frac{E_0}{\pi^{1/2}\tau_L}e^{-(t/\tau_L)^2} ,$$

where E_0 is the total energy. Patel and Tam (PT) (1981) have found the solution for this simplest case to be

$$P_{\rm PT}(r,t)=-\frac{v\beta\alpha E}{\pi(\pi^{1/2})C_p\tau_L^3}\int_{-\infty}^{t-r/v}\frac{t'e^{-(t'/\tau_L)^2}dt'}{[v^2(t-t')^2-r^2]^{1/2}} . \tag{35}$$

Lai and Young (LY) (1982) have obtained a more general solution for $p_{\rm th}(r,t)$, to be referred to as $P_{\rm LY}(r,t)$, with the source not necessarily narrow. They used the following Gaussian form to describe the excitation-pulse laser beam intensity $I_{\rm LY}(r,t)$:

$$I_{\rm LY}(r,t)=\frac{E}{(2\pi)^{3/2}R^2\tau_p}\exp\left[-\frac{r^2}{2R^2}-\frac{t^2}{2\tau_p^2}\right] ,$$

where E is the laser pulse energy, t is the time measured from the peak of the laser pulse, R is a measure of the laser beam radius, and τ_p is a measure of the pulse duration. Lai and Young (1982) have solved the acoustic wave equation with a source term due to the thermal expansion produced by $I_{\rm LY}(r,t)$ and obtained the PA pressure $P_{\rm LY}(r,t)$ in terms of Bessel functions,

$$P_{\rm LY}(r,t)=K\tau_e^{-3/2}\frac{d\Phi_0(\xi)}{d\xi} , \tag{36}$$

where

$$K=(\alpha\beta E/8\pi^{1/2}C_p)(v/r)^{1/2} , \tag{37}$$

$$\tau_e=(\tau_p^2+\tau_a^2)^{1/2} , \tag{38}$$

$$\Phi_0(\xi)=|\xi|^{1/2}\exp(-\xi^2/4)\times\left[\frac{\sqrt{2}}{\pi}K_{1/4}\left[\frac{\xi^2}{4}\right]+2\Theta(\xi)I_{1/4}\left[\frac{\xi^2}{4}\right]\right] , \tag{39}$$

$$\xi=(t-r/v)/\tau_e=t'/\tau_e . \tag{40}$$

Here, K determines the magnitude of the PA pulse, τ_e is a time-scale factor that determines the width and the magnitude of the PA pulse, and $d\Phi_0/d\xi$ determines the shape of the pulse. The symbols used have the following meanings: α is the optical absorption coefficient, β is the volume expansion coefficient, C_p is the specific heat at constant pressure, v is the acoustic velocity, $\tau_a=R/v$ is an acoustic transit time in the source, t' is the retarded time, with $t'=0$ at the moment r/v after the laser peak, ξ is a normalized retarded time, $K_{1/4}$ and $L_{1/4}$ are Bessel functions of imaginary argument, and Θ is the unit step function.

Independently, Heritier (1983) has also solved the thermoelastic wave equation for excitation by a Gaussian laser beam, with an intensity distribution $I_H(r,t)$ defined by

$$I_H(r,t)=\frac{2E}{\pi^{3/2}w_0^2\tau_L}\exp\left[-\frac{2r^2}{w_0^2}-\frac{t^2}{\tau_L^2}\right].$$

Here, w_0 is known as the beam waist (Yariv, 1975) and τ_L is the e^{-1} half-width of the laser pulse, related to the full width at half maximum τ_{FWHM} by

$$\tau_{FWHM}=1.665\tau_L . \tag{41}$$

The solution of the PA pressure $P_H(r,t)$ obtained by Heritier due to the thermal expansion produced by $I_H(r,t)$ in a weakly absorbing medium is

$$P_H(r,t)=K'\varepsilon^{-3/2}F(x) , \tag{42}$$

where

$$K'=[\alpha\beta E/(2\pi)^{3/2}C_p](v/r)^{1/2} , \tag{43}$$

$$\varepsilon=(\tau_L^2+w_0^2/2v^2)^{1/2} , \tag{44}$$

$$x=[t-(r/v)]/\varepsilon=t'/\varepsilon , \tag{45}$$

and

$$F(x)=[\Gamma(\tfrac{3}{4})\,{}_1F_1(-\tfrac{1}{4};\tfrac{1}{2};x^2) -2x\Gamma(\tfrac{5}{4})\,{}_1F_1(\tfrac{1}{4};\tfrac{3}{2};x^2)]\exp(-x^2) . \tag{46}$$

Here, similar to Lai and Young's solution in Eqs. (36)—(40), K' is an amplitude factor, ε is a time-scale factor, and F is the shape function expressed in terms of the confluent (or degenerate) hypergeometric function ${}_1F_1(a;b;z)$. The symbols not previously introduced are x, which is the retarded dimensionless time equal to the retarded time t' divided by ε, and Γ which is the gamma function.

The solutions in Eqs. (36) and (42) state that the shape of the PA pressure pulse is dependent on time t only through the retarded dimensionless time $\xi=t'/\tau_e$ in Lai and Young's result and $x=t'/\varepsilon$ in Heritier's result. Due to their different definitions of the Gaussian spatial and temporal dependence of the laser pulse, it should be noted that the two "time-scale parameters" ε and τ_e differ by a factor of $\sqrt{2}$:

$$\varepsilon=\sqrt{2}\tau_e . \tag{47}$$

We have found that the solution for the time-dependent PA pressure profile $P_{LY}(r,t)$ and $P_H(r,t)$ given in Eqs. (36) and (42), respectively, are essentially equivalent. Numerical evaluations of these equations show that the separation between the peak and the trough of the PA pressure variation is $\Delta x=1.66$, corresponding to a time separation

$$\Delta t_{pk\text{-}tr}=1.66\varepsilon=2.35\tau_e . \tag{48}$$

It is interesting to note that the identical detailed solutions of Lai and Young (1982) and of Heritier (1983) agree very well with the simpler and more intuitive solutions presented earlier. We shall examine two cases, the broad and the narrow PA source comparison case, and the solution of Patel and Tam (1981).

In Eq. (22) we have estimated the ratio of the peak PA amplitude for a "broad" PA source to that for a "narrow" PA source; "broad" and "narrow" are defined according to whether $v\tau_L$ is smaller or larger than the excitation beam waist w_0. According to Eq. (42),

$$\frac{\text{peak pressure for broad source}}{\text{peak pressure for narrow source}}=\left[\frac{\varepsilon(\text{narrow source})}{\varepsilon(\text{broad source})}\right]^{3/2} , \tag{49a}$$

where, according to Eq. (44),

$$\varepsilon(\text{broad source})\approx w_0/\sqrt{2}v \tag{49b}$$

and

$$\varepsilon(\text{narrow source})\approx\tau_L . \tag{49c}$$

We thus see that Eqs. (49a)—(49c) are consistent with Eq. (22) obtained by semiquantitative arguments.

We now compare Patel and Tam's pressure profile in Eq. (35) with that of Heritier's (1983) in Eqs. (42)—(46). In the limit of very narrow laser beam waist, we may replace ε by τ_L [see Eq. (49c)]. Conversely, the solution for a finite beam waist w_0 can be obtained from that for a narrow beam waist by changing τ_L to ε. Thus, without loss of generality, we need to compare Eq. (35) with Eqs. (42)—(46) only for the case of very narrow source radius. The numerical integration of Eq. (35) is shown in Fig. 9 in comparison with the solutions given by Eqs. (36)—(40) and by Eqs. (42)—(46). All profiles are found to be very similar.

Another integral form of the thermoelastic PA pressure for the limit of very short laser pulse duration (i.e., broad source case) has been given by Brueck *et al.* (1980):

$$P_B(r,t)=\frac{1}{(2\pi^3)^{1/2}}\frac{E}{w_0v}\frac{\alpha\beta}{C_p}\frac{\partial}{\partial t}G , \tag{50}$$

where

$$G=\int_r^\infty\left\{\exp\left[-2\left[\frac{s-vt}{w_0}\right]^2\right] -\exp\left[-2\left[\frac{s+vt}{w_0}\right]^2\right]\right\}\frac{ds}{(s^2-r^2)^{1/2}} . \tag{51}$$

We have also computed the line shape for Eq. (50), which is also found to be similar to that of Eq. (35).

We have only discussed direct thermoelastic or electrostrictive PA generation for weak absorption (i.e., bulk generation due to deep penetration) so far. In general, the optical penetration depth may not be deep. In particular, the case of direct thermoelastic PA generation for opaque samples (i.e., surface generation) is important, and has been studied by many authors, e.g., White (1963), Sigrist and Kneubühl (1978), Dewhurst *et al.* (1982), and Terzic and Sigrist (1984).

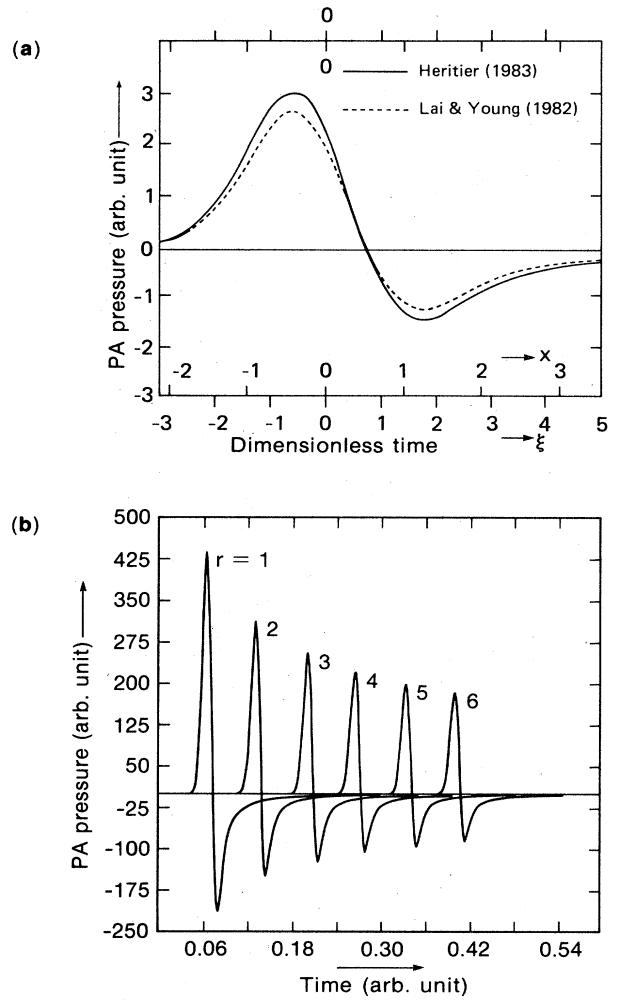

FIG. 9. Pulsed PA signal shapes according to various theoretical calculations. (a) Theoretical PA pressure profiles according to Lai and Young (1982) and to Heritier (1983). The amplitudes of the two profiles are made slightly different to show clearly the shape of each. The retarded dimensionless time used by Lai and Young is ξ, and by Heritier x. (b) Theoretical PA profiles according to the calculation of Patel and Tam (1981) for several propagation distances r (in arbitrary units) from a line PA source.

B. Indirect PA generation

In general, indirect PA generation requiring acoustic detection in a coupling fluid in contact with the sample does not provide as high a sensitivity as the direct PA generation for detecting weak absorptions. However, indirect PA generation is very valuable for the opposite case of weak absorption, i.e., when the optical absorption is so strong that no light passes through the sample.

1. Simple theory of indirect PA generation by "thermal piston"

A simple case of indirect PA generation is indicated in Fig. 10. Let the incident laser beam of radius r, modulat-

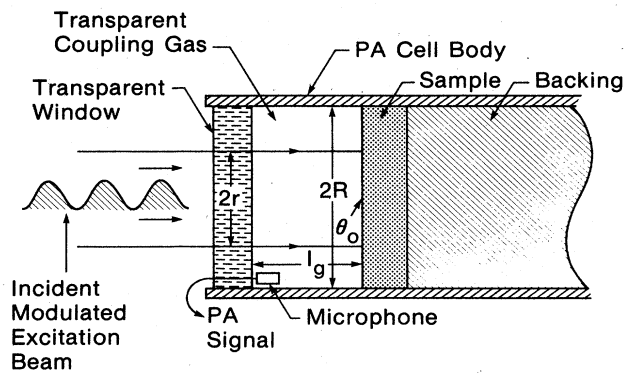

FIG. 10. A schematic PA cell relying on indirect PA generation using a coupling gas.

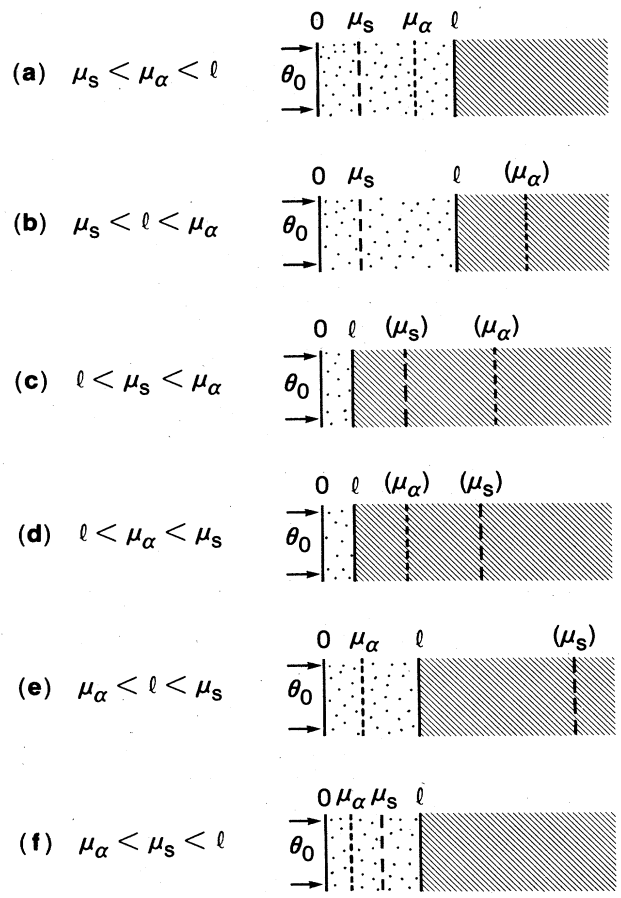

FIG. 11. Various possible cases of "thermal piston" PA generation, depending on the relative magnitude of sample thermal diffusion length μ_s, sample optical absorption length μ_α, and sample thickness l. θ_0 is the amplitude of the temperature oscillation at the sample surface in contact with the coupling gas. The dotted area indicates the sample in contact with the coupling gas on the left and with the backing material (shaded) on the right; when μ_s or μ_α is larger than l, the location of μ_s or μ_α is indicated assuming that the backing has the same thermal diffusivity and optical absorption coefficient as the sample.

ed at frequency f, be incident on the sample of thickness l in a cylindrical cell of radius R and coupling gas thickness l_g. Let the sample optical attenuation coefficient be α at the excitation wavelength, and the optical absorption length be $\mu_\alpha = 1/\alpha$. The modulated component of the laser-induced heating is distributed over a diffusion length μ_s given by

$$\mu_s = [D_s/(\pi f)]^{1/2} \tag{52}$$

when D_s is the thermal diffusivity of the sample. We assume that the optical wavelength and the modulation frequency are chosen so that μ_s is shorter than l and μ_α, as indicated in case (a) in Fig. 11. Let the modulated laser beam intensity be represented by

$$I(t) = \tfrac{1}{2} I_0 (1 + \sin 2\pi f t) . \tag{53}$$

The "active" heat produced within the diffusion length μ_s (which is the depth in communication with the coupling gas) is only a fraction μ_s/μ_α of the power input, which is absorbed over a depth μ_α. The equation for heat conduction applied to the geometry of Fig. 11(a) can be written as follows:

(thermal conductivity) $\times$ (thermal gradient)

$$= (\text{thermal power within diffusion length}) \tag{54}$$

which means

$$k_s(\theta_0/\mu_s) \approx I_0(\mu_s/\mu_\alpha) . \tag{55}$$

Thus

$$\theta_0 \approx I_0 \frac{\alpha \mu_s^2}{k_s} , \tag{55'}$$

where k_s is the sample conductivity, $\alpha = 1/\mu_\alpha$, and θ_0 is the amplitude of the temperature variation on the sample surface, which is thermally coupled to an active volume V_{act} of the gas, given by

$$V_{\text{act}} \approx \pi r^2 s_g , \tag{56}$$

where

$$s_g = \begin{cases} \mu_g & \text{for } l_g > \mu_g , \\ l_g & \text{for } l_g < \mu_g . \end{cases} \tag{56'}$$

Here, μ_g is the gas thermal diffusion length. Using the ideal-gas law, the amplitude δV of the volume change of V_{act} is

$$\delta V = V_{\text{act}} \theta_0 / T , \tag{57}$$

where T is the absolute temperature. Now the volume fluctuation δV causes a pressure fluctuation δP at the microphone. Assuming the adiabatic pressure-volume relation, we have

$$\delta P = \gamma P \delta V / V_0 , \tag{58}$$

where γ is the ratio of the specific heats and V_0 is the total cell volume, given by

$$V_0 = \pi R^2 l_g + V_r , \tag{59}$$

where V_r is the residual volume in the PA cell (Tam and Wong, 1980; Korpiun *et al.*, 1985,1986). Combining Eqs. (55)—(59), we obtain the PA amplitude δP as

$$\delta P \approx \frac{\gamma P s_g r^2}{T(R^2 l_g + V_r/\pi)} \theta_0 \approx \frac{\gamma P s_g r^2 I_0}{T(R^2 l_g + V_r/\pi)} \frac{\alpha \mu_s^2}{k_s} . \tag{60}$$

Equation (60) indicates that the PA magnitude is proportional to the sample absorption coefficient α; thus the

TABLE III. Various cases of indirect PA signal observed for a sample of thickness l mounted on a semi-infinite substrate. F is $\gamma P s_g r^2/T(R^2 l_g + V_r/\pi)$, where s_g is the smaller of μ_g and l_g [see Eq. (56')].

Case	Heat conduction equation (provides solution for θ_0)	PA signal: Approximate magnitude ($\approx \theta_0 F$)	PA signal: Phase factor
(a) $\mu_s < \mu_\alpha < l$	$k_s \frac{\theta_0}{\mu_s} \approx I_0 \frac{\mu_s}{\mu_\alpha}$	$\frac{\alpha \mu_s^2}{k_S} I_0 F$	$-i$
(b) $\mu_s < l < \mu_\alpha$	$k_s \frac{\theta_0}{\mu_s} \approx I_0 \frac{\mu_s}{\mu_\alpha}$	$\frac{\alpha \mu_s^2}{k_s} I_0 F$	$-i$
(c) $l < \mu_s < \mu_\alpha$	$k_b \frac{\theta_0}{\mu_b} \approx I_0 \alpha l$	$\frac{\alpha l \mu_b}{k_b} I_0 F$	$1-i$
(d) $l < \mu_\alpha < \mu_s$	$k_b \frac{\theta_0}{\mu_b} \approx I_0 \alpha l$	$\frac{\alpha l \mu_b}{k_b} I_0 F$	$1-i$
(e) $\mu_\alpha < l < \mu_s$	$k_b \frac{\theta_0}{\mu_b} \approx I_0$	$\frac{\mu_b}{k_b} I_0 F$	$1-i$
(f) $\mu_\alpha < \mu_s < l$	$k_s \frac{\theta_0}{\mu_s} \approx I_0$	$\frac{\mu_s}{k_s} I_0 F$	$1-i$

normalized PA signal $\delta P/I_0$, measured for a range of excitation wavelength λ, can provide the absorption spectrum $\alpha(\lambda)$ as in the direct PA generation case considered in Sec. III.A. The unusual advantage here is that spectra of totally opaque or highly light-scattering materials can now be measured.

The other cases of indirect PA generation indicated in Fig. 11 correspond to other permutations of the magnitudes of the three lengths characterizing the sample, namely, μ_s, μ_α, and l. The sample is assumed to be mounted on a thick substrate or backing material of thermal conductivity k_b and thermal diffusion length μ_b. However, the substrate properties are only important for cases (c), (d), and (e). The only differences among the various cases of Fig. 11 are the equations of heat conduction; the other equations governing indirect PA generation, namely, Eqs. (56)—(59), are the same for all the cases. We thus see that the PA signal given by the right side of Eq. (60) has a first factor that is invariant for the various cases, and a second factor that varies in accordance with the heat conduction equations. The results for the various cases calculated similar to case (a) above are given in Table III. These semiquantitative results obtained by intuitive arguments are in agreement with the results of Rosencwaig and Gersho (1976), who also calculated the "phase factor" of the PA signal; however, they only considered the condition $l_g > \mu_g$ and $V_r \ll \pi R^2 l_g$. The phase factor corresponds to the time lag of the PA signal with respect to the excitation modulation, and the values given by Rosencwaig and Gersho (1976) are also listed in Table III. The above theory for "thermal piston" PA generation is intuitive and semiquantitative. Theories more elaborate than that of Rosencwaig and Gersho (1976) have been developed by Bennett and Forman (1977), Wetsel and McDonald (1977), Aamodt and Murphy (1978), Korpiun and Büchner (1983), and others. Furthermore, gas viscosity effects that are important for $l_g \lesssim \mu_g$ have been considered by Korpiun *et al.* (1985,1986).

2. Other causes of indirect PA generation

Besides the "gas piston" or "thermal piston" source discussed in Sec. III.B.1., there are several other mechanisms for indirect PA generation, i.e., optical excitation of a specimen causing sound generation in an adjacent fluid. Such mechanisms include surface vibrations, gas evolution, and bending of plate specimens, as indicated in Fig. 12. McDonald and Wetsel (1978) first suggested that, in some circumstances, additional effects may be generated when the acoustic wave produced in the sample causes the interface to vibrate. However, this "surface vibration" effect is frequently small compared to the effect of the gas piston, except for the case when the sample is sufficiently transparent (e.g., $\alpha < 1$ cm^{-1}) and the modulation frequency f is sufficiently large (e.g., $f > 10^3$ Hz). In this case, McDonald and Wetsel (1978) and McDonald (1979) have shown that a "composite piston" model must be

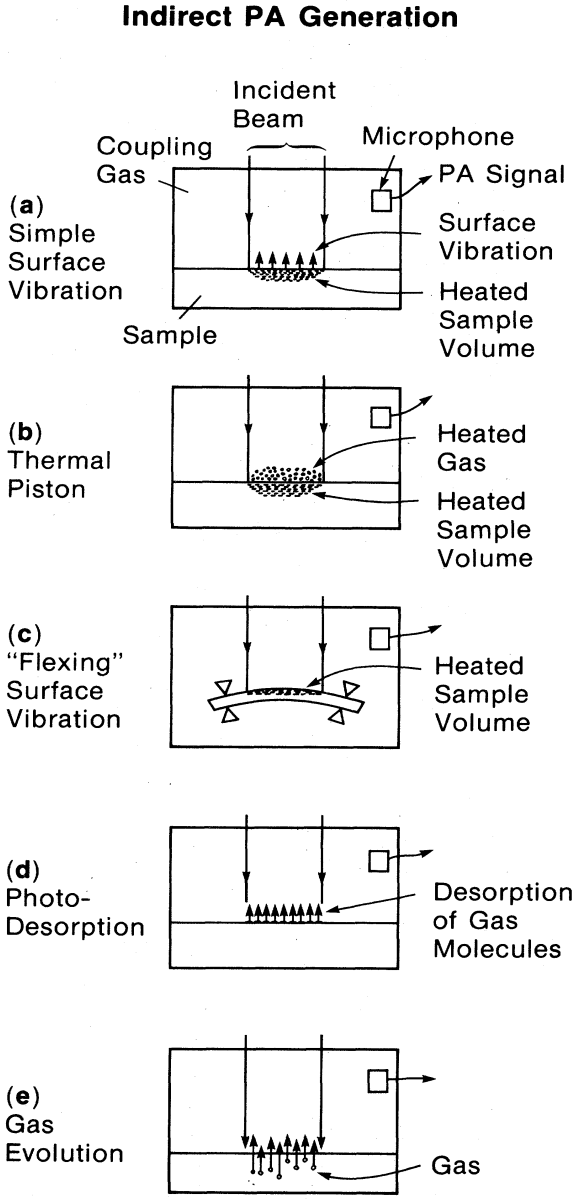

FIG. 12. Various possible causes of indirect PA generation.

used, i.e., the gas piston effect and the sample vibration effect both contribute significantly to the observed PA signal.

Gas evolution causes an additional component in the PA signal, especially when the sample is porous (with adsorbed gases) or is photochemically active (as in active chloroplasts undergoing photosynthesis when oxygen is evolved). Most PA measurements of powders in a gas-phase microphone cell are expected to have this gas evolution effect to some extent (Monchalin *et al.*, 1984). Somasundaram and Ganguly (1983) and Ganguly and Somasundaram (1983) have exploited such a gas evolution effect to enhance PA signals strongly. They reported that the PA signal for solid powders can be increased several

times when a highly volatile liquid like ether is introduced into the PA cell.

Bending of a thin solid sample in a PA cell can cause a large PA signal under certain circumstances when the sample plate acts like a "bimorph." In this case, PT heating by the incident beam causes thermal expansion on only one side of the plate, while the temperature variation in the other side is much smaller. Large bimorph-type bending can thus occur under certain boundary conditions. Rousset *et al.* (1983) have investigated the magnitude of this kind of thermoelastic bending of thin plates in comparison with magnitudes of thermal piston PA signal at various chopping frequencies.

C. Surface acoustic waves

PT heating due to the absorption of an excitation beam at a surface can both generate surface acoustic waves and affect the propagation of surface acoustic waves. The former effect is sometimes called PA Rayleigh surface-wave generation, while the latter can be called surface-wave probing of PT generation.

The effect of PA Rayleigh surface-wave generation was first observed by Lee and White (1968), who used a spatially periodic excitation of an aluminum film on a fused quartz substrate to generate Rayleigh surface waves of about 1-MHz frequency. In this case, the spatially periodic PT heating causes a directional generation of the Rayleigh surface wave, with a wavelength defined by the repetition distance of the illumination pattern. Several other authors have also studied PT Rayleigh surface-wave generation. For example, generation efficiencies have been investigated by Huard and Chardon (1983), and novel applications are indicated by Brueck *et al.* (1983).

The use of surface acoustic waves for probing physical properties near an interface has been extensively investigated, since these waves can be very surface specific. Stearns *et al.* (1983,1984) have used a cw modulated laser beam that is absorbed on a surface to modify the phase velocity of a surface acoustic wave that is generated and detected by suitable wedge transducers. Using a phase-detection technique, they indicated that PT modulation of $\sim 10^{-7}$ °C can be probed by surface acoustic waves.

D. PA amplification

PA generation is frequently understood to be due to thermoelastic expansion and is limited to the energy absorbed from the excitation beam. Most other PA generation mechanisms indicated in Fig. 6 are also limited to the energy absorbed. An important exception is the photochemical chain reaction; in this case, a large PA signal can be produced by a small absorbed energy. Thus, monitoring the PA signal can provide information on the chain reaction.

Chance and Shand (1980) have demonstrated the PA detection of a photoinduced chain reaction by observing the solid-state photopolymerization of diacetylenes. The thermal energy evolved is found to be four times greater than the light energy absorbed; this corresponds to about eight polymerized diacetylene units produced per photon absorbed. Independently, Diebold and Hayden (1980) have reported the PA detection of the photoinduced chain reaction in a halogen (X_2) and hydrogen mixture,

$$X_2 \xrightarrow{\text{photon}} X \xrightarrow{H_2} H \xrightarrow{X_2} X \xrightarrow{H_2} H \xrightarrow{X_2} \cdots . \tag{61}$$

Diebold and Hayden (1980) reported that the PA signal is directly proportional to the photochemical chain length in reaction (61), i.e., chemical amplification of the PA effect occurs. They estimated that a "chemical amplification factor" of several orders of magnitude is possible and showed that the PA measurements provide a determination of the chain length without prior knowledge of the photon flux or detailed rate constant. O'Connor and Diebold (1983) have reported further work on PA amplification in a $H_2 + Cl_2$ mixture. They showed that PA detection provides a direct monitor of the progress in the photochemical reaction because the acoustic signal depends on the reaction kinetics and on the time-dependent reactant concentrations.

IV. PA DETECTION

A. Spectral or spatial dependence

The PA signal for a sample is frequently monitored over a range of excitation wavelengths or over a range of excitation locations. The former measurement is usually called PA spectroscopy and the latter measurement is frequently called PA imaging. There are two broad types of detection techniques for performing PA spectroscopy or imaging. The first technique is a point-by-point measurement, i.e., the wavelength or the position is scanned, and the corresponding PA signal for *each* wavelength or position is recorded. The second approach is a multiplexed technique, whereby the sample is simultaneously excited by many wavelengths or at many locations. Suitable transform techniques can be used to convert the "multiplexed PA signal" back into the conventional PA spectrum or the PA image. Of these transform techniques, perhaps the best known is the Fourier transform.

The technique of Fourier transform PA spectroscopy, analogous to the well-known Fourier transform absorption spectroscopy, was introduced by Farrow *et al.* (1978) to overcome the difficulty of low spectral brightness per solid angle for a lamp source. The advantages of Fourier transform PA spectroscopy are that data at all spectral wavelengths emitted by the light source are simultaneously measured (Fellgett's advantage), and the optical throughput of the Michelson interferometer used in the Fourier transform PA technique is much larger than that of a dispersive spectrometer (Jacquinot's advantage).

A schematic Fourier transform PA spectrometer is shown in Fig. 13. The top part of Fig. 13 is a Michelson interferometer with a fixed mirror at distance l_0 and

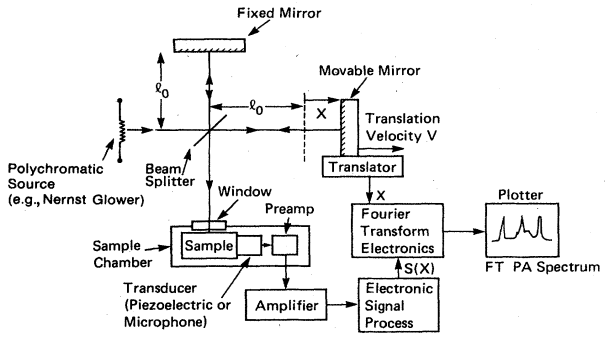

FIG. 13. Schematic of a Fourier transform PA spectrometer. The movable mirror is translated through a range of displacements X to produce the PA signal $S(X)$, which is then converted into the Fourier transform PA spectrum.

a movable mirror at a distance l_0+X from the beam splitter. Constructive or destructive interference of the two beams recombining at the beam splitter occurs when $X=\lambda/2,\lambda,3\lambda/2,\ldots,$ or $X=\lambda/4,3\lambda/4,5\lambda/4,\ldots,$ respectively, for a given optical wavelength λ. Hence the X-dependent component of the spectral intensity $I(\lambda,X)$ *incident* on the sample is

$$I(\lambda,X)=A(\lambda)\cos[2\pi X/(\lambda/2)]\,, \tag{62}$$

where $A(\lambda)$ is the spectral intensity *emitted* by the light source at λ. Consider the case of a thin sample with either indirect PA detection [cases (c) and (d) of Table III] or direct PA detection. The PA signal $S(\nu,X)$ is proportional to the optical absorption coefficient α at λ and to the reciprocal of the modulation frequency f at λ ($f=2u\nu$ where u is the movable mirror velocity):

$$S(\nu,X)=A(\nu)\alpha(\nu)\cos(4\pi X\nu)/(2u\nu)\,, \tag{63}$$

where $\nu=1/\lambda$. The total PA signal $S(X)$ due to all emitted wavelengths for mirror position X is the detected quantity and is given by

$$S(X)=\int S(\nu,X)d\nu\,, \tag{64}$$

where the integration is over the spectral range of the radiation incident on the sample. Equations (63) and (64) indicate that the PA signal, detected at $X=$(velocity)$\times$(time), is a Fourier transform of the quantity $A(\nu)\alpha(\nu)\nu^{-1}$. By measuring $S(X)$ over an extended range of X, an inverse Fourier transform of $S(X)$ can be performed, providing $A(\nu)\alpha(\nu)$ as a function of ν. Since $A(\nu)$ is either known or can be measured by using a black absorber in place of the sample, the desired PA spectrum $\alpha(\nu)$ can be derived.

The Fourier transform PA spectroscopy technique indicated in Fig. 13 was first used by Eyring and co-workers (Farrow *et al.*, 1978; Lloyd, Riseman, Burnham, and Eyring, 1980; Lloyd, Burnham, Chandler, Eyring, and Farrow, 1980). In their experiment, a white light source (e.g., a 100-W tungsten-iodide lamp) was used, and the transducer was either a piezoelectric transducer or a microphone. They obtained Fourier transform PA spectra of various samples like Nd-doped glass, La_2O_3, whole blood, etc., and showed that the combined multiplexing and throughput advantages of the method significantly reduce the data collection time and/or improve the signal-to-noise ratio.

In the infrared regime, Rockley and co-workers were the first to demonstrate the applicability of Fourier transform PA spectroscopy (see Rockley, 1979,1980a, 1980b; Rockley and Devlin, 1980; Rockley *et al.*, 1980,1981). In their work, a commercial Fourier transform infrared (ir) spectrometer (Digilab FTS-20 vacuum spectrometer) is modified so that the sample chamber contains a small nonresonant PA cell of volume ≈ 1 cm^3. A General Radio GR-1962 $\frac{1}{2}$-inch foil electret microphone amplified by an Ithaco 143L preamp is used as the sound transducer. Rockley has used this Fourier transform ir spectrometer to examine PA spectra of polystyrene films, aged and freshly cleaved coal surfaces, ammonium sulphate powders, and so on. This clearly shows the tremendous potential of Fourier transform PA spectroscopy for characterizing infrared materials without the extensive "sample preparation" procedures frequently needed in conventional ir transmission spectroscopy.

Another important advantage of Fourier transform infrared PA spectroscopy has been pointed out by Royce and collaborators (Laufer *et al.*, 1980; Royce *et al.*, 1980; Teng and Royce, 1982). The conventional spectroscopy method of transmission or reflection monitoring frequently suffers from spectral distortions when powdered solids dispersed in a transparent matrix are examined. The reason is that light scattering decreases when the refractive index of the matrix equals that of the powdered solid, causing an increased transmission of the pellet. This undesirable spurious increase in transmission (the Christiansen effect) causes distortions in the shape of the band by transmission monitoring, but is eliminated in Fourier transform infrared PA spectroscopy. In the work of Royce and co-workers, a commercial Fourier-transform ir spectrometer (Nicolet 7199) is used, with the normal detector replaced by a PA cell of about 1 cm^3 in volume, containing a $\frac{1}{2}$-inch B&K 4165 microphone of about 50 mV/Pa sensitivity. Spectra between 400 and 4000 cm^{-1} are obtained at a resolution of 4 cm^{-1}. The elimination of the Christiansen effect for powders like AgCN was clearly demonstrated.

Besides multiplexing in wavelengths, multiplexing in space has also been demonstrated. For example, Coufal *et al.* (1982a,1982b) have indicated that spatial excitation with masks based on a Hadamard transform or Fourier transform can make PA imaging much faster than pointwise excitation measurements.

B. PA cell design

PA generation is caused by a modulated absorption, which can be due either to a modulated light beam or to some modulated absorption characteristics of the sample.

Modulation methods for the light source include Q switching, mode locking, flash-lamp pumping, wavelength switching, mechanical chopping, electro-optic or acousto-optic modulating, wavelength modulating, etc. Modulation of the absorption characteristics of the sample is possible by applying modulated magnetic or electric fields to the sample. For example, Kavaya *et al.* (1979) have demonstrated that Stark modulation of a gas sample by a modulated electric field is excellent for PA detection because the "background signal" or noise is 500 times smaller in Stark modulation than in the conventional chopped light beam case. This is because the background signal (e.g., due to absorption by the cell windows or the buffer gas) has little dependence on the electric field. In a sense, the Stark modulation method is equivalent to a wavelength-modulation method, as used by Lahmann *et al.* (1977) for PA studies of liquids. Castleden *et al.* (1981) have described a simple wavelength-modulated PA spectrometer, which generates differentiated PA spectra. This provides an apparent enhancement in the resolution and results in increased precision in locating the absorption features in the sample.

The PA cell is a container for the sample and for the microphone or transducer, such that the incident excitation beam is absorbed by the sample to produce an acoustic signal. Many designs of PA cells have been described in the literature, aiming at various aspects of signal improvement, noise reduction, and ease of use. We may classify PA cells into two general kinds: cells designed for gaseous samples, and those designed for condensed matter samples. The former generally utilize a microphone (with a relatively "soft" deflecting diaphragm) to sense the gaseous pressure fluctuations produced by the optical absorption; some examples are shown in Fig. 14. Here, we show some of the techniques for signal-to-noise improvement, for example, the use of Brewster windows

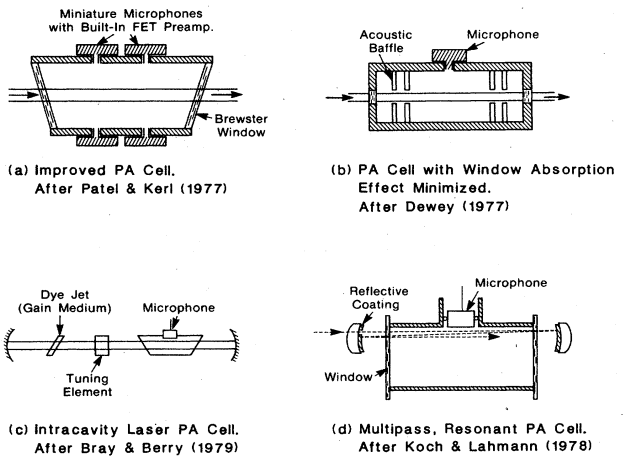

FIG. 14. Examples of various PA cells for high-sensitivity detection in gaseous samples: (a) Brewster window cell of Patel and Kerl (1977); (b) acoustically baffled cell of Dewey (1977); (c) intracavity cell of Bray and Berry (1979); (d) multipass resonant cell with excitation located to produce a suitable antinode position of Koch and Lahmann (1978).

for reducing stray reflections causing spurious signals, the use of acoustic baffles to reduce noise due to window absorption, and the methods of intracavity and extracavity multipassing. Besides microphone detection, fiber-optic detection and optical probe-beam-deflection detection can also be used for gaseous samples; more details are given in Sec. IV.C. In the second type of cells, for condensed matter, both microphones and piezoelectric transducers are in common use for detection. Some examples are shown in Fig. 15. The microphone detection schemes shown in Figs. 15(a) and (15b) are based on the detection of the indirect PA signal due to thermal coupling from the sample into the gas (Sec. III.B), while the piezoelectric detection schemes illustrated in Figs. 15(c) and 15(d) are based on direct PA detections (Sec. III.A), usually providing a higher detection sensitivity. Other PA cells for condensed matter have been described by Callis (1976), McClelland and Kniseley (1976a,1976b), Cahen, Lerner, and Auerback (1978), Kanstad and Nordal (1978), Patel and Tam (1979a), and Tam and Patel (1979b,1980). At low enough modulation frequencies or long enough pulse durations of the excitation beam, the exact geometry of the PA cell is important, since the acoustic wave can be reflected from the cell walls to produce interference and resonances. Hess (1983) has reviewed the effects of acoustic resonance upon PA detection sensitivity. Noise can be reduced by locating the excitation beam entrance and exit positions at acoustic nodes in a resonant cell. On the other hand, at very high modulation frequency or very short pulse duration of the excitation beam, effects of reflections from cell walls are unimportant, and so is the geometry of the PA cell; indeed, "leaky" or "open" PA cells can be used in such cases.

C. Acoustic detection

Many different types of acoustic detection are available, and those most commonly used in PA detection are discussed in this section. The choice of method depends on impedance matching, ruggedness, ease of operation, sensitivity, and whether noncontact detection is required.

1. Microphone

The sound transducer used in a gas-phase PA cell (whether it is used to investigate a gaseous sample or a condensed matter sample via indirect PA generation monitored in a coupling gas) is usually a commercial microphone, which is typically a capacitance sensor that senses the deflection of a diaphragm in contact with the gases. Electrets and piezoelectric microphones are also sometimes used. Many commercial brands are available, and the choice should depend on the best compromise among sensitivity, bandwidth, size, and noise. Sensitivity as high as ~ 100 mV/Pa is available in commercial microphones (e.g., those produced by Bruel and Kjaer), and a bandwidth ~ 100 kHz is also available; however, high sensitivity is usually available only as a tradeoff for lower

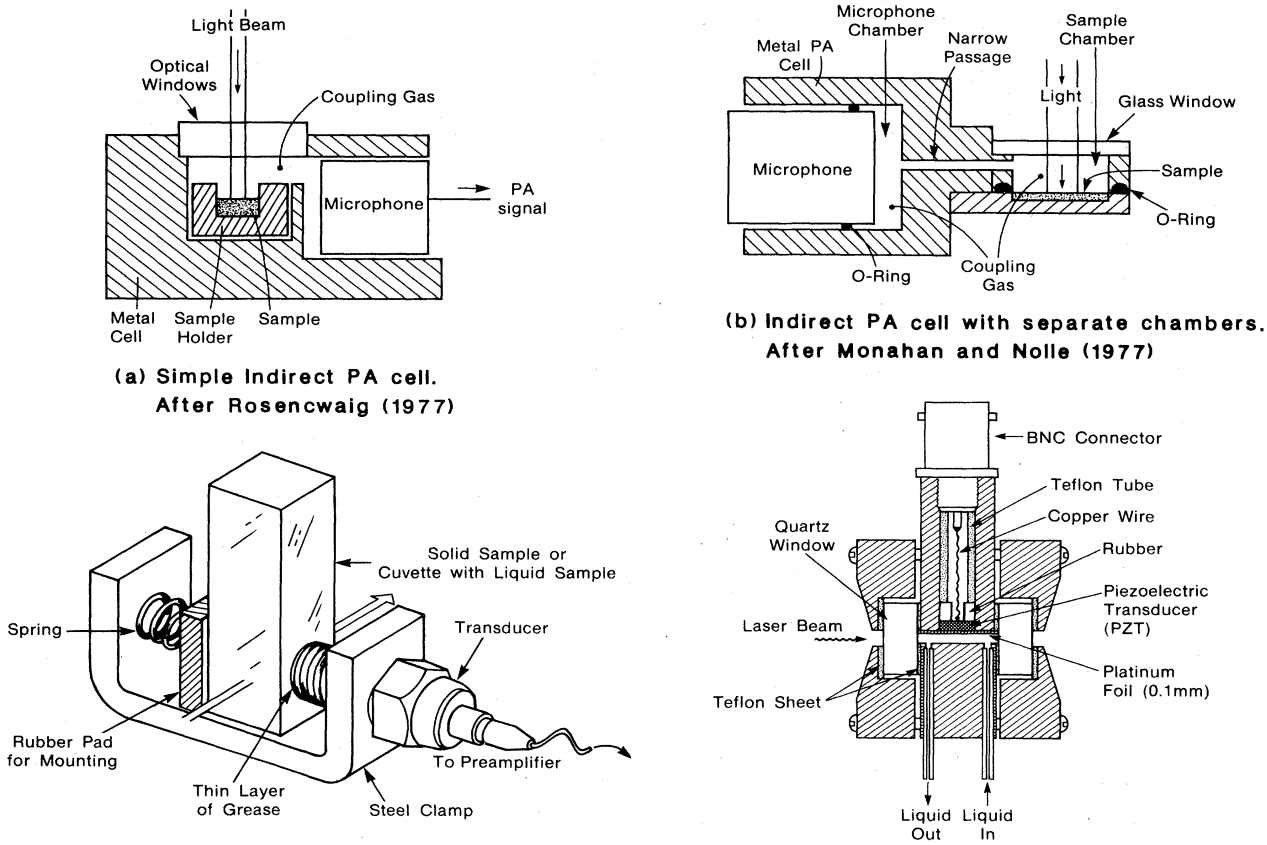

FIG. 15. Examples of various PA cells for condensed matter samples: (a) simple gas-microphone cell of Rosencwaig (1978); (b) separated-chamber cell (with Helmholtz resonance possibility) of Monahan and Nolle (1977); (c) simple direct piezoelectric detection (with the arrow through the sample indicating the path of a pulsed laser beam) of Tam and Patel (1980); (d) PA flow cell for liquids used by Sawada and Oda (1981).

bandwidths and larger microphone size. Exotic "microphones" have also been reported. For example, Choi and Diebold (1982) have developed a "laser Schlieren microphone," which relies on the use of a "probe laser" to monitor the deflection of a diaphgram due to the pressure modulation in a PA cell.

2. Piezoelectric transducers

For detecting the direct PA signal produced in condensed matter, microphones are typically not suitable because of the serious acoustic impedance mismatch at the sample-gas interface, which means that typically less than 10^{-4} of the acoustic pressure amplitude is transmitted from a solid sample into a coupling gas. Piezoelectric ceramics are more suitable for detecting the direct PA signal in condensed matter. Many types of piezoelectric ceramics or crystals are commercially available, e.g., lead zirconate titanate (PZT), lead metaniobate, lithium niobate, crystalline quartz, etc.; these transducers are reviewed by Mason and Thurston (1979). For PA detection, the piezoelectric element with metallized electrodes should be mounted in a suitable manner. One way of mounting is described by Tam and Patel (1979b). A PZT cylinder (PZT5A from Vernitron, Ohio) of 4 mm diameter and 4 mm height is pressed against a stainless-steel diaphragm that is polished on both sides. The PZT element is enclosed in the stainless-steel shell to minimize electromagnetic pickup, corrosion, and absorption of stray light. The sensitivity of such a PZT transducer is typically ~ 3 V/atm. This is much smaller than that of a sensitive microphone (e.g., B&K model 4166) with a sensitivity $\sim 5\times 10^3$ V/atm. However, PZT transducers are preferred over microphones for pulsed PA detection in condensed matter because of their much faster rise times and better acoustic impedance matching.

Thin polymeric films that are made piezoelectric are also frequently used for PA monitoring in condensed matter. These are highly insulating polymeric films that can be poled in a strong electric field at elevated temperatures, or can be subjected to charged-beam bombardment

so that they become polarized by trapping charges and exhibit a piezoelectric character. Such films include polyvinylidene difluoride (PVF_2), Teflon, Mylar, etc., with PVF_2 being the most commonly used. There is strong interest in the use of PVF_2 films as transducers (Sussner *et al.*, 1973) for acoustic imaging (especially for body scanning in medicine) because of the nonringing characteristic of the film (its mechanical Q factor is much lower than PZT), fast rise time, good flexibility, and good acoustic impedance matching to liquids like water. A disadvantage of PVF_2 is that its sensitivity is typically much lower than that of conventional piezoelectric materials like PZT or lithium niobate. However, to make transducers with a fast rise time, a thin slice of the conventional piezoelectric material must be lapped, coated, and mounted suitably, requiring considerable effort. PVF_2 foils, on the other hand, are inexpensive, easily cut to size, and readily available commercially (e.g., from Pennwalt, Pennsylvania). Many ways to mount a PVF_2 film are possible, e.g., as described by Bui *et al.* (1976), Ambrosy and Holdik (1984), and Bur and Roth (1985). We have found that another mounting method, indicated in Fig. 16, gives a PVF_2 transducer that is fast (rise time <2 nsec), reproducible, and durable for detecting PA pulses in solids with minimum electromagnetic interference because of the "grounded" enclosure. Tam and Coufal (1983a,1983b) and Tam and Leung (1984b) have used such a PVF_2 transducer for ringing-free detection of PA pulses produced by a pulsed N_2 laser of ~ 8-nsec duration.

Other thin-film piezoelectric materials are needed to achieve ultrafast rise times on the order of 1 nsec or shorter. Thin ZnO film sputtered onto a polished flat surface of a single-crystal sapphire rod (frequently called a "buffer rod") has been used for high-frequency acoustic measurements and for acoustic microscopy (Khuri-Yakub and Kino, 1977; Wickramasinghe *et al.*, 1978). Tam (1984) has shown that ultrashort PA pulses (of width <1 nsec) excited by a short N_2 laser pulse of 0.5-nsec duration can be detected by using such a ZnO transducer, and the multiple reflections of such PA pulses in thin films of thickness ~ 10 μm can be measured with high accuracy.

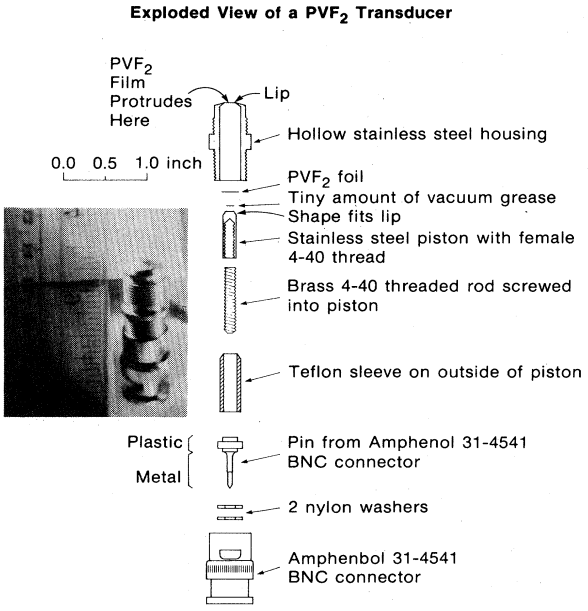

FIG. 16. A new method for mounting a PVF_2 piezoelectric film to produce a fast transducer with rise time $\lesssim 2$ nsec.

3. Capacitance transducer

When a PA pulse arrives at a surface, the displacement of the surface can be detected as a change in capacitance. Here, the sample surface (which must be an electrical conductor) is one "plate" of the capacitor, while a fixed probe (called the "capacitance probe") near the surface is the other "plate." In most cases, the sample surface is grounded, and a constant voltage is applied onto the capacitance probe so that a capacitance change is detected as a variation in charge. To achieve high detection sensitivity, the probe must be kept close to the surface (which must be sufficiently flat and smooth) at a separation of, say, several μm. Good designs of capacitance transducers with high sensitivities (detecting displacements $\sim 10^{-2}$ Å or better) have been described by Cantrell and Breazeals (1977), Scruby and Wadley (1978), and Hutchins and Macphail (1985). Dewhurst and co-workers (Hutchins *et al.*, 1981; Aindow *et al.*, 1981; Dewhurst *et al.*, 1982) have used such capacitance probes to detect PA pulses in metal samples excited by a pulsed Nd:YAG laser.

4. Voltage pickup for electret-type samples

If a sound pulse is produced in an electret-type sample (i.e., a sample with internal trapped charge), a voltage pulse can be detected by using an electrode on or near the sample surface. Sessler and co-workers (1982) have used such a detection technique in conjunction with pulsed PA generation via ablation for studying charge distribution in electrets.

5. Fiber-optic sensor

Optical fibers have been used to detect many physical quantities like pressure and temperature. Leslie *et al.* (1983) have shown that a 20-m-long single-mode optical fiber that is wrapped onto a perforated cylinder can be used as a PA gas detector with a minimum detectable absorption of 1.6×10^{-7} $cm^{-1}W/Hz^{1/2}$. In this arrangement, the PA pressure impinging onto the fiber-optic coil causes a change in the refractive index in the fiber, and hence a phase change of the light propagating in the fiber; such a phase change can be detected by interferometry. Another type of fiber-optic displacement transducer relies on the use of a bundle of fibers whose ends are located

close to the sample surface. Some of these fibers transmit light, which is reflected back into the other fibers leading to a photodetector. The detected light intensity varies according to the sample surface displacement from the fiber bundle tip. Cook and Hamm (1979) have analyzed the performance of such a transducer and obtained a displacement detectability as good as 2×10^{-12} m $Hz^{-1/2}$, with a bandwidth $\sim$1 MHz possible.

6. Noncontact optical PA detection

Noncontact optical probing of surface movements due to acoustic waves has been studied by numerous workers because of its important materials testing applications. Earlier reviews were those of Whitman and Korpel (1969) and Stegeman (1976). A general summary of noncontact ultrasonic transducers for nondestructive testing has been given by Hutchins (1983).

In this section we describe in some detail two general classes of techniques that have been used for noncontact optical PA detection, namely, surface-distortion probing and refractive-index monitoring. Such noncontact techniques are useful for fast ultrasonic testing and imaging and for remote sensing of samples that are "inaccessible" (e.g., in a vacuum chamber, in hostile environments, or not to be contaminated).

A method of optical detection of photothermal surface distortion developed by Amer (1983) has been described in Sec. II.C. It is based on the deflection of a probe beam reflected from the surface. PA surface distortions can be detected similarly. The distinctions between PT distortion and PA distortion may be described as follows: PT distortion is due to the thermal expansion associated with the local temperature rise, follows the temperature decay via diffusion, and remains close to the excitation region: PA distortion, on the other hand, propagates at a sound speed away from the excitation region. Only PA monitoring can provide values of sound speed and attenuation. At distances more than several thermal diffusion lengths away from the excitation regime, only PA distortion can be detected. Sontag and Tam (1985a) have extended the probe-beam-deflection technique of Amer (1983) for detecting multiply reflecting PA pulses in a silicon wafer excited by a pulsed N_2 laser.

Another method of optical sensing of PA surface distortion relies on interferometry. In this case, a probe beam is split into two parts, one being reflected from the sample surface and another from a reference surface. The reflected beams are recombined, and the resultant intensity is monitored. Kino and his associates (Jungerman *et al.*, 1982,1983; Bowers, 1982) have developed a coherent fiber-optic interferometry technique for measuring acoustic waves on a polished or even on a rough surface. Palmer *et al.* (1977) have analyzed a Michelson interferometry system for measuring displacement amplitudes in acoustic emission; their analysis was subsequently criticized by Kim and Park (1984). Bondarenko *et al.* (1976), Calder and Wilcox (1980), and Hutchins and Nadeau (1983) have used Michelson interferometry for detecting the PA pulse shape excited by a powerful pulsed laser (e.g., ruby, Nd:glass, or Nd:YAG laser) in metal plates, while Suemune *et al.* (1985) have extended this work to detect photoacoustic vibration in a GaAs plate produced by a focused diode laser beam modulated at $\sim$100 Hz. Cielo (1981) has described an optical detection method of acoustic waves for the characterization of samples with unpolished surfaces.

The second technique for noncontact PA monitoring relies on detecting the refractive-index change associated with the PA pulse. The detection of refractive-index variation caused by acoustic waves is not new; for example, this has been reported by Lucas and Biquard (1932) and Davidson and Emmony (1980). The present discussion is focused on its use for PA detection, which is similar to a PT detection scheme described earlier (Sec. II.B). This method can be called optical probing of the acoustic refractive-index gradient (OPARIG) and is applicable only for materials transparent to the probe beam. Here, the transient deflection of the probe due to the traversal of the PA pulse is detected. By using two or more probe beams at different displacements from the source and detecting their deflections at different times, acoustic velocity and attenuation of the sample can be detected. Quantification of the OPARIG signal $S(t)$ has been given by Sullivan and Tam (1984), using a photodiode with a small active area as a fast deflection sensor (see Fig. 17). When the PA pulse produced by the excitation beam crosses the probe beam, a transient angular deflection (Klein, 1970) φ of the probe is produced,

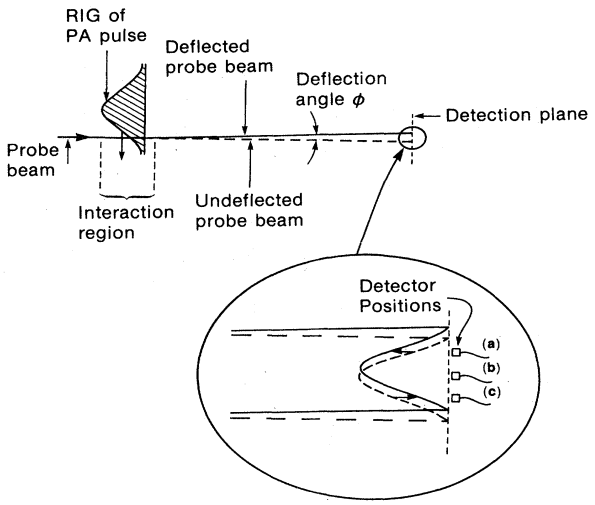

FIG. 17. A probe-beam-deflection method for noncontact transmission detection of PA pulses due to transient deflection of a narrow collimated probe beam by the refractive-index gradient (RIG). Three possible locations of a small detector, (a), (b), and (c) are indicated. The centered (b) position gives nearly zero signal for small deflections. (a) and (c) give the maximum signals (with opposite phase) if they are situated at the positions of maximum intensity slopes.

$$\varphi(r,t)\approx\frac{l}{n_0}\frac{\partial n(r,t)}{\partial r}\propto\frac{\partial P(r,t)}{\partial t}\ , \tag{65}$$

where n_0 is the normal refractive index of the sample, $n(r,t)$ is the change in the refractive index, which is proportional to the PA pressure $P(r,t)$, and l is the interaction length of the PA pulse with the probe laser. The small transient probe deflection φ causes the probe beam to move across the detection photodiode. The observed probe-beam-deflection signal $S(t)$ from the photodiode is given by

$$S(t)=GI_p'(r_d)L\varphi\ , \tag{66}$$

where G is a constant depending on the photodiode sensitivity and electronic gain of the detection system, $I_p'(r_d)$ is the lateral spatial derivative of the probe-beam intensity distribution at the photodiode position r_d (with the active area of the photodiode being sufficiently small), and L is the "lever arm" of the probe beam (i.e., distance from the interaction region in the cell to the photodiode). Combining Eqs. (65) and (66), we have

$$S(t)\propto\frac{\partial P(r,t)}{\partial t}\ , \tag{67}$$

which means that our experimental probe-beam-deflection signal is a measure of the *time derivative* of the PA pulse at the probe-beam position. Sullivan and Tam (1984) have used OPARIG for a reliable determination of PA pulse profiles generated by laser beams of durations in the μsec or nsec regimes to verify the theoretical profiles described in Sec. III.A.4. A novel application of OPARIG for acoustic absorption spectroscopy in gases, to be called "PA spectroscopy of the second kind" (to distinguish it from the well-known first kind concerned with optical absorption spectroscopy) has been reported by Tam and Leung (1984a). This is described in more detail in Sec. VII.D. Thus optical methods of PA pulse profile monitoring should open up new noncontact ultrasonic velocity, relaxation, and dispersion measurements. For example, chemical reactions, nucleations, precipitations, and some other changes in a system frequently result in changes in the ultrasonic absorption or dispersion spectra, detectable by monitoring the profiles of the probe-beam-deflection signals at several propagation distances.

7. Other PA detectors

Other types of PA detectors are possible, e.g., electromagnetic acoustic transducers, laser Doppler vibrometers, ultrasonic Doppler vibrometers, Bragg scattering, and so on. Indeed, almost all acoustic sensors can be adapted for PA detection, with proper care taken for the sensitivity and detection bandwidth needed. For example, Hutchins and Wilkins (1985) have used electromagnetic acoustic transducers to detect PA polarized shear waves produced by a laser line source. Williams (1984) has used Bragg scattering of a probe that is collinear with a modulated pump beam for high-frequency PA detection ($\sim$1 GHz) in a gas.

V. RECENT DEVELOPMENTS IN PA SPECTROSCOPY

A. Weak absorption

PA spectroscopy typically involves the measurement of PA signal amplitude $S(\lambda)$ divided by the excitation energy $E(\lambda)$ as the excitation wavelength λ is scanned. This "normalized" PA spectrum is proportional to the linear absorption spectrum of the sample in certain cases [see, e.g., Eqs. (18), (21), and (60)]. The wavelength-dependent excitation energy $E(\lambda)$ can be measured by a pyrometer, or by monitoring the PA spectrum of a "reference" flat absorber (Coufal, 1982).

The sensitivity of laser PA detection in gases has now advanced to an absorption measurement capacity of $\sim10^{-10}$ cm^{-1} with a cell length of $\sim$10 cm, using a continuously modulated laser for excitation (see Patel and Kerl, 1977). The detection of weak bulk absorption in condensed matter by pulsed PA spectroscopy has been described in an earlier article by Patel and Tam (1981). The minimum absorption detectable in a liquid has been shown to be $\sim10^{-6}$ cm^{-1} with a cell length of $\sim$1 cm and with a pulsed laser of 1 mJ energy and 1-μsec duration for excitation. In comparison, conventional absorption techniques like extinction or reflection measurements are "gross" methods, i.e., the incident and exit intensities are each measured to obtain the difference, which includes absorption plus all scattering losses. These gross methods cannot be readily used to monitor absorption coefficients less than $\sim10^{-3}$ cm^{-1}. Better sensitivities are possible with PA or PT methods, which detect a *net* macroscopic effect, namely acoustic or thermal effects, and are zero-background, which means that the detected signal is zero if there is no absorption.

There are other ultrasensitive techniques for spectroscopic detection that may have sensitivities better than the laser PA technique, notably the single-atom detection method of Hurst *et al.* (1979), using multistep laser excitation and ionization, and also luminescence monitoring with pulsed laser excitation. Although the laser PA method is less sensitive compared to such detections of net microscopic effects, it does offer the advantages of simplicity, convenience, and general usefulness. Only a simple experimental arrangement and a sound transducer are required. PA measurement is convenient, since little sample preparation is needed. Furthermore, PA measurements are applicable to diverse types of samples (including "difficult" samples like opaque materials, aerosols, powders, flames, and so on), since nonradiative thermal relaxations occur very generally (may be only partial in certain highly fluorescent or chemically active systems), while ion attachment, diffusion, recombinations, and

TABLE IV. Comparison of various weak-absorption measurements.

Method	Examples	Sample	Typical sensitivity for absorption detection (cm^{-1})
Gross method (measure incident and exit intensities to get absorption)	Transmission monitoring Reflection measurement	No restriction.	10^{-2}—10^{-4}
New macroscopic effect (measure macroscopic effects due to absorbed energy)	Photoacoustics Probe-beam refraction or reflection Probe-beam deflection Photothermal radiometry Photothermal calorimetry Photoconductivity Optogalvanic effect	Sample should produce heat or other macroscopic effects with sufficient efficiency. Intermolecular collisions or interactions usually needed.	10^{-5}—10^{-10}
Net microscopic effect (measure quantum effects after exciting a molecule)	Fluorescence Resonant ionization spectroscopy	Sample is placed in special environments (e.g., vacuum) so that the quantum effects are not quenched.	$<10^{-10}$

quenching phenomena may impose serious limitations on the other detection schemes involving ionization or luminescence. A comparison of various types of weak-absorption measurements is given in Table IV.

One obvious application of weak-absorption detection capability is the monitoring of trace pollutants. Much work has been published in the literature, and some important examples are given in Table V. For trace pollutant detection in the atmosphere, a tunable infrared PA differential-absorption spectrometer is quite useful, as described by Chen *et al.* (1982) and by Wang *et al.* (1982), all of Changchun Institute of Applied Chemistry, China. Such an infrared PA spectrometer based on a tunable CO_2 laser is now commercially available. Other examples of PA weak-absorption monitoring have been given by Burt *et al.* (1980) and Huard and Chardon (1981), who monitored absorption in optical fibers, Hordvik (1977) and Hordvik and Schlossberg (1977), who measured absorption in transparent solids, Sawada and Oda (1981), who measured trace impurities in liquids, and Patel and Tam (1979b), Patel *et al.* (1979), Tam *et al.* (1979), and Fang and Swofford (1982), who measured

TABLE V. Photoacoustic detection of trace material.

Author	Trace material	Sensitivity (part per billion)	Experimental features of the PA detection
Gases			
Kreuzer *et al.* (1972)	NH_3	0.4	Selected ir lines from a grating-tunable CO_2 or CO laser; output power $\sim$1 W
	C_6H_6	3	
	NO	0.4	
	NO_2	0.1	
Angus *et al.* (1975)	NO_2	10	Modulated cw dye laser
Claspy *et al.* (1977)	NO_2	15	Pulsed dye laser
Koch and Lahmann (1978)	SO_2	0.1	Frequency-doubled dye laser at uv spectral region
Gerlach and Amer (1978)	CO	150	CO laser oscillating in the (1,0) vibrational transition near 4.8 μm
Vansteenkiste *et al.* (1981)	CO	5×10^4	Lead-salt diode laser
Liquids			
Lahmann *et al.* (1977)	carotene in chloroform	0.012	Direct-contact PZT transducer and Ar ion laser with wavelength switching
Oda *et al.* (1978)	cadmium in chloroform	0.014	Direct-contact PZT transducer and modulated Ar ion laser
Voigtman *et al.* (1981)	pyrene in heptane	0.2	Contact PZT transducer and pulsed N_2 laser

overtone absorptions in transparent liquids.

A summary of the factors involved in achieving high-sensitivity PA detection is given in the Appendix.

B. Thin films

Weak absorption can be due to a low bulk concentration of absorbing material, as in the above, or to a thin layer of absorbing material on a substrate. Indeed, since the pulsed PA technique of Patel and Tam (1981) can detect fractional absorptions of 10^{-6} (i.e., absorption coefficients of 10^{-6} cm^{-1} for a 1-cm path length), it may be expected to be capable of detecting absorptions by thin films of 10^{-8}-cm thickness if the absorption coefficient is 10^{2} cm^{-1} or larger. In practice, it requires great care to achieve high detection sensitivities for thin films because of difficulties associated with acoustic coupling to thin films, light scattering by interfaces causing spurious transducer signals, and especially absorption by the substrate.

The use of PA techniques for measuring absorption due to thin films, monolayers, or even submonolayers have been reported by several workers. For thin films of powders or of liquids, Tam and Patel (1979c) and Patel and Tam (1980) have attached a PZT transducer onto the substrate carrying the film sample. To avoid the effect of scattered light, they used a substrate with bends (see Fig. 18), so that the sample and the transducer are located near opposite ends of the substrate. In this way, scattered light emitted from the sample cannot easily reach the transducer; however, PA waves can readily reach the transducer by diffraction because the acoustic wavelength is much larger than the optical excitation wavelength. Furthermore, the PA arrival time is much later than the scattered-light arrival time for a sufficiently long effective path length, so that the real PA signal can be distinguished from the spurious signal (due to scattered light) for pulsed excitation.

To minimize the effect of substrate absorption, several compensation schemes have been used by Träger *et al.* (1982) and Coufal *et al.* (1983,1984), and these schemes are indicated in Fig. 19. If the film has much stronger polarization-dependent absorption than the substrate, we can use two excitation beams of different polarization and alternating intensities to excite the sample and substrate. These beams can be directed at suitable incidence angles with respect to the substrate. If the film has much stronger wavelength-dependent absorption than the substrate, compensation can also be obtained by alternating two excitation beams of wavelengths λ_1 and λ_2, which are absorbed quite differently by the film but not by the substrate. A third method for substrate compensation is by position modulation, where the excitation beam is switched between a substrate location with film and a substrate location without film. Using the technique of polarization modulation [Fig. 18(a)], Coufal *et al.* (1984) demonstrated a PA detection sensibility of $\sim 10^{-3}$ of a monolayer of NH_3 on silver by using a tunable CO_2 laser for excitation and a PZT transducer for contact detection. Other work on PA thin-film monitoring has been reported in the literature, e.g., Kerr (1973), Parker (1973), Nordal and Kanstad (1977), Kanstad and Nordal (1980a,1980b), Low and Parodi (1980), and Fernelius *et al.* (1981).

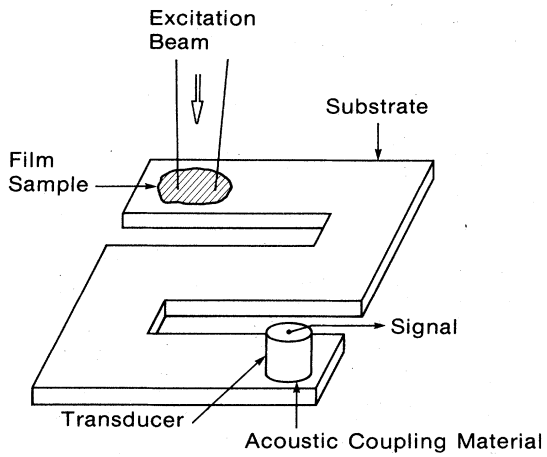

FIG. 18. A PA detection apparatus suitable for a highly light-scattering sample on a substrate.

C. Opaque materials

A very powerful feature of PA spectroscopy is its ability to measure totally opaque materials, in contrast to con-

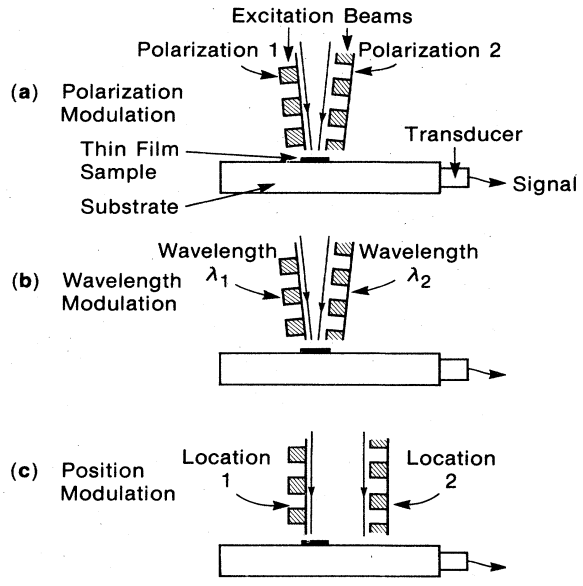

FIG. 19. Compensation schemes for PA spectroscopy of thin films on a substrate, using two excitation beams with intensity modulations that are opposite in phase and that have different (a) polarizations, (b) wavelengths, and (c) positions. Substrate absorption signal is suppressed if it is insensitive to polarization for (a), or insensitive to wavelength variations for (b), or insensitive to location for (c).

ventional transmission monitoring, which is not applicable when no light is transmitted. The key to PA spectroscopy of opaque materials by a continuously modulated excitation beam is to use a very short thermal diffusion length μ_s, so that μ_s is small compared to the absorption length μ_α over the entire spectral range of interest. This is the case (a) in Table III (treated in Sec. III.B), where it is shown that the PA signal magnitude is proportional to the absorption coefficient α.

If μ_s is not always small compared to μ_α over the spectral range studied, we say that "PA saturation" occurs. The intuitive explanation of PA saturation (already implied in Sec. III.B) for a totally opaque sample with wavelength-dependent absorption length μ_α is as follows. When the sample thermal diffusion length μ_s is shorter than μ_α at wavelength λ, the effective heat source $H(\lambda)$ is $I_0\mu_s/\mu_\alpha$, since the incident light amplitude $I_0(\lambda)$ is absorbed in a thickness μ_α, but only a thinner layer of thickness μ_s can communicate with the coupling gas and hence contribute to the PA signal. Hence we see that the $H(\lambda)$ is proportional to the absorption coefficient $\alpha(\lambda)$, and hence the PA signal magnitude is linear in $\alpha(\lambda)$. This is nonsaturation. However, if the modulation frequency f is decreased so that μ_s is longer than μ_α at a wavelength λ_1, the heat $H(\lambda_1)$ is now equal to $I_0(\lambda_1)$, since all the heat generated in the depth μ_α at this wavelength can communicate with the coupling gas. This indicates that $H(\lambda_1)$ has reached the maximum value $I_0(\lambda_1)$, independent of $\alpha(\lambda_1)$. Thus PA saturation has occurred. A way to avoid PA saturation for opaque samples is to make sure that the modulation frequency is large enough.

D. Light-scattering materials

Although PA spectroscopy can be applied to light-scattering materials like powders in the sense that a PA spectrum resembling a bulk absorption spectrum can be obtained, it is usually advisable to minimize the amount of light scattered onto the cell walls or onto the microphones or transducers. The reason is that light absorption at these surfaces can result in spurious acoustic signals. One way to minimize this is to use a PA cell with a passage connecting the sample and the microphone chambers [see, for example, Fig. 15(b)], as was done by McClelland and Kniseley (1976a,1976b), Monahan and Nolle (1977), Aamodt and Murphy (1977), Bechthold *et al.* (1981), and others. The passage can also serve other purposes besides reducing light-scattering effects, for example, providing a condition for Helmholtz resonance to enhance the PA signal, and permitting high or low temperatures of the sample chamber.

The PA absorption spectroscopy of aerosols (e.g., Roessler, 1982; Bruce and Richardson, 1984), colloids (e.g., Oda *et al.*, 1980), powders (e.g., Tam and Patel, 1979c; Rosencwaig, 1980a), and all other forms of particulates provides good examples of the usefulness of PA methods in situations where conventional extinction measurements work poorly at best. Other types of PT monitoring for aerosol absorption spectroscopy are also useful, e.g., phase-fluctuation optical heterodyne spectroscopy, PT modification of aerosol Mie scattering, photophoretic particle displacement, and PT radiometry. Some of these PT aerosol spectroscopic measurements have been described by Lin and Campillo (1985) and by Sontag and Tam (1986).

Measurement of the absorption due to fine particles is very important in basic science and in applied technologies like the automobile industry, smog control, pigment manufacturing, coal conversion, etc. PA measurement is sensitive to the heat deposited in the particulates, and generally not sensitive to light scattering, unlike extinction methods. However, strong light scattering can significantly affect the magnitude of the PA signal because light scattering can modify the "effective penetration depth" $\bar{\mu}_\alpha$ of the incident light. In the absence of light scattering, $\bar{\mu}_\alpha$ is the same as the bulk penetration depth μ_α. In the presence of light scattering, μ_α can be much shorter because a large fraction of light is back-reflected at each scattering site. This is qualitatively explained in Fig. 20 for collimated light incident on (a) a weakly light-scattering sample and (b) on a strongly light-scattering sample. We see that the light intensity near the sample surface is greatly enhanced for case (b). If the thermal diffusion length μ_s is short compared to the optical attenuation length (i.e., thermally thick case), the PA signal is generated by the heat deposited in a skin layer of thickness μ_s, and so the signal will be greatly increased for large light scattering. However, for the opposite case, when the thermal diffusion length is long (thermally thin

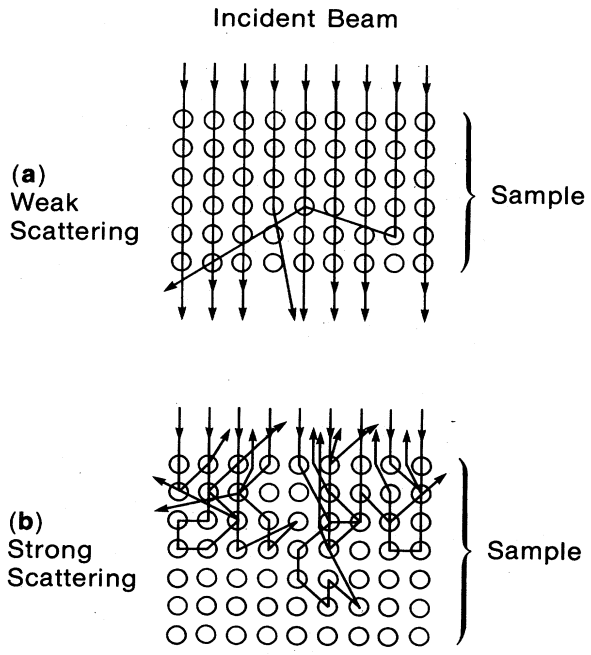

FIG. 20. Effect of weak (a) and strong (b) light scattering on the PT signal of a powdered sample indicated as spheres.

case), heat generated deep in the sample also contributes to the PA signal, and so light scattering does not necessarily increase the PA signal. Quantifications of these considerations have been given by Helander and Lundström (1980), Tilgner (1981), Yasa *et al.* (1982), and Monchalin *et al.* (1984). Figure 21 indicates some of the quantitative results given by Yasa *et al.* (1982), showing the variation of the PA signal magnitude with light scattering $\alpha_s l$ for several absorptions $\alpha_a l$ and for thermally thick and thin cases. Here, l is the sample thickness, α_s is the optical scattering coefficient, α_a is the optical absorption coefficient (denoted as α in other places in this paper), and the total absorption coefficient $\alpha_{\text{tot}}=\alpha_s+\alpha_a$.

The important conclusions concerning PA spectroscopy of light-scattering materials given by Yasa *et al.* (1982) are as follows. The PA signal is independent of light scattering only for optically thin samples when $\alpha_s l < 0.1$. In general, the PA signal can be significantly affected by light scattering when $\alpha_s l \gtrsim 1$. For thermally thin and optically thick samples (i.e., $\mu_s \gg l$ and $\alpha_{\text{tot}} l \gg 1$), PA spectra can be shown to be equivalent to diffuse reflectance spectroscopy. By varying the modulation frequency f of the excitation beam, thermally thin (for $f \to 0$) or thermally thick (for $f \to \infty$) cases can be achieved, and information on α_a and α_s can, in principle, be derived from the frequency-dependent PA spectra by using the theory of Yasa *et al.* (1982).

E. Intermodulated spectroscopy

The technique of laser-intermodulated spectroscopy is well known in the field of luminescence, transmission, and optogalvanic monitoring. It generally involves the use of two monochromatic laser beams that are modulated at different frequencies, f_1 and f_2. When the two laser beams interact with the same molecules (e.g., if they have the same lower state, or if the excited state of one beam is the lower state of the other beam), the two beams exhibit "cross-talk," i.e., the modulation of one beam induces a similar modulation in the other. By wavelength-scanning one or both of the laser beams, high-resolution spectroscopy or state-selective spectroscopy can be performed.

The technique of intermodulation spectroscopy can be applied to PA detection. A simple example of an intermodulated "Doppler-free" spectroscopy technique involving two single-mode laser beams of the same wave number, traveling in opposite directions and modulated at unequal frequencies f_1 and f_2, is shown in Fig. 22. When a highly monochromatic light beam (of bandwidth much less than the Doppler width) at wave number ν_L cm^{-1} is incident on a gas medium, only a small velocity subgroup with velocity component u parallel to the light beam will be excited, as given by

$$\nu_L = \nu_0 + u\nu_0/c_L \ , \tag{68}$$

where ν_0 is the wave number of the absorption line center and c_L is the velocity of light. The lifetime-limited linewidth is assumed to be small. By similar argument, a counterpropagating light beam of the same wave number will excite a velocity subgroup with velocity component $-u$ with respect to the original light beam. Thus the two oppositely directed light beams do not interact with the same velocity subgroup unless $u=0$, in which case Eq. (68) implies that ν_L must be equal to ν_0. In this case, the excited-state density N' will vary as

$$N' \sim \exp(i2\pi f_1 t)\exp(i2\pi f_2 t) = \exp[i2\pi(f_1+f_2)t] \ . \tag{69}$$

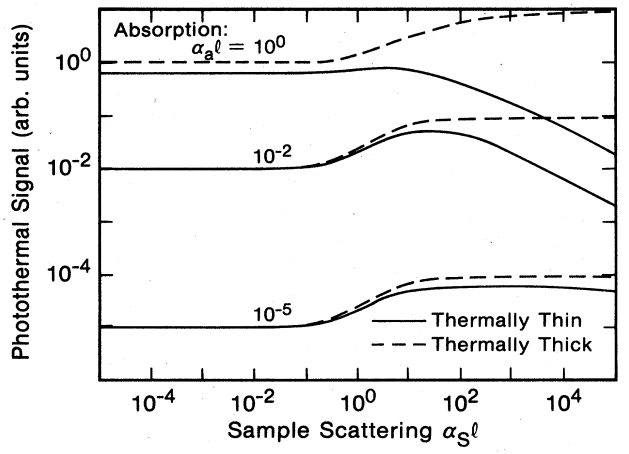

FIG. 21. Computed variation of the PT signal magnitude with light scattering $\alpha_s l$ for several absorptions $\alpha_a l$ for thermally thin or thermally thick samples (after Yasa *et al.*, 1982).

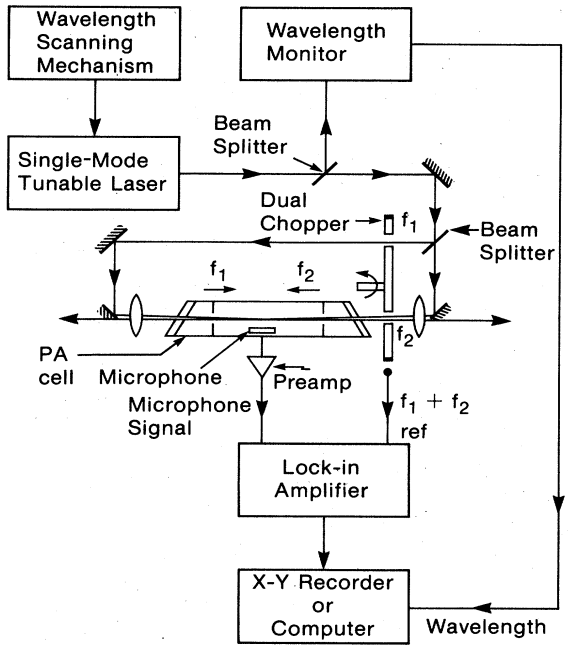

FIG. 22. Schematic arrangement for a Doppler-free intermodulated PA spectroscopy measurement.

Hence the lock-in amplifier will detect the PA signal at the sum frequency f_1+f_2. On the other hand, if the laser wave number is not at ν_0, so that different velocity subgroups are affected, the excited-state density will vary as $\exp(i2\pi f_1 t)+\exp(i2\pi f_2 t)$, and no sum frequency is generated.

In the Doppler-free PA spectroscopy of Marinero and Stuke (1979), the $P(192)$ line of the 11-0 band of the $B\leftarrow X$ transition of I_2 is measured using a single-longitudinal-mode cw dye laser beam, which is split into two equal-intensity beams propagating in opposite directions and chopped at different frequencies. Other work on Doppler-free PA spectroscopy has been reported, for example, by Lieto *et al.* (1979), Inguscio *et al.* (1979), and Abraham *et al.* (1984).

F. Multiphoton absorption

Pulsed lasers are generally used to observe multiphoton absorption by PA detection because of the high light intensity required. Multiphoton PA spectroscopy, together with multiphoton ionization spectroscopy and multiphoton luminescence spectroscopy, are all highly sensitive methods suitable for studying high-lying molecular excited states or other states that are not accessible in a one-photon transition.

Cox (1978) has used a high-power CO_2 TEA laser beam and adjusted its intensity between 16 and 5×10^6 W/cm^2 to excite a SF_6-Ar mixture. At low intensity, the pulsed PA signal S varies linearly with the beam intensity I, as expected for linear absorption. At intermediate I, S is observed to go as $\sqrt{I}$, indicating optical saturation of an inhomogeneously broadened absorption. At large I, rapid increase of S with I is observed, indicating the occurrence of multiphoton absorption. Furthermore, the addition of more buffer gas to increase the collision frequency is observed to quench the multiphoton excitation of SF_6.

Several other workers have performed similar ir multiphoton absorption spectroscopy with PA detection. Fukumi (1979) has used CO_2 laser lines to observe multiphoton PA signals in ethylene; by measuring the dependence of the PA signal magnitude on the laser energy, Fukumi (1979) has shown that the absorption at 949 cm^{-1} is due to a single-photon transition in ethylene, while the absorptions at 953 and 939 cm^{-1} are due to two-photon transitions. Brenner *et al.* (1980) have studied multiphoton absorption in propynal in a collisionless environment and performed both PA detection and laser-induced fluorescence detection. Webb *et al.* (1980) have measured the two-photon PA spectroscopy of symtriazine and derived the vibronic assignments in the $^1E''$ state. Weulersse and Genier (1981) have obtained multiphoton absorption cross sections for CO_2 laser lines in CF_3I at a vapor pressure of 0.2 Torr. Chin *et al.* (1982) have studied two-photon absorption effects in gases due to CO_2 laser excitation. Tam and Patel (1979a) were the first to measure two-photon absorption cross sections in liquids by a PA technique. Other multiphoton absorption measurements in solids have been reported by Bass *et al.* (1979) and by Bae *et al.* (1982).

Another interesting multiple photon effect observed by PA spectroscopy is the Raman-gain effect. This detection technique is frequently called "PA Raman spectroscopy" or PARS. PARS was first suggested by Nechaev and Ponomarev (1975) and was observed by Barrett and Berry (1979) and by Patel and Tam (1979c). Raman-gain spectroscopic technique is of strong current interest because of its potentially high sensitivity for measuring Raman frequencies and cross sections, and its applicability to cases of luminescent samples or hostile environments (flames, discharges, etc.) where spontaneous Raman scattering cannot be easily performed. To produce stimulated Raman scattering, a "pump beam" of intensity I_p and wave number ν_p, and a "signal beam" of intensity I_s and lower wave number ν_s, are incident on a Raman-active medium collinearly. One of the beams is tunable. When the difference wave number $(\nu_p-\nu_s)$ equals a Raman frequency ν_R of the medium, Raman gain occurs, i.e., I_p is attenuated and I_s is amplified, photon for photon. Since a "pump photon" is of higher energy (being of larger wave number) than a "signal photon," energy is deposited in the medium due to the stimulated Raman scattering. This deposited energy can produce heat due to vibrational-translational relaxations in the medium.

For the case of weak Raman gain (i.e., when the signal intensity increase ΔI_s is much less than I_s), it can be shown (see Barrett and Berry, 1979; Patel and Tam, 1979c) that the energy W deposted in the medium due to a pulsed signal beam of energy E_s is

$$W=G_s l\bar{I}_p E_s \nu_R/\nu_s \ , \tag{70}$$

where G_s is the Raman-gain coefficient that depends on the Raman cross section, l is the gain path length, and $\bar{I}_p$ is the averaged pump intensity, during the signal pulse.

Equation (70) is the basis of the PARS work of Barrett and co-workers. In their first experiments (Barrett and Berry, 1979), continuous laser sources incident on CH_4 were used. The pump beam was an Ar^+ laser mechanically chopped at 573 Hz, while the signal beam was a continuous dye laser beam tuned near 6054 Å. With microphone detection, the symmetric stretch vibrational mode of methane near 2900 cm^{-1} was detected. In their later experiments on PARS, West and Barrett (1979) and Siebert *et al.* (1980) reported that greatly enhanced sensitivity could be obtained using a pulsed laser to provide the pump and probe beams. This is obvious from Eq. (70), which can be rewritten as

$$W\propto E_p E_s/(\tau_p A_p) \ , \tag{71}$$

where E_p is the incident pump beam energy, τ_p is the duration of the pump pulse, and A_p is the cross-sectional area of the pump beam. Thus, for constant energies E_p and E_s, the PARS signal is inversely proportional to τ_p and A_p. This method of enhancing a PARS signal by using pulsed lasers instead of cw lasers is in agreement with the work of Patel and Tam (1979c), who have obtained

PARS data for several liquids, including benzene, acetone, trichloroethane, toluene, and hexane.

VI. PA MONITORING OF DEEXCITATIONS

After optical absorption in a medium, deexcitation mechanisms frequently involve heat evolution. The simplest case occurs when there is only thermal deexcitation. In this case, PA monitoring can be a powerful way to detect the energy deposited in a medium. Shaw (1980) has, in fact, used this effect to construct a PA laser energy monitor.

In general, several deexcitation channels occur, usually involving a thermal deexcitation channel in competition with another deexcitation channel like fluorescence, photochemistry, photoelectricity, or energy transfer. For an energy W_0 absorbed in a system, the energy W_{heat} released as heat can be expressed in the following general form:

$$W_{\text{heat}} = W_0 \left[1 - \sum_i \varphi_i f_i \right] , \tag{72}$$

where φ_i is the branching ratio for an ith state, which decays with a fraction f_i of its energy not producing heat and a fraction $(1-f_i)$ of its energy producing heat. Since the PA signal S is proportional to W_{heat}, we may write

$$S = S_0 \left[1 - \sum_i \varphi_i f_i \right] , \tag{72'}$$

where S_0 represents the PA signal if only heat is produced. Equation (72') is the basis of many different types of PA measurement for deexcitation quantum efficiency, as discussed below.

A. Fluorescence quantum yields

When a luminescent material that is optically excited can decay only by fluorescence or by heat generation, the measurement of the absolute optical energy absorbed W_0 and the absolute heat energy generated W_{heat} provides the fluorescence quantum efficiency φ for a simple two-level system,

$$\varphi = (W_0 - W_{\text{heat}})/W_0 , \tag{73}$$

which is a special case of Eq. (72). Thus absolute calorimetry is one way to obtain information on the fluorescence quantum efficiency. In practice, a luminescing system is frequently not a simple two-level system if intersystem crossing to a triplet state occurs. In this case, two components of heat generation may be observable, a fast component due to nonradiative relaxation of the singlet excited state and a slow heat component due to the nonradiative relaxation of the triplet state. Callis *et al.* (1969) have developed a flash calorimetry technique to examine quantum yields in such a system, for example, anthracene in ethanol, where triplet formation quantum yields is 66%. In the work of Callis *et al.* (1969), the detection of the slow and fast heat production (only $\sim 10^{-5}$ cal) is accomplished by means of a capacitance microphone measuring the thermal volume change of the liquid. This work appears to be the first PA experiment to monitor a triplet quantum yield.

A key issue in measuring fluorescence quantum yield by Eq. (73) is that absolute heat energy is involved; however, the PA signal is only proportional to the modulated heat generated, with the proportionality constant usually poorly known. The best way to avoid this difficulty is to perform the PA measurement twice, first with the desired luminescence quantum yield φ_f, and secondly with the quantum yield altered in a known way. This provides two equations with two unknowns, and so φ_f can be solved. As concrete examples, consider the energy-level diagram of Fig. 23. For optical excitation to a low excited singlet state S_1 at energy E_1, the heat energy W_{heat} per unit volume produced by an incident optical intensity I_{in}, pulse duration τ, and absorption coefficient α is given by

$$W_{\text{heat}} = I_{\text{in}} \alpha \tau (E_1 - \varphi_f E_1') , \tag{74}$$

where E_1' is the energy of the lowest S_1 excited state and relaxation from E_1 to E_1' is assumed to be fast and nonradiative. Now, since the PA signal S is proportional to W_{heat}, we have

$$S = K I_{\text{in}} \alpha \tau (E_1 - \varphi_f E_1') , \tag{74'}$$

which contains two unknowns: the proportionality constant K and the luminescence quantum efficiency φ_f.

Two methods for evaluating φ_f are indicated in Fig. 23. The first method is the quenching method (a). In essence, the method consists of doping the sample by the addition of a small concentration of an efficient "quencher" molecule, so that φ_f in the doped sample becomes zero, without affecting any other properties. Thus

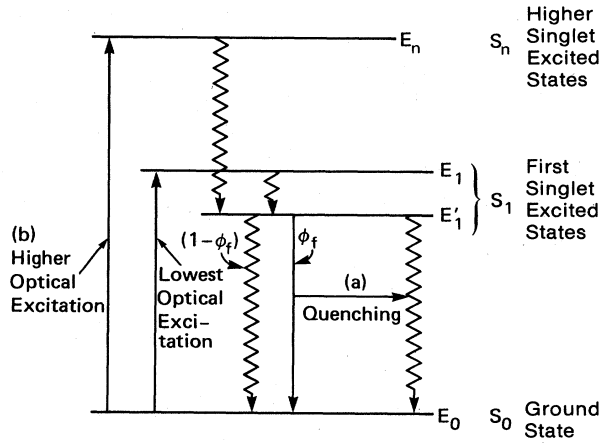

FIG. 23. Schematic of some methods for measuring the luminescence quantum yield φ_f from the lowest singlet excited state: (a) by a quenching technique; (b) by a higher-state excitation technique. Straight lines indicate radiative transitions and jagged lines indicate nonradiative transitions.

$$S' = KI_{\text{in}}\alpha\tau E_1 , \tag{75}$$

where S' is the PA signal for the doped sample at the same wavelength, and Eqs. (74') and (75) can be solved for φ_f. Such quenching methods have been used by Hall *et al.* (1976) for absolute fluorescence quantum yield studies of benzene vapor in the near ultraviolet, by Starobogatov (1977), Lahmann and Ludewig (1977), Adams, Highfield, and Kirkbright (1977), Adams, Beadle, and Kirkbright (1977), and Adams *et al.* (1981) for measuring φ_f of dye solutions, by Merkle and Powell (1977), Quimby and Yen (1978), and Auzel *et al.* (1979) for measuring φ_f of solids, and by Murphy and Aamodt (1977a,1977b) for explaining the nonradiative processes affecting the concentration-dependent metastable-state quenching rates in ruby at liquid-N_2 temperatures.

The second method (b) in Fig. 23 relies on the possibility of optically exciting higher excited states S_n that decay nonradiatively to the lowest state in S_1. This higher excitation method was first proposed and demonstrated by Rockley and Waugh (1978). The mathematical basis of the method is that the PA signal S'' due to the higher excitation is given by

$$S'' = KI''_{\text{in}}\alpha''\tau''(E_n - \varphi_f E'_1) , \tag{76}$$

where I''_{in} is the incident optical intensity to excite S_n with a pulse width τ'' and absorption coefficient α''. Thus Eqs. (74') and (76) provide two equations with two unknowns (K and φ_f), and hence φ_f can be solved. Using this higher excitation method to provide an "internal standard," Rockley and Waugh (1978) were able to obtain φ_f for a crystal violet solution.

The measurement of φ_f with PA methods can be very useful for studying laser materials. For example, the fluorescence quantum yield of laser dyes in various solvents at various concentrations can be measured to understand the effect of solvent quenching and concentration quenching. New laser solid materials in the form of powders can be tested without the necessity of growing macroscopic crystals as conventional methods of measuring φ_f would require.

Electrical excitation of materials can also produce heat and luminescence in certain materials, and fluorescence quantum yields due to electrical excitation can also be measured as in the optical cases. As an example, semiconductor diode laser materials have been tested acoustically by Suemune *et al.* (1980); in that work, current-injection-induced acoustic signals were detected in GaAs-GaAlAs double-heterostructure lasers. The dependence of the acoustic intensity on the injection current showed an anomaly close to the threshold of laser action. Such work may have important applications in the research and manufacturing of semiconductor lasers.

B. Photochemistry

Photochemical effects can cause characteristic acoustic emissions due to different mechanisms; hence PA monitoring can provide a new and sensitive way to study or to monitor photochemistry. The simplest mechanism by which photochemistry influences the magnitude of the PA signal or a photothermal signal in general is that of complementarity; when the two branches are complementary (assuming the luminescence and photoelectricity branches to be zero), the increase of one branch must mean the decrease of the other. This complementary effect is always present in all the photochemical monitoring studies discussed below, but may be overwhelmed by the other effects like gas evolution. The complementary effect is well demonstrated in the important photosynthesis work of Cahen and co-workers (Cahen, Garty, and Caplen, 1978; Cahen, Malkin, and Lerner, 1978; Malkin and Cahen, 1979). In that work, lettuce chloroplast membrane in a liquid medium was contained in the sample chamber of a differential PA cell. They observed that, for samples with active photosynthesis, the PA spectrum and the optical absorption spectrum actually differed by an amount corresponding to the conversion into chemical energy (called the "photochemical loss"). Furthermore, "poisoned" chloroplasts give PA signals that were larger than those obtained with active chloroplasts because of the absence of photochemical loss in the poisoned case.

Energetics in the purple membrane of *Halobacterium halobrium* represent another important photochemical effect that has been studied by PA techniques (Cahen, Garty, and Caplen, 1978; Cahen, Malkin, and Lerner, 1978; Ort and Parson, 1978,1979). This membrane contains a single protein, bacteriorhodopsin, covalently bonded to a retinal molecule. Absorption of light by the retinal molecule causes a cyclic photochemical process, involving a proton transfer from one side of the membrane to the other. Ort and Parson (1978,1979) have used a capacitance microphone PA cell to detect the volume changes due to the proton transfer following an optical flash excitation. This is performed in an aqueous buffered solution at 3.4 °C, when thermal expansion effects are negligible.

Another mechanism of photochemical-induced acoustic generation is gas evolution or consumption, which may be very large compared to that caused by the thermal expansion effects alone. Diebold (1980) has considered the case of a periodic ultraviolet photodissociation of a diatomic gas. Since the equilibrium point of the photodissociation depends on the slow reverse process, namely, a three-body recombination, a phase lag is introduced in the PA signal. The amplitude and phase lag of the PA signal provide important information on the photodissociation process. Gray and Bard (1978) have studied both photochemical gas generation and consumption by PA detection. Gas evolution was demonstrated for the heterogeneous photocatalytic oxidation of acetic acid to methane and CO_2 at a platinized TiO_2 catalyst. Gas consumption was shown for the case of O_2 depletion due to photo-oxidation of rubrene.

Photochemical chain reactions can cause extremely large and prolonged PA emission signals, which can provide important information on the chain reaction. Such PA "amplifications" or "gains" have been described in Sec. III.D.

C. Photoelectricity

When part of the light energy is converted into electrical energy (e.g., in a photovoltaic or photoconductive device), the thermal energy produced in the optical excitation will be less than the absorbed light energy. Under circumstances in which released free carriers do not cause any volume change in the sample (e.g., by electrostriction or by electrical current heating), the observed PA signal from the sample should be smaller when the sample is photoelectrically active than the signal when it is inactive. However, if electrostriction or Joule heating by the photocarrier are important, the PA signal still shows a photoelectrical effect, but the interpretation of the results becomes more complex.

Cahen (1978) was the first to demonstrate the PA monitoring of photoelectrical effects. The PA signal $S(R)$ from a solar cell device depends on the photoelectrical generation efficiency $\varphi_e(R)$, which is dependent on the external load R,

$$S(R)=KI_0[1-\varphi_e(R)] , \tag{77}$$

which is a particular case of Eq. (72'). Here K is a constant for a fixed PA cell geometry and a fixed optical wavelength, and I_0 is the modulation amplitude of the incident light ntensity. Under open circuit conditions, the PA signal S' is simply given by

$$S'=KI_0 , \tag{78}$$

since $\varphi_e=0$ at open circuit. Combining Eqs. (77) and (78), we have

$$\varphi_e(R)=1-[S(R)/S'] . \tag{79}$$

Cahen's (1978) experiment was performed on a Si solar cell; he measured simultaneously $S(R)$ and the electrical power output $P_{\text{out}}(R)$, as R was varied from a small value ($\sim 0.1\ \Omega$) to a large value ($\sim 100\ \Omega$). His results, indicated in Fig. 24, show that $S(R)$ is at a minimum while $P_{\text{out}}(R)$ is at a maximum when $R=6\ \Omega$, which is presumably the internal resistance of the solar cell. By using Eq. (79), Cahen obtained a value of $\varphi_e=18\%$ (at $6\ \Omega$) at the wavelength used. Cahen's experiment may have important applications in the testing and quality control of solar cells for measuring the conversion efficiency averaged over the whole cell surface or at different parts of the surface. Furthermore, efficiencies of individual elements of a solar cell array can be measured without any disconnection.

Tam (1980) extended Cahen's (1978) idea of PA monitoring of photoelectricity to other systems. Tam (1980) used a PA method for the first time to study the photoconductive quantum efficiency φ_e of a thin organic dye film. Here, φ_e was defined as the averaged number of mobile electrons or holes generated per photon absorbed. The photoconductive sample used was a multilayer film suitable for electrophotographic applications. The special, highly photoconductive dye (see Tam, 1980) was coated onto an aluminized Mylar sheet, and the dye film

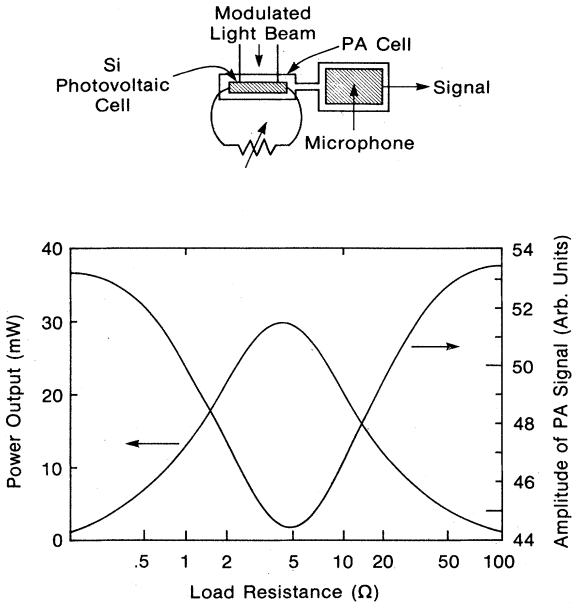

FIG. 24. An experimental demonstration of PA monitoring of photoelectric generation efficiencies in a silicon solar cell (after Cahen, 1978). The PA signal amplitude is minimum when the external power is maximum for a load resistance equal to the internal solar cell resistance.

thickness was from 0.1 to 1 μm. It was overcoated with a 20-μm thick "transport layer," which was a doped polycarbonate film that transported holes. A piezoelectric transducer was spring loaded against the Mylar with a thin layer of grease used between the piezoelectric transducer and the Mylar for acoustic coupling. The sample was excited by a modulated Kr^+ laser beam with sufficient attenuation so that the light intensity at the sample never exceeded 0.1 mW/cm^2 to avoid material damage. The PA signal S was found to be very much dependent on the modulation frequency f; strong enhancement (by a factor of ~ 100) of S occurred when f equaled a fundamental mechanical resonance frequency of the sample-transducer assembly (about 40 kHz in this experiment). To measure φ_e at a laser wavelength (e.g., 676 nm), the modulation frequency was fixed at a resonance frequency, and $S(\varepsilon)$ was measured for various electric fields ε across the sample. It is well known (see Tam, 1980) that φ_e in organic dyes is very dependent on ε, and φ_e is zero at $\varepsilon=0$. Hence the situation was analogous to Cahen's (1978) case in Eqs. (77) and (78), with ε being the variable instead of R, and hence $\varphi_e(\varepsilon)$ could be measured.

Equation (79) can be regarded as a general prescription for obtaining quantum efficiency φ which depends on a parameter R if there is a known value φ_0 for the quantum efficiency at a parameter value R_0. However, we must remember that the use of Eq. (79) to obtain photoelectrical quantum efficiencies is not unconditional: luminescence, photochemistry, Joule heating by carriers, and photocarrier-induced strain (which was recently demonstrated in Si by Stearns and Kino, 1985) should all be

negligible for this simple equation to be valid. These conditions should be examined before Eq. (79) is used.

There are several other recent papers on the use of photoacoustic monitoring of photoelectrical carrier generation or related effects in semiconductors and organic dyes. Thielemann and Neumann (1980) have applied a photoacoustic technique similar to Cahen's (1978) to determine the photocarrier generation quantum efficiency in a Schottky diode. Wasa *et al.* (1980) have investigated nonradiative states in GaAs and InP by PA spectroscopy. Tokumoto *et al.* (1981) have used PA spectroscopy to study Si, Ge, InSb, GaAs, and GaP in the region above the fundamental absorption edge. Iwasaki *et al.* (1979) have used laser PA spectroscopy to examine voltage-dependent electron recombination processes at a semiconductor electrode-dye solution interface. Iwasaki *et al.* (1981) have used PA methods to study spectral sensitization effects by dyes on ZnO powders.

D. Energy transfer

There are at least two ways to achieve energy transfer. The most commonly used way is by collisions, i.e., either self-collision of the excited molecules with the ground state of the same molecules, or collision of the excited-state molecules with foreign molecules. Another less common but very powerful way is stimulated transition by light.

The simplest explanation of the technique of PA monitoring of the energy transfer process is as follows. For a simple two-level system in a gas phase involving the ground state of density N and excited state of density N', optical excitation by a photon flux Φ with absorption cross section σ can be described by the rate equation

$$\left[\frac{d}{dt}+\tau^{-1}\right]N'=N\Phi\sigma\ , \tag{80}$$

where

$$\tau^{-1}=\tau_n^{-1}+\tau_c^{-1} \tag{81}$$

is the total excited-state decay rate composed of the natural decay rate τ_n^{-1} and the collision-induced decay rate τ_c^{-1}. We have assumed that there is no optical saturation.

The incident light flux is assumed to be sinusoidally modulated, i.e.,

$$\Phi=\Phi_0(1+e^{i\omega t})\ , \tag{82}$$

where only the real part has physical meaning. We may drop the constant term in Eq. (82) since we are only interested in the modulated heat source, which generates a corresponding PA signal. The steady-state solution of Eqs. (80) and (82) is

$$N'=\frac{N\Phi_0\sigma\tau}{(1+\omega^2\tau^2)^{1/2}}e^{i(\omega t-\psi)}\ , \tag{83}$$

where

$$\psi=\tan^{-1}(\omega\tau) \tag{84}$$

is the phase lag of the excited-state density with respect to the excitation. Such phase lag is large when $\omega\gtrsim\tau^{-1}$, i.e., when the excited-state decay rate is slower than the modulation rate of the light intensity.

The heat source term H is given by the product of the excited-state density N' and the average thermal energy E' released due to a collision of the excited state and the collision rate τ_c^{-1}

$$H=N'E'\tau_c^{-1}\ . \tag{85}$$

Combining Eqs. (82), (83), and (85), we have

$$H=\frac{\Phi_0\alpha\tau E'\tau_c^{-1}}{(1+\omega^2\tau^2)^{1/2}}\exp(i\omega t-\psi)\ , \tag{86}$$

where $\alpha=N\sigma$ is the absorption coefficient.

The effects of energy transfer on Eq. (86) are twofold. (a) The branching ratio $A_n=\tau_c^{-1}\tau$ for nonradiative collisional decay is altered, e.g., it is increased by more quenching collisions so that the magnitude of the PA signal increases. (b) The net lifetime τ is changed by energy transfer processes, e.g., with increased quenching collisions, τ decreases, which causes a decrease in the phase lag ψ and an increase in the magnitude of the PA signal through the factor $(1+\omega^2\tau^2)^{1/2}$. Conversely, by measuring the dependence of the magnitude and phase of the PA signal on, for example, gas pressures and composition, chopping frequencies, etc., quantities of interest like A_n and τ can be derived. This is for the modulated cw beam excitation case. In the case of pulsed excitation, the idea is the same, namely, a time-resolved detection of the PA signal provides information on the excited-state radiationless processes, as discussed by Wrobel and Vala (1978).

Parker and Ritke (1973) performed some of the pioneering work on the PA measurement of collisional deactivation time of the first vibrationally excited level of the $^1\Delta_g$ electronic state of O_2, and obtained a pressure×lifetime product of 0.05 sec atm for pure oxygen. Robin and collaborators (Kaya *et al.*, 1974,1975; Robin and Kuebler, 1975; Robin, 1976, Robin *et al.*, 1980) performed a series of experiments in organic vapors which beautifully demonstrate the use of PA spectroscopy to measure energy transfer processes when various triplet or singlet excited states are produced. An example of their results in the study of biacetyl is shown in Fig. 25. In this work, Kaya *et al.* (1975) demonstrated for the first time that radiationless decay from S_1 of biacetyl when excited at wavelengths longer than 4430 Å involves a very slow $T_1\rightarrow S_0$ step with a decay rate of $\sim 10^{-3}$ sec^{-1}. However, at shorter wavelengths, a second fast channel is possible, namely $T_2\rightarrow S_0$. Addition of O_2 causes the $T_1\rightarrow S_0$ relaxation to become faster.

Hunter and co-workers (Hunter *et al.*, 1974; Hunter and Stock, 1974; Hall *et al.*, 1976) have also performed a series of experiments on energy transfer processes in vapors of organic materials (e.g., biacetyl) using PA monitoring. For example, Hunter and Stock (1974) derived a triplet yield of 97% in a biacetyl vapor excited at wave-

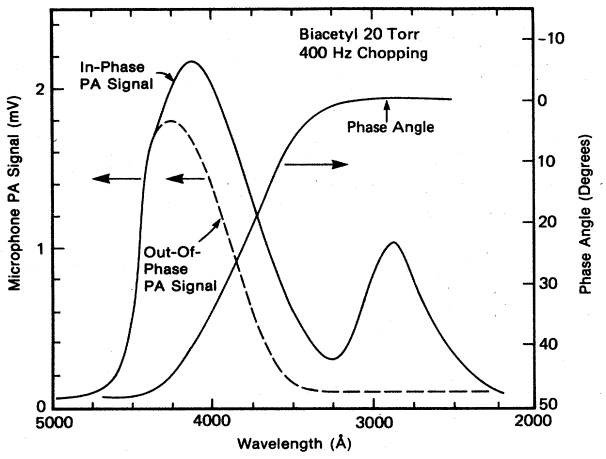

FIG. 25. Radiationless decays in biacetyl, as studied by PA detection (after Kaya *et al.*, 1975). The changes in phase angles at different excitation wave lengths are due to different deexcitation pathways and lifetimes.

length of 436 nm. This large triplet yield is due to the fast intersystem crossing in biacetyl, where S_1 and T_1 are only 3000 cm^{-1} apart. Hunter *et al.* (1974) also obtained a much more refined theory [compared to Eq. (86)] taking into account both fast heat release and slow heat release (due to nonradiative decays of S_1 and T_1, respectively) after optical excitation.

Vibrational relaxations of CO_2 in collision with itself or with other molecules like N_2, He, CO, etc., represent an important field of research, both scientifically and technologically. Huetz-Aubert and Tripodi (1971) first used a spectrophone (i.e., a PA cell) to investigate such vibrational relaxation rates in CO_2. Subsequently, Lepoutre and co-workers (Huetz-Aubert and Lepoutre, 1974; Lepoutre *et al.*, 1979; Taine and Lepoutre, 1980) investigated in detail the collisional deactivation rates of vibrationally excited CO_2 with a host of other molecules at temperatures ranging from 170 to 400 K. Gelfand and co-workers (Gelfand *et al.*, 1979; Rohlfing *et al.*, 1980,1981) have used tunable dye laser PA spectroscopy to examine the pressure-broadening and relaxation rates of high vibrational overtones in simple molecules like CH_4 and HD. Hess and co-workers (Karbach *et al.*, 1984) have used PA resonance profile measurements to obtain relaxation times and thermoelastic properties of gases.

Relaxation rates in solids have also been measured by monitoring the phases and magnitudes of PA signals similar to the gas-phase measurements above. Theories of such PA measurements for condensed matter have been developed by Mandelis *et al.* (1979) and Mandelis and Royce (1980a,1980b). Powell *et al.* (Powell, Neikirk, Flaherty, and Gualtien, 1980; Powell, Neikirk and Sardar, 1980) have applied PA methods to the study of lifetimes in laser materials, e.g., NdP_5O_4, and Peterson and Powell (1978) have studied the radiationless relaxations in Cr^{3+}:MgO and found them to be different from the case of Cr^{3+}:Al_2O_3, that is, ruby.

Up to now, we have discussed only energy transfer due to collisions. Another technique for achieving energy transfer (or more accurately, state transfer) is that of stimulated transitions by light. Allen *et al.* (1977) and Anderson *et al.* (1981) have ingeniously applied such a technique to obtain the quenching rate in a flame. PA techniques are, of course, ideally suited for acoustic generation in a flame because of their noncontact nature. If a microphone is used for detection, it must be located outside the flame, as in the experiment of Allen *et al.* (1977). Photorefractive methods can be used in detection instead of a microphone, making the PA probing method totally noncontact and suitable for hostile environments (see Tam *et al.*, 1982). In the experiment of Allen *et al.* (1977), the flame was doped with Na atoms, and a pulsed dye laser beam tuned to the resonant transition (Na-Na*) was used to excite the Na in the flame. The laser intensity was varied so that the excitation rate (Na$\rightarrow$Na*) and the stimulated emission rate (Na*$\rightarrow$Na) was correspondingly changed. The Na*$\rightarrow$Na competed with the other two decay process of Na*, namely, radiative decay and quenching collision. Since the stimulated emission rate was known, as given by an Einstein coefficient, and the radiative decay rate was known, the quenching rate Q could be derived. Allen *et al.* (1977) obtained $Q=2.6\times10^{10}$ sec^{-1} under their flame conditions. The use of stimulated emission to cause state transfer has also been applied to condensed matter by Razumova and Starobogatov (1977) for organic dye solutions.

VII. PA MATERIALS TESTING

The generation and propagation of acoustic waves in a sample depend critically on the thermoelastic and physical properties of the sample. By monitoring the PA signal, we are able to probe or measure such properties, as acoustic velocities, elasticity, density, thickness, specific heat, properties at high pressures, electrostrictive coefficients, material discontinuities, crystallinity, phase transitions, and so on. By focusing the light beam, some of these physical properties may be measured locally, and hence by scanning the beam over the sample, PA imaging of the property concerned can be obtained. A review of pulsed photoacoustic methods for materials characterization is given by Hutchins and Tam (1986). Moreover, the use of light beams is not necessary, since any other type of beam (electron, ion, or other forms of energy) which can generate heat in a sample can be used to do the same probing as the light beam. Applications relying on beams other than light are discussed in Sec. IX.

A. Generating large-amplitude acoustic waves

Although many methods for generating acoustic waves in materials are possible, the pulsed PA generation method is especially useful for producing very-large-amplitude acoustic waves (shock waves). PA generation efficiency due to thermoelastic expansion increases linear-

ly with the optical absorption for small absorptions. Thus intense pulsed lasers should have much higher efficiency for generating acoustic waves than continuous light sources, and this is why intense PA generations are all performed with pulsed lasers. Teslenko (1977) has investigated the efficiency of conversion of radiation into mechanical energy as a result of breakdown in liquids. He defined the photoacoustic coefficient as the ratio of acoustic shock-wave energy to the incident optical pulse energy. Using a ruby laser of 1 J energy and 20-nsec duration, Teslenko (1977) reported a photoacoustic coefficient as large as 30% due to laser-induced breakdown in water. This large photoacoustic coefficient may be compared with typical values of less than 10^{-10} in most PA spectroscopy experiments. Several other cases of strong PA generation have been reported since giant pulsed lasers were invented in the early 1960s. For example, Askar'yan *et al.* (1963) made the first qualitative experimental investigation of strong acoustic wave generation via boiling in a liquid by a pulsed ruby laser. Carome *et al.* (1964) used a Q-switched ruby laser of 0.1 J energy and 50-nsec duration to excite a ferrocyanide aqueous solution contacting a glass backing plate, and reported the observation of large peak acoustic pressures. Silberg (1965) reported that a 50-J ruby laser pulse incident onto a mercury surface caused rapid boiling, producing a strong "reaction force" in the liquid metal. Observations of many cases of high-pressure shock waves in liquids, usually water, have been described, for example, by Bell and Landt (1967), Bushanam and Barnes (1975), Kohanzadeh *et al.* (1975), Emmony *et al.* (1976), Sigrist and Kneubühl (1978), Fairand and Cluer (1979), and others. Such observations of shock waves are of importance not only for better understanding of the fundamental processes of PA generators, but also for possible high-pressure research and for underwater signal transmission and air-to-sea communications applications.

Attempts have been made to understand the time development of the shock wave generated by pulsed lasers. For example, Felix and Ellis (1971) used Schlieren photography to provide a step-by-step account of the expanding cavitation due to laser-induced breakdown in liquids. Gordienko *et al.* (1978) used a stroboscope to examine PA generation by a Nd:YAG laser of 50 mJ energy and 10-nsec duration in a $CuCl_2$ aqueous solution.

Intense PA generation is also possible in gases as well as in condensed matter. An example is the work of Tam *et al.* (1982), who demonstrated that strong blast waves are produced in a metal vapor due to the transient ionization and plasma formation induced by a pulsed dye laser. Nonideal-gas acoustic behaviors were observed. This work provides an example of totally noncontact acoustic measurements that are suitable for a high-temperature, hostile environment. Thus the method is useful for flame or plasma diagnostics.

B. PA pulse propagation

Low-amplitude PA pulse generation is useful in several ways. (a) Short-duration acoustic pulses of well-defined shape can be produced. (b) Acoustic waves can be generated in "difficult" samples like powders. (c) Distributed PA sources can be produced. These are discussed further below.

1. Generation of single short PA pulses

There is much interest in the use of PA short-pulse generation for materials testing applications in industry. Such applications have up to now been mainly performed by conventional acoustic generation techniques, using power transducers that are attached to the sample. The advantages of PA generation are that (a) no instrumental effects due to the excitation transducer is involved (a single narrow acoustic pulse can be generated reproducibly without requiring acoustic coupling materials), (b) the laser excitation region is small (so that scanning for defects is possible and acoustic path lengths are well defined), (c) the excitation technique is noncontact and hence fast and noncontaminating (in comparison, excitation transducers must be rigidly attached, and different transducers with different attachment methods are needed for generating surface, longitudinal, or shear waves), and (d) longitudinal, shear, and surface acoustic pulses may all be generated.

The amplitude and shape of PA pulses produced by laser pulses have been measured by several authors, e.g., by Dewhurst *et al.* (1982) using a capacitance transducer held close to a solid plate sample, by Sigrist and Kneubühl (1978) using a piezoelectric transducer in a liquid, and by Sullivan and Tam (1984) using a probe-beam-deflection scheme in a liquid. Sullivan and Tam (1984) have also shown that the PA pulse length τ_a is related to the laser pulse duration τ_L and the "acoustic transit time" τ_t, defined as the acoustic propagation time across the PA source of length l *in the direction of observation:*

$$\tau_a \approx (\tau_L^2 + \tau_t^2)^{1/2} . \tag{87}$$

For optical excitation of a highly opaque solid (or liquid), l is equal to the optical attenuation length for an end-on measurement (i.e., normal to the solid surface); in this case, if $l \approx 10^{-5}$ cm (for a highly opaque sample), and v = velocity of sound $\approx 10^6$ cm/sec, $\tau_t \approx 10^{-11}$ sec is obtained, which means that in principle τ_a on the order of 10 psec can be achieved for sufficiently short τ_L. In practice, factors like large attenuation, detector rise time, surface roughness, and so on may make the detection of very narrow acoustic pulses ($<$ 10-nsec duration) difficult.

Tam (1984) made a first attempt in the nondestructive PA generation of ultrashort acoustic pulses in solids, with $\tau_a \lesssim 1$ nsec, which was limited by the laser pulse duration, detector rise time, and sample surface roughness. Such narrow acoustic pulses with highly reproducible shapes are ideally suitable for measuring thin film properties like thickness, d, acoustic velocity v, or attenuation α. v and α are highly correlated with physical properties of the film like porosity (Imaino and Tam, 1983,1984), strain

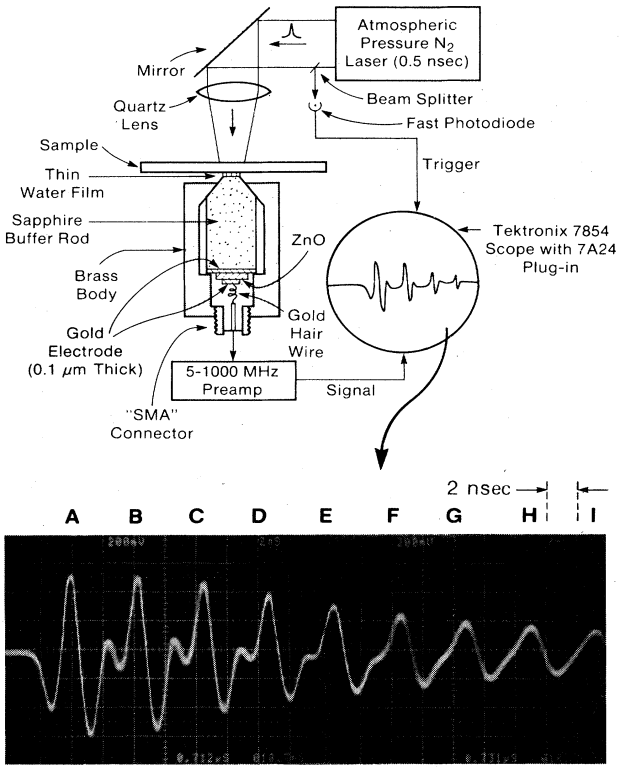

FIG. 26. Top: Experimental arrangement (not to scale) to generate and detect PA pulses of duration $\lesssim 1$ nsec in solids. Bottom: Observed PA pulse and multiple reflections in a type 302 stainless-steel film of thickness 12.6 μm. The first PA pulse labeled A is delayed from the laser pulse by 0.892 μsec. The equally-spaced echoes B to I due to thickness reflections show clearly progressive broadening. Horizontal scale is 2 nsec/division (after Tam, 1984).

(Kino *et al.*, 1980), grain size (Papadakis, 1965), and field distribution (Migliori and Hofler, 1982).

Tam's (1984) experimental arrangement to demonstrate the generation and detection of PA pulses with $\tau_a \approx 1$ nsec is indicated in Fig. 26. The pulsed-excitation source was an atmospheric-pressure N_2 laser (PRA model LN1000) producing laser pulses at 337 nm, of duration $\tau_L = 0.5$ nsec, and energy $E = 1$ mJ. The laser beam was weakly focused to a spot size of 2×0.5 mm^2 on a sample, e.g., polished type 302 stainless-steel film of thickness d, ranging from 12 to 260 μm. The PA pulse was detected "end-on" with the use of a transducer coupled to the sample with a thin film of water. The role of the acoustic coupling liquid was to fill the gaps (due to sample surface roughness of ~ 1 μm) at the contact interface between the sample and the transducer. The ultrafast transducer consisted of a ~ 5-μm-thick ZnO film between 1000-Å gold electrodes; this whole structure was rf-sputtered on a polished surface of a single-crystal sapphire buffer rod. The other end of the buffer rod had the shape of a truncated cone with a flat polished surface of diameter about 2 mm. The transducer rise time τ_r was $\lesssim 1$ nsec, and causes some broadening of the measured PA pulse widths. The observed signals for a stainless-steel film of thickness 14 ± 2 μm (as measured by a micrometer) are shown in Fig. 26. Here, the first pulse A is the PA pulse directly arriving at the ZnO film without undergoing any multiple reflections. The full width at half maximum of the positive-going part of pulse A is about 0.8 nsec, which is larger than $\tau_L = 0.3$ nsec (τ_t is on the order of 10^{-11} sec and is negligible). The time delay of A with respect to the laser firing is 0.892 μsec and is mainly due to the length of the sapphire buffer rod. Pulses B—I in Fig. 26 are due to multiple reflections at the surfaces of the sample with the round-trip time τ_{RT} of the sample being given by the equal spacing between adjacent pulses. It is also clear from Fig. 26 that the pulses progressively become broader with more reflections, i.e., longer propagation distance in the sample. This is because of the phenomenon of frequency-dependent absorption, whereby higher Fourier frequency components are expected to be more strongly absorbed (Papadakis, 1965) in the steel sample. Thus this work shows that such ultranarrow PA pulse measurements are ideally suited for measuring thickness, acoustic velocity, or acoustic attenuation in thin films. Accuracy in thickness measurements of 1% was demonstrated for the 12-μm-thick stainless-steel films once v was known; such high accuracies for thin films of 10 μm thickness was previously very difficult with pulsed transducer measurements.

In another experiment, Tam and Leung (1984b) have shown that nondestructive laser-induced short ultrasonic pulse generation, together with broadband detection, are useful for detecting and measuring the small elastic anisotropy in opaque solids quickly and precisely. This was demonstrated for extruded aluminum alloy of type 6061-T6. A measurement of laser-induced acoustic pulse propagating over a path length of 47 mm provided an accuracy of 0.02% for the longitudinal ultrasonic velocity. The longitudinal velocities at $\pm 45°$ from the extruding direction Z were found to be 2% larger than the velocity along Z, indicating that most of the aluminum crystallites were oriented with a principal axis parallel to Z. This high accuracy for the velocity measurement was obtained in a single-pulsed measurement (which took ~ 10 μsec). Conventional techniques such as the sing-around method (Millero and Kubinski, 1975) and pulse-overlapping method (McSkimin, 1964) can achieve comparable or even better precision, but at the expense of much longer measuring time (of the order of seconds) because of the "time-average" nature of these methods.

Many other applications of the generation and detection of short PA pulses for materials testing have been reported in the literature. Short PA pulses induced by PT ablation of a coating on a sample have been utilized by Sessler *et al.* (1982) for measuring charge distributions in electret samples. Subsequently, Sessler *et al.* (1985) used short laser pulses of duration 70 psec and energy 1—10 mJ to irradiate graphite-coated plastic films with surface trapped charges; an electrode was held near the surface

charges on the sample to detect the arrival of the PA pulse, which had a half-width ~0.5 nsec. Ultrasonic velocity and attenuations in the sample were obtained. Sontag and Tam (1985a) used nondestructive PA generation by a nitrogen laser and PA detection by a probe-laser-deflection technique for noncontact acoustic velocity measurements in silicon wafers at different crystal directions.

2. PA propagation measurement in powders or porous materials

Conventional methods of studying the acoustic properties of powders, porous materials, colloids, gels and other "difficult" materials rely on contact transducers for acoustic generation (Anderson and Hampton, 1980). Imaino and Tam (1983,1984) have shown that acoustic pulse velocity, attenuation, and dispersion in powders can be measured using the technique of PA pulse generation. The advantages of PA generation in powders include the following. (a) Acoustic pulses can be produced on a free surface. (b) Complexities due to the properties of the generating transducer (rise time, ringing, etc.) are eliminated. (c) The serious impedance mismatch between the generating transducer and the powder is eliminated. (d) A wide range of acoustic signals can be produced by varying the temporal or spatial profiles of the laser beam. The apparatus used by Imaino and Tam (1984) to study acoustic pulse propagation in carbon-loaded epoxy powders (toners) is shown in Fig. 27. A prism mounted on the end of a Pyrex tube directed the unfocused flashlamp-pumped dye laser beam onto the powder/glass interface. The powder was a commercially available monocomponent toner of median particle size ~12 μm. The spot size of the laser on the sample was ~1 cm in diameter, and the laser pulse (1-μsec duration; 20 mJ energy) generated an acoustic pulse which could be detected by a PVF_2 (polyvinylidene difluoride) foil or by a lead zirconate titanate detector with similar results. The signal from the detector was amplified by a preamplifier of 1-MHz bandwidth, and digitized and accumulated by a signal-averaging oscilloscope. The digitized waveform was stored by a personal computer, and then was sent to a host computer for Fourier transform computation.

Some observed PA pulse shapes at different powder path lengths are shown in Fig. 28. The results are for a toner powder sample at low pressures (~1 atm) and high porosities (~50%). The pulse shapes shown in Fig. 28 are remarkably similar to PA pulse shapes in liquids (e.g., Sigrist and Kneubühl, 1978; Sullivan and Tam, 1984). Figure 28 shows that the amplitude of the pulse decreases with increasing sample path lengths, and higher frequencies are more strongly attenuated. Imaino and Tam (1984) showed that Fourier transforms of the PA pulse signals shown in Fig. 28 provide both the absorption coefficient $\alpha(f)$ and the velocity $v(f)$ of the powder sample, depending on the sound frequency f. They also found that α and v are very much dependent on the porosity of the sample.

3. Distributed PA sources

Westervelt and Larson (1973) theoretically treated the problem of a PA array produced by a system of laser beams. They showed that highly directional sound beams in water or in other materials can be produced. The theory was later verified by Muir *et al.* (1976) using ruby or Nd:glass laser excitations in a fresh-water lake.

Using the interference effect by merging two coherent laser beams in a solid, Nelson and Fayer (1980) have produce three-dimensional PA "fringes" in solids.

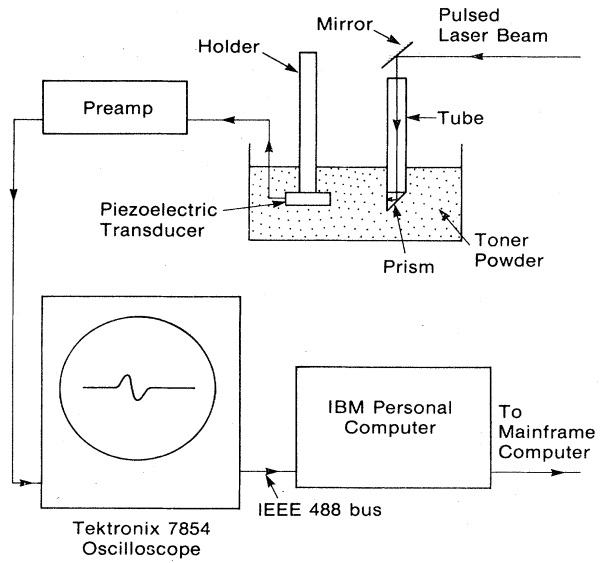

FIG. 27. Schematic diagram of an apparatus used to measure acoustic propagation in loose unconsolidated powders in air, using photoacoustic generation and piezoelectric transducer detection.

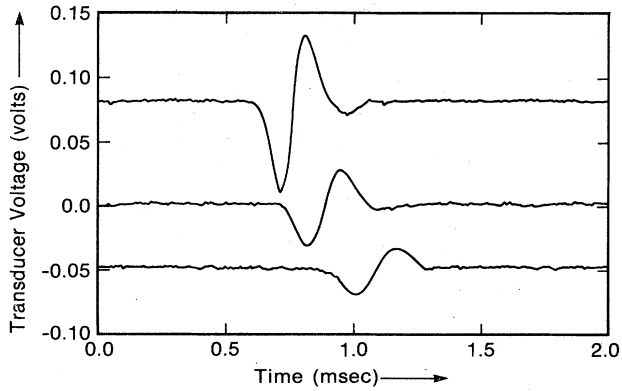

FIG. 28. Plot of acoustic waveforms detected by a lead zirconate titanate transducer for three different path lengths of carbon-loaded epoxy powders. The individual waveforms have been shifted vertically for clarity and "windowed" to eliminate the delayed arrival of pulse reflections.

C. Noncontact measurements of flows and temperatures; flame diagnostics

Zapka and Tam (1982b,1982c) have demonstrated a new application of the laser-induced acoustic source for measurements in a flowing fluid. They show that the flow velocity of a pure particle-free gas (as well as of a liquid) can be measured to an accuracy of 5 cm/sec, and simultaneously the fluid temperature can be obtained to an accuracy of 0.1 °C. Such noncontact measurements were not possible previously by other known laser scattering methods (like laser Doppler velocimetry, coherent anti-Stokes Raman scattering, or stimulated Raman-gain spectroscopy). The experimental arrangement for the simultaneous measurement is shown in Fig. 29. An acoustic pulse in a flowing air stream is produced at position 0 by a pulsed-excitation laser (Nd:YAG laser, ~ 10 mJ energy and 10-nsec duration). Three probe HeNe laser beams, 1, 2, and 3, at distances l_1, l_2, and l_3 from 0, are used to monitor the acoustic pulse arrival times t_1, t_2, and t_3, respectively. The acoustic pulse arrival at each beam is signified by the transient deflections of the beam and can be detected by using a knife edge and a photodiode of suitable rise time. Zapka and Tam (1982c) have shown that the probe beams provide enough data to give both the flow velocity and the fluid temperature simultaneously, and possible errors due to a blast wave or a shock wave produced at the origin 0 can be minimized.

Noncontact techniques are generally required for measurements in flames or other highly corrosive environments. Since PA generation is a noncontact method for production of acoustic pulses, it can be applied to flames, as shown by Allen *et al.* (1977) and by Tennal *et al.* (1982). However, in these early PA flame studies, microphones located outside the flames were used to monitor the acoustic signal, and thus acoustic propagation measurements were comparatively inaccurate because the acoustic signal had to cross the turbulent flame boundaries to be detected; moreover, rise times of microphones are typically slow (many microseconds). Zapka *et al.* (1982) performed the first totally noncontact PA measurements in flames, using one or more cw laser beams to probe the PA signal excited by a pulsed laser beam (similar to the measurements of Zapka and Tam in a flowing gas, as shown in Fig. 29). The active regions of all the laser beams were well within the flame, and so the acoustic pulse never crossed the turbulent flame boundary to be detected. Thus accurate, spatially resolved PA measurements could be performed; for example, they showed that temperature mapping of the flame is possible by monitoring the position-dependent ultrasonic velocity. Furthermore, since microphones are not used, the method is applicable for large flames or enclosed combustions if small windows for the excitation and probe laser beams can be provided. A vertical temperature profile obtained for a horizontal propane/air premixed flame is shown in Fig. 30. Such a temperature profile agrees in shape with a profile obtained by direct thermocouple measurements, although the thermocouple reading is typically about 15% smaller than the temperature value from the acoustic measurement at the same position (probably due to conduction loss in the thermocouple wires, which are 0.5 mm in diameter). This study clearly shows that the flame temperature profiles can be mapped by the simple noncontact PA probing technique. In a flame, strong noise is generated by the combustion process, but such noise generally has frequencies below ~ 100 kHz, and hence a bandpass filter can be used for the signal which has frequencies $\gtrsim 500$ kHz. The results of Fig. 30 represent new *translational* temperature measurement in flames. Previous light-scattering measurements (e.g., Raman scattering) usually provided only *vibrational* or *rotational* tem-

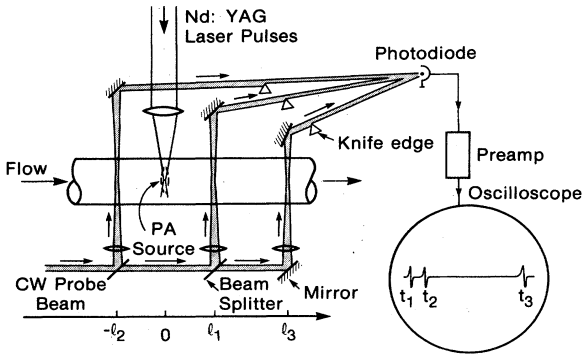

FIG. 29. Experimental arrangement for noncontact photoacoustic monitoring of flow velocity and temperature simultaneously in a pure unseeded gas or liquid.

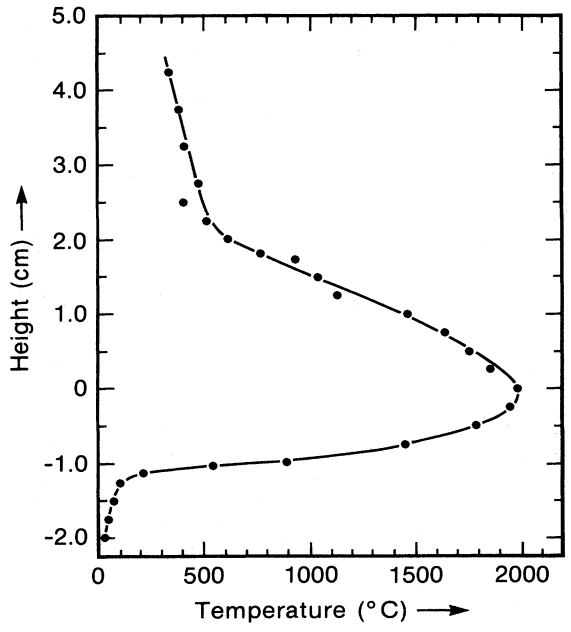

FIG. 30. Photoacoustic measurement of the temperature profile in a horizontal-burning premixed propane/air flame along a vertical line 9 cm from the burner nozzle (after Zapka *et al.*, 1982).

peratures; only Doppler profile measurement can provide translational temperature if other broadening mechanisms are negligible.

Besides the *photoacoustic* technique of flow and temperature monitoring indicated above, *photothermal* probe-beam-deflection schemes can also be used for noncontact flow, temperature, and composition measurements in fluids. In fact, both photoacoustic and photothermal deflection are generally observable with the same experimental setup, with the photoacoustic deflection occurring earlier for displaced excitation and probe beams. Loulergue and Tam (1985) have shown temperature measurement in an unconfined hot gas by probe-beam deflection. Sontag and Tam (1985b), Sell (1985), and Weimer and Dovichi (1985) have shown flow and composition measurement in a gas by monitoring the traveling thermal lens. Usually, photothermal deflection is more suitable for slow flow velocities, and photoacoustic deflection is more suitable for fast flows.

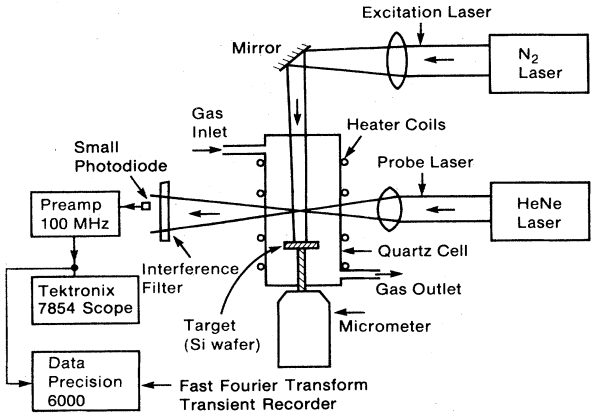

FIG. 31. Experimental arrangement for ultrasonic absorption spectroscopy by an all-optical method. The probe-deflection signal is Fourier analyzed, and the difference between two Fourier spectra at different displacements x between the acoustic source and the probe location provides the ultrasonic absorption spectrum (after Tam and Leung, 1984a).

D. Optical method for ultrasonic absorption spectroscopy

The absorption spectrum of high-frequency sound (frequency f much larger than 1 MHz) in gases has traditionally been very difficult to measure. This is because of the lack of a controllable high-frequency source with good acoustic coupling to the gas, and of a sensitive detection method with fast response. Thus classical methods (Lindsay, 1982) using ultrasonic transducers are usually limited to frequencies less than 1 MHz. The absorptions and velocities of high-frequency waves (e.g., with f approaching a molecular collisional frequency, or wavelength approaching a collisional mean free path) remains unknown for many gases. Tam and Leung (1984a) have made a first demonstration of an all optical Fourier-multiplexed method for measuring ultrasonic absorption spectra of gases and mixtures near normal temperature and pressure at frequencies up to tens of MHz. This technique is new in two respects. (a) It is all optical and is noncontact, and hence applicable for hostile environments. (b) It is a frequency-multiplexed technique relying on pulse shape and magnitude measurement and fast Fourier transform analysis, and hence is applicable for "real-time" monitoring under rapidly changing conditions.

The experimental arrangement of Tam and Leung (1984a) is shown in Fig. 31. The gas being studied is contained in a temperature-controlled quartz cell. A pulsed N_2 laser beam (1 mJ energy and 8-nsec duration) is directed onto an absorption target (highly polished Si wafer) in the cell to produce a narrow acoustic pulse. The laser spot size at the target is 2 mm, and the laser intensity is sufficiently small to cause no damage at the target. A continuous HeNe laser beam is carefully focused into the cell such that it is parallel to the target surface and the focus is vertically above the irradiated spot at the target. The acoustic pulse produced at the irradiated target propagates through a distance x before it arrives at the probe laser focus, causing a transient deflection of the probe beam. The distance x can be finely adjusted by a micrometer. The probe deflection is converted into an intensity variation by using a small photodiode suitably positioned at a wing of the transmitted probe beam (but not at its center), as explained in Fig. 32. The amplified probe-deflection signal is accumulated on a Data Precision Model 6000 transient recorder with fast Fourier transform capability. The observed signals for a gas mixture of CO_2+20-Torr H_2O at 1 atm total pressure and 22 °C show that the acoustic pulse broadens quickly with propagation distance, and fast Fourier transform analysis provides the ultrasonic absorption spectra, as shown in Fig. 33.

E. Radiation damage, crystallinity change, and phase transitions

The PA signal obtained from a sample may change for several reasons. For the direct-coupling case, the generation of an acoustic wave by thermal expansion is determined by the expansion $(\Delta V)_{\rm th}$ of the heated volume V_0

$$(\Delta V)_{\rm th}=\beta H/(C_p\rho)\ , \tag{88}$$

where β is the volume expansion coefficient, H is the heat deposited in volume V_0, C_p is the specific heat at constant pressure per unit mass, and ρ is the density. Thermal losses from V_0 are neglected in Eq. (88). Thus the acoustic efficiency is characterized by a PA "figure of merit" $M_{\rm PA}$,

$$M_{\rm PA}=\beta/(C_p\rho)\ . \tag{89}$$

$M_{\rm PA}$ has appeared earlier in several equations describing

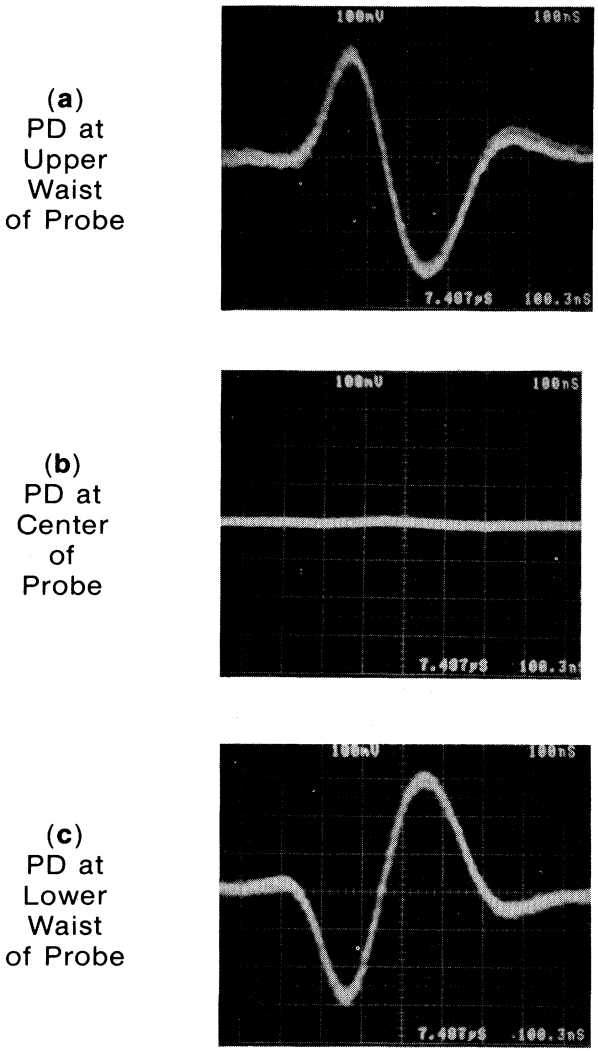

FIG. 32. Observed probe-deflection signal $S(x,t)$ for dry N_2 at 22 °C and $x=2.7$ mm. The photodiode (PD) is located at one wing, at center, and at the other wing of the probe-beam cross section for (a), (b), and (c), respectively (corresponding to the situations in Fig. 17). Each scope picture is delayed by 7.487 μsec from the laser pulse, and the horizontal scale is 100 nsec/division (after Tam and Leung, 1984a).

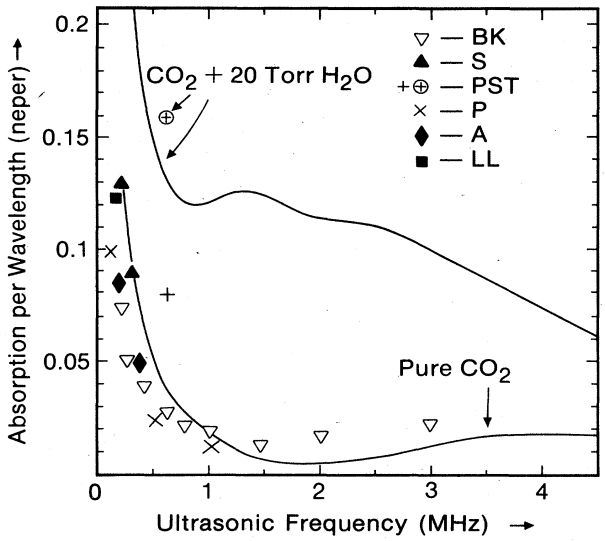

FIG. 33. Ultrasonic absorption spectra measured by PA generation and optical detection for pure CO_2 and for CO_2 + 20-Torr H_2O vapor at 22 °C and 1 atm total pressure. Previous data for comparison are BK (Bashlachev and Kerimov, 1972), S (Shields, 1957), PST (Pielemeier, Saxton, and Telfair, 1940), P (Pielemeier, 1943), A (Angona, 1953), and LL (Lewis and Lee, 1965) (after Tam and Leung, 1984a).

PA generation. If the M_{PA} of a sample or its optical absorption or reflectivity change with time or position, the acoustic signal produced will also change accordingly. The measurement of a position-dependent PA signal is usually referred to as "PA microscopy" or "PA imaging," and will be treated in detail in Sec. VII.F. In this section, we are more concerned with the measurement of a time-dependent PA signal due to modifications of the sample (e.g., ion bombardment, laser annealing, structural change, etc.).

An important case of a time-dependent PA signal is considered by McClelland and Kniseley (1979a,1979b) and by Macfarlane and Hess (1981). They applied PA methods to the monitoring of laser annealing of semiconductors, where it is important to control the semiconductor surface heating during the irradiation by the annealing laser, to monitor dopant concentrations and their diffusions, to know the degree of recrystallization, and to detect any possible damages associated with the intense irradiation. In an actual application, the PA signals can be obtained either from the annealing laser or with the use of an auxiliary probe laser. Real-time monitoring of the laser annealing is possible by observing the change in the PA signal when crystallinity changes, which causes changes in the value of M_{PA}, optical absorption coefficient or reflectivity, and possibly the degree of thermal coupling of the sample with the gas for the microphone detection case.

Other cases in which crystallinity, structural, or chemical changes affect PA signals have also been published. Florian *et al.* (1978) appear to be the first to have reported such effects. Luukkala and Askerov (1980) have observed that plastic deformation of a polycrystalline Al sample results in a larger PA signal in a gas-microphone cell using a cw laser beam chopped at a few hundred Hz for excitation; they suggest that the thermal conductivity k of plastic-deformed Al is smaller than that of polycrystalline Al, causing a larger microphone signal. Schneider *et al.* (1982) have reported that photoisomerization of DODCI (3,3'-diethyldicarbocyanine iodide) results in an intensity-dependent change in the PA spectrum.

The above PA detection methods for crystallinity changes are all based on continuously modulated excitation beams. Tam (1982) has shown that pulsed PA gen-

eration can also be used to detect such changes. He used a sharp punch to slightly indent a steel sample, and subsequently used a milling machine to take off a surface layer so that no punch mark was visible anymore on the sample. On scanning the steel surface with a focused pulsed laser beam (1-μsec duration and 10 mJ energy), the PA signal was observed to change significantly in the vicinity of the invisible stressed area.

F. Photoacoustic imaging

The technique of PA imaging is concerned with the detection of subsurface thermoelastic property variations in a sample. In particular, if little lateral resolution is desired, and the PA imaging is mainly concerned with the property variation in the thickness direction, the technique is usually called "PA depth profiling." On the other hand, if high lateral resolution is required, the technique is called "PA microscopy." All variations of PA imaging rely on the detection of the magnitude or the shape of the PA signal depending on the modulation frequency of the excitation beam, or depending on the location on the sample.

1. PA depth profiling

PA depth profiling is a technique of using the PA signal to find out the depth-dependent properties of a sample. Such a technique can be destructive or nondestructive.

An example of destructive PA depth profiling is given by Yeack *et al.* (1982), who monitored the PA signal due to laser ablation of a composite, layered sample. By continuously monitoring the PA signal obtained from successive laser pulses incident on the same region of the layered sample, they showed that they could control the depth of the thermal ablation in the sample. The PA pulse was detected by a piezoelectric ring positioned close to the ablation spot, and no special acoustic cell was needed. Yeack *et al.* (1982) used this PA monitoring technique to control the optical ablation of composite materials so that the ablation was stopped after a desired depth was reached. Their method of PA monitoring of stepwise ablation by laser pulses may be extended to many other novel technological or medical applications where optical ablation, evaporation, coagulation, polymerization, or other chemical or physical changes can be performed stepwise with light pulses. In these applications, the PA pulse signal can be continuously monitored, and the completion of the desired operation (e.g., drilling through a certain layer) can be indicated by a characteristic change in the pulsed PA signal.

Nondestructive depth-profiling techniques are of more general use. Usually, depth profiling is obtained by a "chopping-frequency dependence" measurement of the PA signal with a gas-coupled microphone. The qualitative idea for an opaque sample is simple: the modulated thermal coupling at the gas-sample interface occurs between a sample thermal diffusion length μ_s and a gas thermal diffusion length μ_g. Since the diffusion lengths depend on the chopping frequency f as $f^{-1/2}$, higher chopping frequency corresponds to probing the sample closer to the surface. A good example is the chopping-frequency dependence of the visible PA spectra of an apple peel or of a spinach leaf reported by Rosencwaig (1978), Adams and Kirkbright (1976), and others. At a comparatively high chopping frequency (e.g., $f \approx 300$ Hz, $\mu_s \approx 10$ μm), the PA spectrum corresponds to the optical absorption of the top waxy layer of the plant matter, while at a lower chopping frequency (e.g., $f \approx 30$ Hz, $\mu_s \approx 33$ μm), the PA spectrum corresponds to absorption by the pigment below the top layer as well.

Photoacoustic depth profiling for the instructive case of a simple layered structure (see Fig. 34), composed of a thin transparent layer of thickness h on a thick opaque substrate, can be semiquantitatively understood as follows. Since no heat is generated in the transparent layer, the temperature T within it satisfies the diffusion equation

$$D\partial^2 T/\partial x^2 = \partial T/\partial t \ , \tag{90}$$

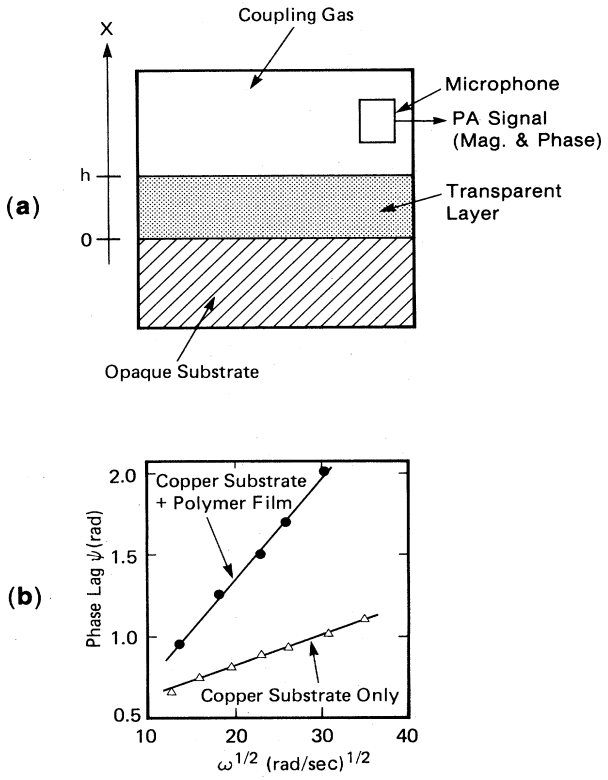

FIG. 34. The technique of PA depth profiling for a simple layered structure. (a) Schematic of the apparatus; the excitation beam can be incident on the opaque substrate from the top or from the bottom. (b) Variation of phase lag ψ with the angular chopping frequency ω for a bare copper substrate and a coated copper substrate for incident radiation from the top, i.e., through the coupling gas (after Adams and Kirkbright, 1977b).

where D is the thermal diffusivity and only one-dimensional conduction is considered. Assuming that the optical excitation beam has the sinusoidal time dependence $\exp(i\omega t)$, the solution to Eq. (90) is

$$T(x)=T_0\exp(-ax+i\omega t)\ , \tag{91}$$

where

$$a=(i\omega/D)^{1/2}\ . \tag{92}$$

Here T_0 is the temperature at the interface and depends on the incident light amplitude $I_{\rm in}$ (assumed to be totally absorbed by the opaque substrate) and on the chopping period $2\pi/\omega$,

$$T_0=(\text{real constant})\times\frac{I_{\rm in}}{\omega^{1/2}}\exp(i\theta)\ , \tag{93}$$

where θ is independent of the properties of the transparent layer and depends only on the properties of the opaque substrate and on the direction of illumination (i.e., whether the light is incident from the top or from the bottom for the arrangement of Fig. 34). The factor of $\omega^{-1/2}$ in Eq. (93) arises because the present sample (aside from the thin transparent coating) corresponds to case (f) of Fig. 11 and of Table III. Combining Eqs. (91)—(93) (only the real parts have physical meaning), we may write the temperature at the top of the transparent layer, i.e., $T(h)$, as

$$T(h)=(\text{real constant})\times\frac{I_{\rm in}}{\omega^{1/2}}\exp(-h/\mu)\cos(\omega t-h/\mu+\theta)\ , \tag{94}$$

where

$$\mu=(2D/\omega)^{1/2} \tag{95}$$

is the thermal diffusion length in the coating material.

Equation (94) is the basis of PA depth profiling for the simple layered structure. Similar equations have been given by Adams and Kirkbright (1977a,1977b), by Helander *et al.* (1981), and by others. Since the PA signal is determined by $T(h)\times$(gas diffusion length) for sufficiently large gas-column thickness (see Sec. III.B and Table III), Eq. (94) implies that the magnitude and phase of the gas-phase PA signal, denoted by $A_{\rm PA}$ and $\psi_{\rm PA}$, respectively, are given by

$$A_{\rm PA}\propto\omega^{-1}\exp[-h\omega^{1/2}/(2D)^{1/2}]\ , \tag{96}$$

$$\psi_{\rm PA}=-h\omega^{1/2}/(2D)^{1/2}+\theta\ . \tag{97}$$

Thus the value of $h/D^{1/2}$ for the top layer can be obtained by plotting either a semilog plot of $A_{\rm PA}\omega$ vs $\omega^{1/2}$ or a linear plot of $\psi_{\rm PA}$ vs $\omega^{1/2}$. Adams and Kirkbright (1977b) have verified this by obtaining phase lag plots for various thicknesses of polymer coatings on copper substrates; they show that h obtained from such a plot (with D known) agrees with the coating thickness by direct measurements. Some results of Adams and Kirkbright (1977b) are shown in Fig. 34.

Helander *et al.* (1981) have refined the above depth-profiling theory and extended it to multiple layers. They show that the linear dependence of $\psi_{\rm PA}$ on the layer thickness h [Eq. (97)] is only a first approximation, but in general $\psi_{\rm PA}$ and $A_{\rm PA}$ are given by linear combinations of $\cosh(ah)$ and $\sinh(ah)$ functions, with the quantity a being given by Eq. (92). However, the experimental results of Helander *et al.* (1981) for a photographic emulsion on a substrate indicate that Eqs. (96) and (97) are approximately valid if (h/μ) is less than 0.3. More generalized theories on thermal wave propagations in layered structures have been published by Opsal and Rosencwaig (1982), Iravani and Wickramasinghe (1985), and Baumann and Tilgner (1985).

Various PA cells using gas microphones for depth-profiling studies of solid samples have been described in the literature, for example, by Adams and Kirkbright (1976,1977a,1977b). Tam and Wong (1980) have described a PA cell for which the coupling gas and its thickness are changeable, so that the PA signal for a depth-profiling study can be optimized. Depth profiling with the use of direct coupling is also possible, in which case the PA signal with piezoelectric detection is usually larger than the signal with microphone detection. Some of these studies will be discussed in conjunction with PA microscopy. Depth profiling with thermal radiometric detection (see Sec. II.D) or with thermal refractive detection (Sec. II.B) are also possible.

The techniques of PA depth profiling can provide information on the thickness of a surface layer, depth of a sublayer, thermal diffusivity of a coating, thermal barriers, or other irregularities below the surface, and depth-dependent optical absorption features. Such techniques should be quite useful for the semiconductor industry, thin-film technologies, and different branches of surface science. Examples have been given by Bennett and Patty (1981). Furthermore, depth-profiling techniques may be uniquely suitable for certain *in vivo* studies in medicine and biology, where normal optical reflection or extinction measurements cannot be performed without elaborate sample preparations. For example, Campbell *et al.* (1979) have reported some remarkable applications of PA techniques to research in dermatology. They show that drug diffusion, water content, and thermal properties of skin can be measured. They have developed a multilayer model of the PA effect to account for the nonuniform thermal properties of the intact skin due to the gradient of water content. Stadler *et al.* (1981) have proposed PA depth-profiling detection of cancer for medical diagnostics.

2. PA microscopy

PA microscopy is a field that is very quickly expanding and being actively investigated by many research groups because of its potential applications in thin-film technologies, chemical engineering, biology, medical diagnostics, etc. It provides a unique method for obtaining subsurface

imaging of irregularities, flaws, doping concentrations, etc., that cannot be obtained by other nondestructive methods.

A schematic arrangement for PA microscopy is shown in Fig. 35. The most suitable optical excitation source is a tightly focused laser beam at a wavelength that is strongly absorbed by the sample and at an intensity below damage threshold of the sample. If the beam is not strongly absorbed, both PA signal magnitude and spatial resolution decrease. An electron beam or other types of radiation can also be used for excitation. As shown in Fig. 35, the volume of thermal diffusion $V_{\rm th}$ is larger than the volume of optical absorption $V_{\rm op}$ by a distance μ_s, which is the thermal diffusion length of the sample, of thermal diffusivity D. For a sinusoidally modulated laser beam of frequency f,

$$\mu_s=(D/\pi f)^{1/2}\,, \tag{98}$$

while for a pulsed laser beam of duration τ,

$$\mu_s\approx(4D\tau)^{1/2}\,. \tag{99}$$

The volume $V_{\rm th}$ (approximately a hemisphere of radius μ_s for a highly optically opaque material) defines the PA microscopy resolution; for example, for more thermally conductive materials like Al, Au, or Si, $\mu_s\approx 50$ μm at $f=10$ kHz, while for less conductive materials, $\mu_s\approx 15$ μm for Al_2O_3 and $\mu_s\approx 5$ μm for SiO_2 at the same chopping frequency. Three kinds of PA imaging are possible, as pointed out by Rosencwaig (1979,1980b). (1) Any foreign materials or voids included in $V_{\rm th}$ causing a change in the thermal properties of $V_{\rm th}$ would change the amplitude and the phase of the PA signal; this is the basis of PA microscopy by *thermal wave.* (2) Any foreign materials or voids included in $V_{\rm op}$ causing a change in the optical absorption in $V_{\rm op}$ would also change the amplitude of the PA signal; this is the basis of PA microscopy by *optical absorption.* (3) If a piezoelectric transducer is used for detection, the PA wave generated in the sample may be scattered by some foreign materials or voids before reaching the transducer; this is the basis of PA microscopy by *ultrasonic scattering.* Typically, ultrasonic scattering is negligible because the acoustic wavelengths generated in most PA microscopy measurements are larger than the dimension of irregularities in the samples studied. However, Wickramasinghe *et al.* (1978) have shown that PA microscopy via ultrasonic scattering is possible, as described further below. Also, Tam and Coufal (1983a) have provided an example of pulsed PA imaging at low spatial resolution by ultrasonic scattering. They scanned a focused pulsed N_2 laser beam across the surface of an aluminum plate of thickness 12.6 mm, with a shallow

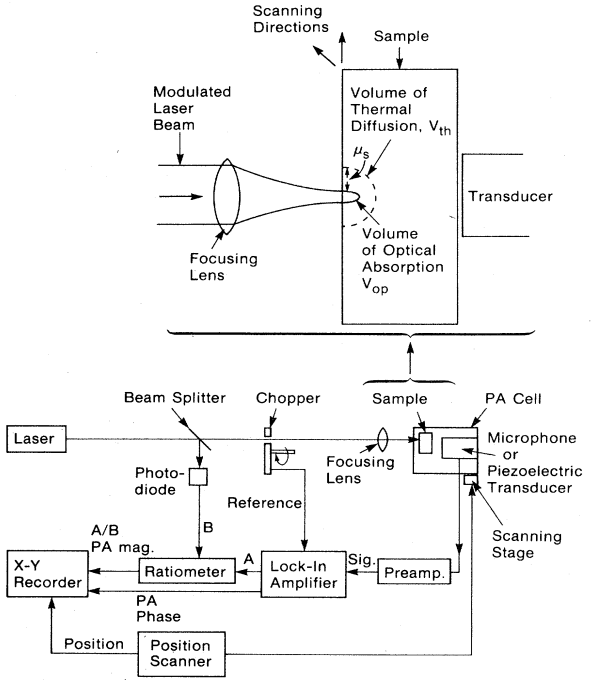

FIG. 35. Schematic arrangement for PA microscopy. The PA signal can be detected by a microphone via gas coupling to the sample, by a piezoelectric transducer via direct coupling, or by other PT detection schemes. The focused excitation spot on the sample surface is scanned to obtain a PA image. The top diagram shows that the resolution is given by the volume of thermal diffusion for a sample without optical absorption variations.

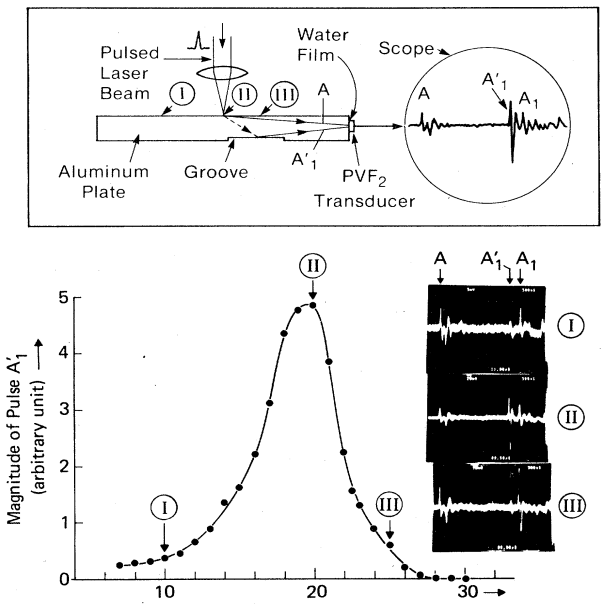

FIG. 36. PA imaging of a deep subsurface groove in an aluminum plate by acoustic scattering. The pulsed N_2 laser of duration 8 nsec produces both longitudinal (solid line) and transverse (dotted line) PA pulses, while the PVF_2 transducer coupled to the edge by a water film detects only longitudinal pulses. Mode conversion at the lower surfaces of the plate produces the longitudinal pulses A_1 and A'_1 at the normal (locations I or III) and grooved (location II) bottom surfaces, respectively. The magnitude of A'_1 displays changes as the laser beam is scanned across the top surface, as shown in the graph.

groove of depth 1.4 mm on the other surface (see Fig. 36). By using a PVF_2 transducer fixed to the edge of the plate, they could detect the presence of the subsurface groove (Fig. 36). Alternatively, a transducer that is fixed end-on with respect to the laser beam can be used, as in most other PA microscopy work described below; this would, however, require a larger transducer of the size of the scanned area, or else moving the transducer with respect to the sample to follow the scanning laser spot.

von Gutfeld and Melcher (1977) were the first to demonstrate that subsurface holes in an Al cylinder could affect the pulsed PA signal detected by a piezoelectric transducer. Wong *et al.* (1978,1979) first reported actual PA images of subsurface structures in solids. In the experiment of Wong *et al.* (1978), an Ar ion laser, chopped at a frequency between 50 and 2000 Hz, was focused onto a silicon carbide ceramic sample used in the manufacturing of turbine blades. They found that any surface microstructures observable with an optical microscope could also be detected by changes in the PA signal when the chopped laser beam was scanned across the microstructure. In addition, Wong *et al.* (1978) observed that the PA signal could detect subsurface inhomogeneities not visible with an optical microscope. In a subsequent paper, Wong *et al.* (1979) provided further experimental quantification of the scanning PA microscopy technique. They showed that for the optically thick case (which is true for their SiC or Si_3N_4 samples excited by 4880- or 5145-Å beams), the PA microscopy detection depth is approximately given by the thermal diffusion length, which is $\sim 100\ \mu$m with chopping frequencies ~ 100 Hz.

Luukkala and Penttinen (1979) used an optical microscope to focus a HeNe laser chopped at 1 kHz onto a photolithographic mask. They obtained a spatial resolution of about 2 μm in the PA image of the mask; here, it is obvious that the high resolution was due to the strong difference of optical absorption between the black and transparent regions of the mask, and not due to the thermal wave produced in the mask. Luukkala (1979) later demonstrated thermal wave imaging for a sample with uniform optical absorption but nonuniform thermal properties by recording the change in PA signal as water soaked through a piece of paper; since water has a much higher heat capacity than dry paper, the moistened area gave a smaller PA signal.

Freese and Teegarden (1979) have shown that inhomogeneities in a layered sample (thin film on a Ge substrate) can be located by raster scanning a focused CO_2 laser of power 75 mW, and nondestructive PA detection of the inhomogeneities is possible at rates in excess of 0.4 sec per resolution point; laser-damaged samples can also be evaluated in this way. They further showed that samples with inhomogeneities located by PA microscopy will usually be damaged by sufficiently intense radiation at the same positions, and thus the PA images may actually be useful to predict the tendency toward laser damage.

Petts and Wickramasinghe (1980) have described a pulsed PA microscope that minimizes the possibility of sample heating by the focused laser beam. They used an electro-optic modulator to produce a train of narrow pulses from a cw tunable laser, and used either microphone or radiometric detection. Such a pulsed excitation scheme not only reduces the risk of sample damage, but also provides information on the depth and the thickness of an inclusion inside a host material.

Thomas and collaborators (Thomas *et al.*, 1980; Favro *et al.*, 1980; Pouch *et al.*, 1980) have performed extensive experimental and theoretical investigations of scanning PA microscopy with either magnitude or phase monitoring for subsurface flaw detection. They included the effects of three-dimensional thermal diffusion, instead of the one-dimensional diffusion considered by many other authors, and successfully produced PA images of an Al sample with a subsurface slot, a Si_3N_4 or SiC sample with subsurface porosity, seeded impurities, and a Knoop indentation, and an integrated circuit sample.

Ash *et al.* (1980), Busse and Rosencwaig (1980), Busse and Ograbeck (1980), Perkowitz and Busse (1980), and Rosencwaig and Busse (1980) have also demonstrated that PA microscopy can be used to map out subsurface features, e.g., in integrated circuits, ceramic substrates, etc., and the PA phase image is usually more valuable than the PA amplitude image because the former is much less affected by the variation in optical absorption, but mainly depends on the variation of thermoelastic properties in V_{th} (see Fig. 35).

McClelland *et al.* (1980) have reported the PA imaging of compositional variation in $Hg_{1-x}Cd_xTe$ semiconductors, which are useful for mid-ir detection. Here, PA imaging is mainly due to the spatial variation of the thermoelastic properties, since the alloy's thermal conductivity depends on the composition. This experiment is a good example of an application of PA detection for industrial quality control; the $Hg_{1-x}Cd_xTe$ can be photoacoustically scanned for homogeneity before fabrication into ir detector arrays, which require compositional uniformity to ensure uniform spectral response across the arrays.

Macfarlane *et al.* (1980) made a very important demonstration of PA mapping of damages due to ion implantation and subsequent recrystallization due to annealing in Si or GaAs, using a cw Nd:YAG laser at 1.06 or 1.32 μm for excitation. They showed that spurious PA signals from the substrate can be eliminated by suitable phase adjustments of the lock-in amplifier. They obtained a PA image of a damaged crystal and showed that laser annealing can change the sample either to single-crystal structure or to a polycrystalline structure.

From the above discussion, we see that in most PA microscopy experiments the image obtained is due either to optical absorption variations with a resolution V_{op} or to thermoelastic property variations with a resolution V_{th}. One notable exception is the PA microscopy experiment of Wickramasinghe *et al.* (1978). They used a mode-locked Q-switched Nd:YAG laser to excite a sample of a metal film with optical pulse trains of duration 0.2 nsec at 210-MHz repetition rate. The PA ultrasonic wave was coupled through a water film and an Al_2O_3 acoustic lens to a zinc oxide thin-film piezoelectric transducer respond-

ing to the PA waves at 840 MHz. Here, the acoustic wavelengths involved were $\lesssim 10$ μm, and so ultrasonic scattering would also affect the PA imaging in this experiment.

Up until now, PA imaging experiments have been performed with point-by-point laser excitation and data-taking. Coufal *et al.* (1982b) have shown that PA imaging could also be performed by a spatial multiplexed technique, e.g., via Hadamard transformations. This method has two advantages. (1) The power density at the sample is reduced, thus lowering the risk of sample damage or spurious effects due to sample heating. (2) Improvements in signal-to-noise is possible because of the multiplexing advantage.

To summarize, PA microscopy techniques have been used for nondestructive imaging of various subsurface features: holes in metals, flaws in ceramics, absorption sites in laser windows, water content in porous materials, inhomogeneities in layered materials, foreign material inclusions in biological samples, defects in integrated circuits and in substrates, compositional variations in alloys, ion-implantation damage in semiconductors, etc. Excitations can be made by modulated cw lasers, pulsed lasers, or other energetic beams, and detection is possible by microphone, piezoelectric transducer, radiometry, probe-beam deflection, and so on. Other examples of PT microscopy via radiometry are given by Busse (1980), and of PT microscopy via probe refraction by Burgi *et al.* (1984). Such techniques should have many valuable applications in industrial quality control, physical and biological sciences, and medical diagnostics.

VIII. PA PRODUCTION OF MECHANICAL MOTIONS

PA effects always produce microscopic mechanical motions, since acoustic waves are always involved. However, under some circumstances, comparatively large "macroscopic" mechanical motions can be produced and exploited. In the present discussion, we are excluding the photon-momentum effects, which are typically small. The area of light-induced mechanical motion (LIMM) is still in its infant state.

Large LIMM can be produced by two methods: (a) an increase in PA generation efficiency or (b) an enhancement of the mechanical motion by suitable sample mounting. Large PA generation is possible, for example, via the mechanism of boiling or ablation instead of the mechanism of thermoelastic expansion that is mainly discussed in this article. Tam and Gill (1982) have reported an effect called photoacoustic ejection from a nozzle (PEN), whereby a light pulse of ~ 1 μJ energy and 1-μsec duration focused onto an ink reservoir connected to a 0.25-mm nozzle can reproducibly cause an ink droplet to be ejected from the nozzle. Thus PEN should have writing applications. The mechanism of PEN is believed to be localized boiling. In fact, we can easily estimate that it takes just 2 nJ of absorbed energy to cause boiling for a sufficiently short laser pulse, if it is focused onto a highly opaque aqueous solution with a spot diameter of 1 μm. Other examples of laser-induced motion due to boiling or ablation have been described by Silberg (1965), Lautherborn (1976), and Koss and Tobin (1983).

Mechanical motion of a sample due to a modulated excitation beam can be enhanced by suitable mounting, sample preparation, or mechanical resonance. Some of these effects have been described in Sec. III. B. For example, a "bimorph" type of bending of suitably supported thin plate excited by a modulated light beam is described by Rousset *et al.* (1983).

IX. GENERALIZED PA EFFECTS

The PA effect relies on the use of a modulated light beam as an excitation source for acoustic waves. To generalize, the excitation may be due to any form of energy, such as radio waves or particle beams. The use of such other modulated excitation sources for acoustic generation is called the generalized PA technique, as summarized schematically in Fig. 37. Some important examples are discussed below.

A. Particle acoustics

The particle-acoustic effect is the production of acoustic waves due to energy deposition by a particle (e.g., photon, electron, ion, muon, molecule, cluster, etc.) in matter. Thus, the particle-acoustic effect includes the photoacoustic effect. There is a general interest in the particle-acoustic effect for detection of high-energy particles like

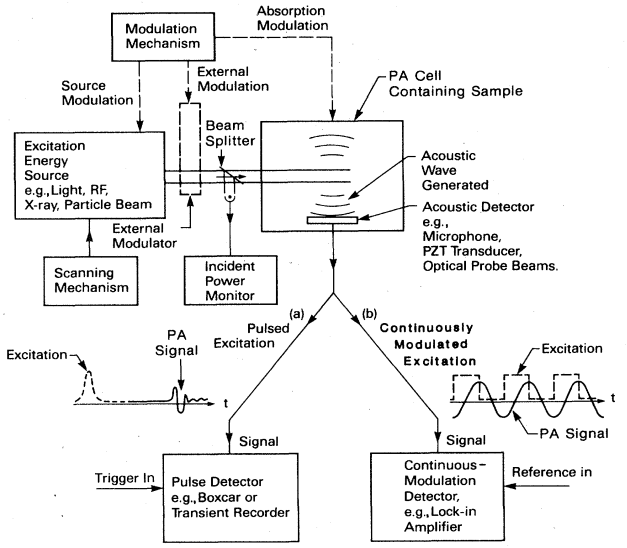

FIG. 37. Schematic of the generalized PA generation and detection technique.

protons or neutrons. There are at least three reasons for this. (1) The acoustic detector is applicable for a very broad range of particles, unlike most other types of detectors, which tend to be limited to certain particles and energies. (2) Acoustic waves can propagate through large distances like kilometers, and thus any detection scheme for particles (like neutrinos) using a large target (like an ocean) would favor acoustic detection, since the detectors can be spaced far apart. (3) Acoustic detectors are relatively inexpensive. For these reasons, several authors (Learned, 1979; Hunter *et al.*, 1981) have studied sound generation by protons in a liquid. A motivation for such studies is the possibility of using acoustics for deep undersea muon and neutrino detection, using arrays of hydrophones under the sea to "hear" the cosmic ray particles instead of the conventional methods of detecting radiation or ionization.

The electron-acoustic effect is a special case of the particle-acoustic effect. Its importance lies in the fact that electron microscopes are well developed, and that modulation, focusing, and deflection devices for electron beams are commerically available. Thus, a scannable electron-acoustic microscope could be readily set up for detecting subsurface defects or for measuring layered structures. Fairly high spatial resolution (~ 1 μm) is possible. Techniques for scanning electron-acoustic microscopy have been reported by Coufal and Pacansky (1979), Nunes *et al.* (1979), Cargill (1980a,1980b), and Brandis and Rosencwaig (1980). Cargill (1980a) modified a commercial scanning electron microscope to obtain an electron beam modulated at 6 MHz and focused to 1-μm spot size at a sample surface, and detected the ultrasonic wave at the same frequency with a piezoelectric transducer attached to the opposite surface of the sample. The transducer output is used to form a scanned, magnified image of the sample. Image contrast comes primarily from spatial variations in the thermal and elastic properties within a resolution radius, which is typically a few micrometers for the sample studied (Au, Cu, Al, and Si). Cargill (1980a,1980b) showed that images of integrated circuits can be obtained with ~ 4-μm resolution and suggested that 0.1-μm resolution is possible in thin-film specimens.

Brandis and Rosencwaig (1980) have reported scanning electron-acoustic microscopy of ceramic substrates. They used a commercial scanning electron microscope modified to accept a sample with an attached PZT transducer. Brandis and Rosencwaig (1980) succeeded in identifying subsurface cracks in alumina substrates with soldering pads by thermal wave imaging with phase optimization. More recently, Rosencwaig and White (1981) have demonstrated that electron-acoustic thermal wave micros-

TABLE VI. Summary of various applications of photoacoustic (PA) techniques.

Type	Principle of operation	Remarks
1. PA spectroscopy	Absorption spectrum is obtained by varying the excitation wavelength to produce a corresponding variation in acoustic response. Constant quantum efficiency for thermal deexcitation is usually assumed.	Contact acoustic detection includes the use of gas-coupled microphones and piezoelectric transducers. Noncontact acoustic detection includes a variety of probe-beam-deflection techniques.
2. PA monitoring of deexcitation	The quantum efficiency for thermal deexcitation is varied (e.g., by changing concentrations, temperature, electric fields, etc.) to make inference on the quantum efficiency of a complementary channel.	Contact acoustic detection has been generally used; complementary channels to thermal deexcitation include luminescence, photochemistry, photoelectricity, and energy transfer.
3. PA sensing of physical properties	The thermal or acoustic waves generated in the sample are used to sense subsurface flaws, layered structure, material composition or crystallinity, change or piezoelectricity profiles, sound velocities, flow rates, temperatures, etc.	Contact acoustic detection has been generally used to sense subsurface features. Noncontact acoustic detection for various velocities and temperature-sensing measurements involve the use of probe beams.
4. PA generation of mechanical motions	PA pulses or shock waves (e.g., due to boiling, ablation, or breakdown) may generate mechanical motions efficiently.	Liquid droplet formation and ejection from a nozzle and laser-induced structural vibrations in metal beams and plates have been demonstrated.

copy can be used at 640-kHz modulation frequency to detect and to image phosphorous doping in a Si wafer. Balk *et al.* (1984) and Balk (1985) have extensively developed scanning electron-acoustic microscopy for applications in the microelectronics industry, and have investigated the important questions of harmonic generation and of contrast mechanisms.

B. Wave acoustics

Since energy can be in the form of particles or of waves, we would expect the existence of "wave acoustics" analogous to "particle acoustics." Many types of long-wavelength electromagnetic waves (beyond the far-infared range) have been shown to generate detectable acoustic waves. Nonelectromagnetic waves could also produce similar effects.

Several authors have demonstrated acoustic detection of the absorption of modulated electromagnetic microwaves or radio-frequency (rf) waves. For example, Melcher (1980) has reported that electron paramagnetic resonance can be detected acoustically; i.e., in magnetic resonance, the modulated rf field (analogous to a modulated light beam in PA experiments) is absorbed, producing a detectable acoustic wave. Melcher (1980) found that magnetic field modulation can also be used instead of rf amplitude modulation. Coufal (1981) has reported further work on the acoustic detection of magnetic resonance. Actual application of ferromagnetic resonance depth profiling for detecting the layered structure of magnetic cassette recorder tapes has been shown by Netzelmann and Pelzl (1984); here depth profiling is performed by measuring the variation of the acoustic signal with respect to the magnetic field modulation frequency. Other types of acoustic detection of magnetic resonances have been reported by Hirabayashi *et al.* (1981) and by DuVarney *et al.* (1981).

X. CONCLUSION

The applications of PA techniques are diverse, both in nature (spectroscopy, deexcitations, physical properties measurements, and mechanical motion generation) and in field (physics, chemistry, biology, technology, geology, medicine, etc.). These applications are summarized in Table VI. Examples of PA applications expected to grow rapidly in the near future include pollutant, drug, and trace-impurity monitoring; particles or aerosol detection; characterization of thin films, surfaces, and powders; PA Fourier transform spectroscopy for materials identification; PA imaging; and other nondestructive materials evaluation in industry. In addition, many interesting scientific investigations with PA monitoring are possible; for example, photochemical chain reactions can cause strong acoustic amplifications (Diebold and Hayden, 1980); weak laser pulses of 1 mJ energy can generate an acoustic shock wave (via breakdown in a vapor) that is observable many centimeters away from the breakdown region (Tam *et al.*, 1982); and ultrashort single acoustic pulses of duration less than 1 nsec can be generated and detected for new ultrasonic testing of materials, with even narrower PA pulses possible (Tam, 1984). The study and application of these various PA generation and detection mechanisms in different systems will be an area of fruitful research.

ACKNOWLEDGMENTS

This work was supported in part by the U.S. Office of Naval Research. The author thanks his colleagues Han Coufal, Wing-Pun Leung, Heinz Sontag, and Werner Zapka for their valuable contributions and discussions, and also greatly appreciates the useful comments of Professor Raj Gupta and Professor Gerhard M. Sessler on this manuscript.

APPENDIX: CONSIDERATIONS FOR HIGH-SENSITIVITY PA DETECTION

The early attention given to photoacoustic sensing techniques is due to their high-sensitivity detection capability, and this remains a popular application, as indicated in Secs. V.A and V.B. We review here the various factors

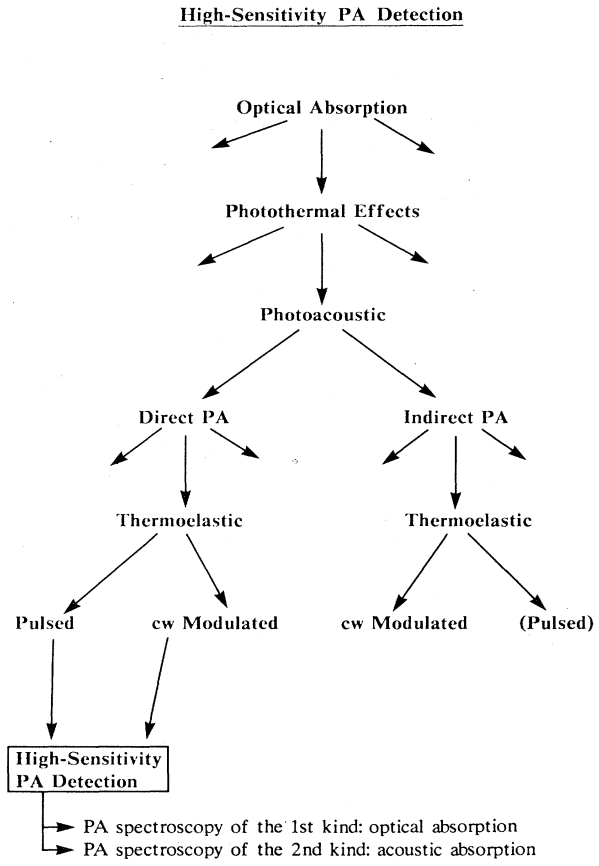

FIG. 38. Routes to high-sensitivty PA detection of optical absorptions.

TABLE VII. Factors to consider to increase PA signal.

(a) Increase PA generation efficiency
Direct thermoelastic case:
Short pulse (limited by transit time, bandwidth, nonlinear effects)
Large expansion coefficient
Small specific heat
Large acoustic velocity
Detector near source
Indirect thermoelastic case:
Low chopping frequency
Optimize buffer gas
High pressure
Low temperature
Gas column length $\approx 2\times$diffusion length
Small residual volume
(b) Increase optical intensity
Multipass cell
Intracavity cell
(c) Acoustic enhancement
Acoustic resonance
Acoustic focusing
Transducer impedance matching
Gas-evolution amplification
Chemical amplification

that contribute to that high sensitivity. A block diagram to explain the sequence leading to high-sensitivity PA detection of optical absorption is shown in Fig. 38. The initial step of optical absorption in a sample can result in many effects (see Fig. 1), some of which are photothermal (see Fig. 2). Photoacoustics is one of the most commonly used photothermal detection schemes, and can be classified into the direct type (Fig. 6) and the indirect type (Fig. 12). Indirect PA detections involve heat diffusion from the sample into an adjacent gas, causing acoustic waves in the gas to be detected, and are generally less sensitive for the purpose of spectroscopic detection of optical absorption. Of the many possible types of direct PA generation exemplified in Fig. 6, providing acoustic generation in the sample itself (without requiring a coupling gas), the thermoelastic PA generation mechanism is generally the most suitable for monitoring spectroscopic absorption in gaseous or condensed samples (even though it is not the strongest PA generation mechanism). The thermoelastic direct PA generation mechanism can be divided into the pulsed type and the cw modulated type (Fig. 7), which are compared in Table II. Whether the pulsed type or the cw modulated type provides a higher detection sensitivity depends on the details of the experimental arrangement and the origins of the noise; both types have been used to demonstrate high sensitivities, as exemplified in Table V. The main advantages of cw modulated detection are the high duty cycle for excitation and the sensitivity of lock-in detection, and so under circumstances when random noise dominates, cw modulated detection is frequently preferable. On the other hand, when systematic noise dominates (like noise due to window, PA cell wall, or substrate absorption), pulsed PA detection is usually preferred, since it provides strong noise suppression by time

TABLE VIII. Possible noise sources and corresponding noise reduction schemes.

Origin	Reduction
1. Undesired absorption (transducer, window, cell wall, substrate)	Proper choice of transducer location and shielding, window location or no window, cell wall material, gated detection, and modulation technique
2. Laser intensity fluctuation	Normalization
3. Vibration and acoustic disturbance	Isolation; avoid noise peaks
4. rf interference (pick-up)	Shield transducer and electronics; minimize transducer cable length
5. Amplifier noise	Optimize amplifier
6. Electrostriction	Suitably long pulse; gated detection
7. Laser pointing noise	Laser stabilization; minimize turbulence
8. Johnson noise	Reduce temperature and bandwidth
9. Fundamental noises (e.g., Brownian motion, deexcitations, statistical fluctuations)	

gating of the PA signal. Since the time gate is typically short, and the pulse repetition rate is generally low, the actual "signal-gathering time" is typically much shorter than in the cw modulated case, and this is the main trade-off factor. Further comparison of the relative merits of pulsed and cw modulated PA detection are given in Table II.

Examples of detectors used in high-sensitivity PA detection of both pulsed and cw modulated types are microphones and probe-beam deflection in gaseous samples, and piezoelectric transducers in condensed samples. The detectors should ideally be acoustically impedance-matched to the sample.

As indicated at the bottom of Fig. 38, high-sensitivity PA detection is useful not only for measuring optical absorption (PA spectroscopy of the first kind), but also for monitoring acoustic absorption (PA spectroscopy of the second kind), which is discussed in Sec. VII. D.

The improvement of detection sensitivity always hinges upon two factors besides signal averaging: increasing the signal and decreasing the noise. This paper has described both aspects in various theoretical and experimental contexts. Tables VII and VIII summarize the considerations. The theories discussed in Sec. III suggest that direct or indirect thermoelastic PA generation efficiencies can be increased as listed in Table VII. An increase in optical intensity and acoustic enhancement will provide a larger signal, although they also may result in larger noise due to window or cell wall absorption. Some of the most common origins of noise some schemes for their reduction are indicated in Table VIII. The noise sources are listed in an order of decreasing magnitude typically. We see that some of the larger noise sources (e.g., undesired absorptions and laser intensity fluctuations) can be reduced by some experimental care. Ultimately, the fundamental noise limits may be reached, which include Brownian motion noise, and statistical fluctuations of the excitation and deexcitation processes.

REFERENCES

Aamodt, L. C., and J. C. Murphy, 1977, J. Appl. Phys. **48**, 3502.

Aamodt, L. C., and J. C. Murphy, 1978, J. Appl. Phys. **49**, 3036.

Abraham, T. O., J. S. Bakos, Z. Sörlei, and T. Juhasz, 1984, Opt. Commun. **49**, 266.

Adams, M. J., B. C. Beadle, and G. F. Kirkbright, 1977, Analyst **102**, 569.

Adams, M. J., J. G. Highfield, and G. F. Kirkbright, 1977, Anal. Chem. **49**, 1850.

Adams, M. J., J. G. Highfield, and G. F. Kirkbright, 1981, Analyst **106**, 850.

Adams, M. J., and G. F. Kirkbright, 1976, Spectrosc. Lett. **9**, 255.

Adams, M. J., and G. F. Kirkbright, 1977a, Analyst **102**, 281.

Adams, M. J., and G. F. Kirkbright, 1977b, Analyst **102**, 678.

Aindow, A. M., R. J. Dewhurst, D. A. Hutchins, and S. B. Palmer, 1981, J. Acoust. Soc. Am. **69**, 449.

Allen, J. F., W. R. Anderson, and D. R. Crosley, 1977, Opt. Lett. **1**, 118.

Ambrosy, A., and K. Holdik, 1984, J. Phys. E **17**, 856.

Amer, N. M., 1983, J. Phys. (Paris) Colloq. **C6**, 185.

Anderson, A. L., and L. D. Hampton, 1980, J. Acoust. Soc. Am. **67**, 1865.

Anderson, W. R., J. E. Allen, and D. R. Crosley, 1981, Technical Report No. ARBRL-TR-02336, U.S. Army Aberdeen Proving Ground, Maryland (unpublished).

Angona, F. A., 1953, J. Acoust. Soc. Am. **25**, 1116.

Angus, A. M., E. E. Marinero, and M. J. Colles, 1975, Opt. Commun. **14**, 223.

Ash, E. A., E. Dieulesaint, and H. Rakouth, 1980, Electron. Lett. **16**, 470.

Askar'yan, G. A., A. M. Prokhorov, G. F. Chanturiya, and G. P. Shipulo, 1963, Zh. Eksp. Teor. Fiz. **44**, 752 [Sov. Phys.—JETP **17**, 1463 (1963)].

Atalar, A., 1980, Appl. Opt. **19**, 3204.

Auzel, F., D. Meichenin, and J. C. Michel, 1979, J. Lumin. **18/19**, 97.

Bae, Y., J., J. Song, and Y. B. Kim, 1982, Appl. Opt. **21**, 35.

Balk, L. J., 1985, *Technical Digest, 4th International Conference on Photoacoustic, Thermal, and Related Sciences, Montreal* (École Polytechnique de Montreal, Montreal), Paper WD1.

Balk, L. J., D. G. Davies, and N. Kultscher, 1984, IEEE Trans. Mag. **MAG-20**, 1466.

Barrett, J. J., and M. J. Berry, 1979, Appl. Phys. Lett. **34**, 144.

Bashlachev, Y.-A., and A. Kerimov, 1972, Akust. Zh. **18**, 312 [Sov. Phys.—Acoust. **18**, 257 (1972)].

Bass, M., and L. Liou, 1984, J. Appl. Phys. **56**, 184.

Bass, M., E. W. Van Stryland, and A. F. Steward, 1979, Appl. Phys. Lett. **34**, 142.

Baumann, J., and R. Tilgner, 1985, J. Appl. Phys. **58**, 1982.

Baumann, T., F. Dacol, and R. L. Melcher, 1983, Appl. Phys. Lett. **43**, 71.

Bebchuk, A. S., V. M. Mizin, and N. Ya. Salova, 1978 Opt. Spektrosk. **44**, 158 [Opt. Spectrosc. (USSR) **44**, 91 (1978)].

Bechthold, P. A., M. Campagna, and J. Chatzipetros, 1981, Opt. Commun. **36**, 369.

Bell, A. G., 1880, Am. J. Sci. **20**, 305.

Bell, C. E., and J. A. Landt, 1967, Appl. Phys. Lett. **10**, 46.

Bennett, C. A., and R. R. Patty, 1981, Appl. Opt. **20**, 911.

Bennett, H. S., and R. A. Forman, 1977, Appl. Opt. **16**, 2834.

Bialkowski, S. E., 1985, Appl. Opt. **24**, 2792.

Boccara, A. C., D. Fournier, W. Jackson, and N. M. Amer, 1980, Opt. Lett. **5**, 377.

Bondarenko, A. N., Yu. B. Drobot, and S. V. Kruglov, 1976, Sov. J. Nondestr. Test. **12**, 655.

Bowers, J. E., 1982, Appl. Phys. Lett. **41**, 231.

Brandis, E., and A. Rosencwaig, 1980, Appl. Phys. Lett. **37**, 98.

Bray, R. G., and M. J. Berry, 1979, J. Chem. Phys. **71**, 4909.

Brenner, D. M., K. Brezinsky, and P. M. Curtis, 1980, Chem. Phys. Lett. **72**, 202.

Brilmyer, G. H., A. Fujishima, K. S. V. Santhanam, and A. J. Bard, 1977, Anal. Chem. **49**, 2057.

Bruce, C. W., and N. M. Richardson, 1984, Appl. Opt. **23**, 13.

Brueck, S. R. J., H. Kidal, and L. J. Bélanger, 1980, Opt. Commun. **34**, 199.

Brueck, S. R. J., T. F. Deutsch, and D. E. Oates, 1983, Appl. Phys. Lett. **43**, 157.

Bui, L., H. T. Shaw, and L. T. Zitelli, 1976, Electron. Lett. **12**, 393.

Bur, A. J., and S. C. Roth, 1985, J. Appl. Phys. **57**, 113.

Burgi, D. S., T. G. Nolan, J. A. Risefelt, and N. J. Dovichi,

1984, Opt. Eng. **23**, 756.
Burt, J. A., K. J. Ebeling, and D. Efthiamiades, 1980, Opt. Commun. **32**, 59.
Bushanam, G. S., and F. S. Barnes, 1975, J. Appl. Phys. **46**, 2074.
Busse, G., 1980, Infrared Phys. **20**, 419.
Busse, G., and P. Eyerer, 1983, Appl. Phys. Lett. **43**, 355.
Busse, G., and A. Ograbeck, 1980, J. Appl. Phys. **51**, 3576.
Busse, G., and K. F. Renk, 1983, Appl. Phys. Lett. **42**, 366.
Busse, G., and A. Rosencwaig, 1980, Appl. Phys. Lett. **36**, 815.
Cahen, D., 1978, Appl. Phys. Lett. **33**, 810.
Cahen, D., H. Garty, and S. R. Caplen, 1978, FEBS Lett. **91**, 131.
Cahen, D., E. I. Lerner, and A. Auerback, 1978, Rev. Sci. Instrum. **49**, 1206.
Cahen, D., S. Malkin, and E. J. Lerner, 1978, FEBS Lett. **91**, 339.
Calder, C. A., and W. W. Wilcox, 1980, Mater. Eval. **38**, 86
Callis, J. B., 1976, J. Res. Natl. Bur. Stand. Sect. A **80A**, 413.
Callis, J. B., M. Gouterman, and J. D. S. Danielson, 1969, Rev. Sci. Instrum. **40**, 1599.
Campbell, S. D., S. S. Yee, and M. A. Afromowitz, 1979, IEEE Trans. Biomed. Eng. **BME-26**, 220.
Cantrell, J. H., and M. A. Breazeals, 1977, J. Acoust. Soc. Am. **61**, 403.
Cargill, C. S., 1980a, Nature (London) **286**, 691.
Cargill, C. S., 1980b, in *Scanned Image Microscopy,* edited by E. A. Ash (Academic, New York), p. 319.
Carome, E. G., N. A. Clark, and C. E. Moeller, 1964, Appl. Phys. Lett. **4**, 95.
Castleden, S. L., G. F. Kirkbright, and D. E. M. Spillane, 1981, Anal. Chem. **53**, 2228.
Chance, R. R., and M. L. Shand, 1980, J. Chem. Phys. **72**, 948.
Chen, C., Y. Liu, C. Ming, C. Wang, W. Wang, J. Xu, Z. Li, and L. Wang, 1982, Chinese Phys. **2**, 452.
Chin, S. L., D. K. Evans, R. D. McAlpine, and W. N. Selander, 1982, Appl. Opt. **21**, 65.
Choi, J. G., and G. J. Diebold, 1982, Appl. Opt. **21**, 4087.
Cielo, P., 1981, J. Acoust. Soc. Am. Suppl. 1 **70**, 546.
Cielo, P., 1984, J. Appl. Phys. **56**, 230.
Cielo, P., 1985, in *International Advances in Nondestrucive Testing,* edited by W. J. McGonnagle (Gordon and Breach, New York), Vol. 11, p. 175.
Cielo, P., X. Maldague, G. Rousset, and C. K. Jen, 1985, Mater. Eval. **43**, 1111.
Claspy, P. C., C. Ha, and Y. H. Pao, 1977, Appl. Opt. **16**, 2972.
Colles, M. J., N. R. Geddes, and E. Mehdizadeh, 1979, Contemp. Phys. **20**, 11.
Cook, R. O., and C. W. Hamm, 1979, Appl. Opt. **18**, 3230.
Cotten, R. J., 1980, Anal. Chem. **52**, 1767.
Coufal, H., 1981, Appl. Phys. Lett. **39**, 215.
Coufal, H., 1982, Appl. Opt. **21**, 104.
Coufal, H., 1984, Appl. Phys. Lett. **44**, 59.
Coufal, H., T. J. Chuang, and F. Trager, 1983, J. Phys. (Paris) Colloq. **C6**, 297.
Coufal, H., U. Möller, and S. Schneider, 1982a, Appl. Opt. **21**, 116.
Coufal, H., U. Möller, and S. Schneider, 1982b, Appl. Opt. **21**, 2339.
Coufal, H., and J. Pacansky, 1979, IBM Tech. Discl. Bull. **22**, 2875.
Coufal, H., F. Trager, T. J. Chuang, and A. C. Tam, 1984, Surf. Sci. **145**, L504.
Cox, D. M., 1978, Opt. Commun. **24**, 336.
Crum, L. A., and G. T. Reynolds, 1985, J. Acoust. Soc. Am. **78**, 137.
Davidson, G. P., and D. C. Emmony, 1980, J. Phys. E **13**, 92.
Davis, C. C., 1980, Appl. Phys. Lett. **36**, 515.
Deem, H. W., and W. D. Wood, 1962, Rev. Sci. Instrum. **33**, 1107.
Dewey, C. F., 1977, in *Opto-acoustic Spectroscopy and Detection,* edited by Y. H. Pao (Academic, New York), p. 47.
Dewhurst, R. J., D. A. Hutchins, S. B. Palmer, and C. B. Scruby, 1982, J. Appl. Phys. **53**, 4064.
Didascalou, S., R. Stewart, and G. Diebold, 1985, *Technical Digest, 4th International Conference on Photoacoustic, Thermal, and Related Sciences, Montreal* (École Polytechnique de Montreal, Montreal), Paper MA7.
Didascalou, S., R. Stewart, and G. Diebold, 1986, Opt. Commun. (in press).
Diebold, G. J., 1980, J. Phys. Chem. **84**, 2213.
Diebold, G. J., and J. S. Hayden, 1980, Chem. Phys. **49**, 429.
Dovichi, N. J., T. G. Nolan, and W. A. Weimer, 1984, Anal. Chem. **56**, 1700.
DuVarney, R. C., A. K. Garrison, and G. Busse, 1981, Appl. Phys. Lett. **38**, 675.
Emmony, D. C., M. Sigrist, and F. K. Kneubühl, 1976, Appl. Phys. Lett. **29**, 547.
Fairand, B. P., and A. H. Cluer, 1979, J. Appl. Phys. **50**, 1497.
Fang, H. L., and R. L. Swofford, 1982, Appl. Opt. **21**, 55.
Farrow, M. M., R. K. Burnham, and E. M. Eyring, 1978, Appl. Phys. Lett. **33**, 735.
Favro, L. D., P. K. Kuo, J. J. Pouch, and R. L. Thomas, 1980, Appl. Phys. Lett. **36**, 953.
Felix, M. P., and A. T. Ellis, 1971, Appl. Phys. Lett. **19**, 484.
Fernelius, N. C., D. V. Dempsey, and D. B. Quinn, 1981, Appl. Surf. Sci. **7**, 32.
Florian, R., H. Pelzl, M. Rosenberg, H. Vargas, and R. Wernhardt, 1978, Phys. Status Solidi A **48**, K35.
Fournier, D., A. C. Boccara, N. M. Amer, and R. Gerlach, 1980, Appl. Phys. Lett. **37**, 519.
Fournier, D., A. C. Boccara, and J. Badoz, 1978, Appl. Phys. Lett. **32**, 640.
Fournier, D., A. C. Boccara, and J. Badoz, 1981, Appl. Opt. **21**, 74.
Freese, R. P., and K. J. Teegarden, 1979, NBS Spec. Publ. (U.S.) **568**, 313.
Fukumi, T., 1979, Opt. Commun. **30**, 351.
Ganguly, P., and T. Somasundaram, 1983, Appl. Phys. Lett. **43**, 160.
Gelfand, J., W. Hermina, and W. H. Smith, 1979, Chem. Phys. Lett. **65**, 201.
Gerlach, R., and N. M. Amer, 1978, Appl. Phys. Lett. **32**, 228.
Glatt, I., Z. Karny, and O. Kafri, 1984, Appl. Opt. **23**, 274.
Gordienki, V. M., A. B. Reshilov, and V. I. Shaml'gauzen, 1978, Akust. Zh. **24**, 132 [Sov. Phys.—Acoust. **24**, 73 (1978)].
Gournay, L. S., 1966, J. Acoust. Soc. Am. **40**, 1322.
Gray, R. C., and A. J. Bard, 1978, Anal. Chem. **50**, 1262.
Hall, L. M., Hunter, T. F. and M. G. Stock, 1976, Chem. Phys. Lett. **44**, 145.
Helander, P., and I. Lundström, 1980, J. Appl. Phys. **51**, 3841.
Helander, P., I. Lundström, and D. McQueen, 1981, J. Appl. Phys. **52**, 1146.
Hendler, E., J. D. Hardy, and D. Murgatroyd, 1963, in *Proceedings of the Fourth Symposium an Temperature, Its Measurement and Control in Science and Industry, Columbus, 1961,* edited by Charles M. Herzfeld (Reinhold, New York), Vol. 3, Part 3, p. 211.

Heritier, J. M., 1983, Opt. Commun. **44**, 267.
Heritier, J. M., J. E. Fouquet, and A. E. Siegmann, 1982, Appl. Opt. **21**, 90.
Hess, P., 1983, in *Topics in Current Chemistry,* edited by F. L. Boschke (Springer, Berlin), Vol. 111.
Hirabayashi, I., K. Morigaki, and Y. Sans, 1981, Jpn. J. Appl. Phys. **20**, L208.
Hordvik, A., 1977, Appl. Opt. **16**, 2827.
Hordvik, A., and H. Schlossberg, 1977, Appl. Opt. **16**, 101.
Hu, C. L., 1969, J. Acoust. Soc. Am. **46**, 728.
Huard, S. J., and D. Chardon, 1981, Opt. Commun. **39**, 59.
Huard, S. J., and D. Chardon, 1983, J. Phys. (Paris) Colloq. **C6**, 91.
Huetz-Aubert, M., and F. Lepoutre, 1974, Physica (Amsterdam) **78**, 435.
Huetz-Aubert, M., and R. Tripodi, 1971, J. Chem. Phys. **55**, 5724.
Hunter, S. D., W. V. Jones, D. J. Malbrough, A. L. Van Buren, A. Liboff, T. Bowen, J. J. Jones, J. G. Learned, H. Bradner, L. Pfeffer, R. March, and U. Camerini, 1981, J. Acoust. Soc. Am. **69**, 1557.
Hunter, T. F., D. Rumbles, and M. G. Stock, 1974, J. Chem. Soc. Faraday Trans. 2 **70**, 1010.
Hunter, T. F., and M. G. Stock, 1974, J. Chem. Soc. Faraday Tras. 2 **70**, 1022.
Hurst, G. S., M. G. Payne, S. D. Kramer, J. P. Young, 1979, Rev. Mod. Phys. **51**, 767.
Hutchins, D. A., 1983, Nondestr. Test. Commun. **1**, 37.
Hutchins, D. A., R. J. Dewhurst, S. B. Palmer, and C. B. Scruby, 1981, Appl. Phys. Lett. **38**, 677.
Hutchins, D. A., and J. D. Macphail, 1985, J. Phys. E **18**, 69.
Hutchins, D. A., and F. Nadeau, 1983, *IEEE 1983 Ultrasonics Symposium Proceedings* (IEEE Piscataway, New Jersey), p. 1175.
Hutchins, D. A., and A. C. Tam, 1986, IEEE Trans. Ultrasonics, Ferroelectrics, and Frequency Control (in press).
Hutchins, D. A., and D. E. Wilkins, 1985, Appl. Phys. Lett. **47**, 789.
Imaino, W., and A. C. Tam, 1983, Appl. Opt. **22**, 1875.
Imaino, W., and A. C. Tam, 1984, Photogr. Sci. Eng. **28**, 213.
Imhof, R. E., D. J. S. Birch, F. R. Thornley, J. R. Gilchrist, and T. A. Strivens, 1984, J. Phys. E **17**, 521.
Inguscio, M., A. Moretti, and F. Strumia, 1979, Opt. Commun. **30**, 355.
Iravani, M. V., and H. K. Wickramasinghe, 1985, J. Appl. Phys. **58**, 122.
Iwasaki, T., S. Oda, T. Sawada, and K. Honda, 1981, Photogr. Sci. Eng. **25**, 6.
Iwasaki, T., T. Sawada, H. Kamada, A. Fujishima, and K. Honda, 1979, J. Phys. Chem. **83**, 2142.
Jackson, W. B., N. M. Amer, A. C. Boccara, and D. Fournier, 1981a, Appl. Opt. **20**, 1333.
Jackson, W. B., N. M. Amer, D. Fournier, and A. C. Boccara, 1981b, *Technical Digest, Second International Conference on Photoacoustic Spectroscopy, Berkeley* (Optical Society of America, Washington, D.C.), Paper WA3.
Jungerman, R. L., J. E. Bowers, J. B. Green, and G. S. Kino, 1982, Appl. Phys. Lett. **40**, 313.
Jungerman, R. L., B. T. Khuri-Yakub, and G. S. Kino, 1983, J. Acoust. Soc. Am. **73**, 1838.
Kanstad, S. O., and P. E. Nordal, 1978, Opt. Commun. **26**, 367.
Kanstad, S. O., and P. E. Nordal, 1980a, Appl. Surf. Sci. **5**, 286.
Kanstad, S. O., and P. E. Nordal, 1980b, Appl. Surf. Sci. **6**, 372.
Karbach, A., J. Röper, and P. Hess, 1984, Rev. Sci. Instrum. **55**, 892.
Kavaya, M. J., J. S. Margolis, and M. S. Shumate, 1979, Appl. Opt. **18**, 2602.
Kaya, K., W. R. Harshbarger, and M. B. Robin, 1974, J. Chem. Phys. **60**, 4231.
Kaya, K., C. L. Chatelain, M. B. Robin, and N. A. Kuebler, 1975, J. Am. Chem. Soc. **97**, 2153.
Kerr, E. L., 1973, Appl. Opt. **12**, 2520.
Khuri-Yakub, B. T., and G. S. Kino, 1977, Appl. Phys. Lett. **30**, 78.
Kim, H. C., and H. K. Park, 1984, J. Phys. D **17**, 673.
Kinney, J. B., and R. H. Staley, 1982, Annu. Rev. Mater. Sci. **12**, 295.
Kino, G. S., D. M. Barnett, N. Grayeli, G. Herrmann, J. B. Hunter, D. B. Ilic, G. C. Johnson, R. B. King, M. P. Scott, J. C. Shyne, and C. R. Steele, 1980, J. Nondestr. Eval. **1**, 67.
Kirkbright, G. F., and S. L. Castleden, 1980, Chem. Br. **16**, 661.
Klein, M. V., 1970, *Optics* (Wiley, New York).
Koch, K. P., and W. Lahmann, 1978, Appl. Phys. Lett. **32**, 289.
Kohanzadeh, Y., J. R. Whinnery, and M. M. Carroll, 1975, J. Acoust. Soc. Am. **57**, 67.
Korpiun, P., and B. Büchner, 1983, Appl. Phys. B **30**, 121.
Korpiun, P., B. Büchner, A. C. Tam, and Y. H. Wong, 1985, Appl. Phys. Lett. **46**, 1039.
Korpiun, P., B. Büchner, A. C. Tam, and Y. H. Wong, 1986, J. Appl. Phys. **59**, 2944.
Koss, L. L., and R. C. Tobin, 1983, J. Sound Vib. **86**, 1.
Kreuzer, L. B., 1971, J. Appl. Phys. **42**, 2934.
Kreuzer, L. B., N. D. Kenyon, and C. K. N. Patel, 1972, Science **177**, 347.
Lahmann, W., and H. J. Ludewig, 1977, Chem. Phys. Lett. **45**, 177.
Lahmann, W., H. J. Ludewig, and H. Welling, 1977, Anal. Chem. **49**, 549.
Lai, H. M., and K. Young, 1982, J. Acoust. Soc. Am. **72**, 2000.
Landau, L. D., and E. M. Lifshitz, 1959, *Fluid Mechanics,* translated by J. B. Sykes and W. H. Reid (Pergamon, Oxford), Chap. VIII.
Laufer, G., J. T. Huneke, B. S. H. Royce, and Y. C. Teng, 1980, Appl. Phys. Lett. **37**, 517.
Lautherborn, W., 1976, Phys. Bl. **32**, 553.
Learned, J. G., 1979, Phys. Rev. D **19**, 3293.
Lee, R. E., and R. M. White, 1968, Appl. Phys. Lett. **12**, 12.
Leite, R. C. C., R. S. Moore, and J. R. Whinnery, 1964, Appl. Phys. Lett. **5**, 141.
Lepoutre, F., G. Louis, and J. Taine, 1979, J. Chem. Phys. **70**, 2225.
Leslie, D. H., R. O. Miles, and A. Dandridge, 1983, J. Phys. (Paris) Colloq. **C6**, 537.
Leung, W. P., and A. C. Tam. 1984a, Opt. Lett. **9**, 93.
Leung, W. P., and A. C. Tam, 1984b, J. Appl. Phys. **56**, 153.
Lewis, J. W., and K. P. Lee, 1965, J. Acoust. Soc. Am. **38**, 813.
Lieto, A. D., P. Minguzzi, M. Tonelli, 1979, Opt. Commun. **31**, 25.
Lin, H.-B., and A. J. Campillo, 1985, Appl. Opt. **24**, 422.
Lindsay, R. B., 1982, in *Physical Acoustics,* edited by W. P. Mason and R. N. Thurston (Academic, New York), Vol. 16, p. 1.
Liu, G., 1982, Appl. Opt. **21**, 955.
Lloyd, L. B., R. K. Burnham, W. L. Chandler, E. M. Eyring, and M. M. Farrow, 1980, Anal. Chem. **52**, 1595.
Lloyd, L. B., S. M. Riseman, R. K. Burnham, and E. M. Eyring, 1980, Rev. Sci. Instrum. **51**, 1448.

Long, G. R., and S. E. Bialkowski, 1985, Anal. Chem. **57**, 1079.
Loulergue, J.-C., A. C. Tam, 1985, Appl. Phys. Lett. **46**, 457.
Low, M. J. D., and G. A. Parodi, 1980, Appl. Spectrosc. **34**, 76.
Low, M. J. D., C. Morterra, A. G. Severdia, and M. Lacroix, 1982, Appl. Surf. Sci. **13**, 429.
Low, M. J. D., C. Morterra, and A. G. Severdia, 1984, Mat. Chem. Phys. **10**, 519.
Lucas, R., and P. Biquard, 1932, J. Phys. Radium **3**, 464.
Luukkala, M., 1979, in *IEEE 1979 Ultrasonics Symposium Proceedings,* edited by J. deKlerk and B. R. McAvoy (IEEE, Piscataway, New Jersey), p. 412.
Luukkala, M. 1980, in *Scanned Image Microscopy,* edited by E. A. Ash (Academic, New York), p. 273.
Luukkala, M., and S. G. Askerov, 1980, Electron. Lett. **16**, 84.
Luukkala, M., and A. Penttinen, 1979, Electron. Lett. **15**, 326.
Lyamshev, L. M., and L. N. Sedov, 1981 Akust. Zh. **27**, 5 [Sov. Phys.—Acoust. **27**, 4 (1981)].
Macfarlane, R. A., and L. D. Hess, 1981, Appl. Phys. Lett. **36**, 137.
Macfarlane, R. A., L. D. Hess, and G. L. Olson, 1980 in *IEEE 1980 Ultrasonics Symposium Proceedings,* edited by B. R. McAvoy (IEEE, Piscataway, New Jersey), Vol. 1, p. 628.
Malkin, S., and D. Cahen, 1979, Photochem. Photobiol. **29**, 803.
Mandelis, A., and B. S. H. Royce, 1980a, J. Appl. Phys. **51**, 610.
Mandelis, A., and B. S. H. Royce, 1980b, J. Opt. Soc. Am. **70**, 474.
Mandelis, A., Y. C. Teng, and B. S. H. Royce, 1979, J. Appl. Phys. **50**, 7138.
Marinero, E. E., and M. Stuke, 1979, Opt. Commun. **30**, 349.
Mason, W. P., and R. N. Thurston, 1979, Eds., *Physcial Acoustics* (Academic, New York), Vol. XIV.
McClelland, J. F., and R. N. Kniseley, 1976a, Appl. Opt. **15**, 2658.
McClelland, J. F., and R. N. Kniseley, 1976b, Appl. Opt. **15**, 2967.
McClelland, J. F., and R. N. Kniseley, 1979a, Appl. Phys. Lett. **35**, 121.
McClelland, J. F., and R. N. Kniseley, 1979b, Appl. Phys. Lett. **35**, 585.
McClelland, J. F., R. N. Kniseley, and J. L. Schmit, 1980, in *Scanned Image Microscopy,* edited by E. A. Ash (Academic, New York), p. 353.
McClenny, W. A., C. A. Bennett, G. M. Russwurm, and R. Richmond, 1981, Appl. Opt. **20**, 650.
McDonald, F. A., 1979, Appl. Opt. **18**, 1363.
McDonald, F. A., and G. C. Wetsel, Jr., 1978, J. Appl. Phys. **49**, 2313.
McSkimin, H. J., 1964, in *Physical Acoustics,* edited by W. P. Mason (Academic, New York), Vol. 1, Part A, p. 271.
Melcher, R. L., 1980, Appl. Phys. Lett. **37**, 895.
Merkle, L. D., and R. C. Powell, 1977, Chem. Phys. Lett. **46**, 303.
Migliori, A., and T. Hofler, 1982, Rev. Sci. Instrum. **53**, 662.
Millero, F. J., and T. Kubinski, 1975, J. Acoust. Soc. Am. **57**, 312.
Monahan, E. M., and A. W. Nolle, 1977, J. Appl. Phys. **48**, 3519.
Monchalin, J.-P., L. Bertrand, G. Rousset, and F. Lepoutre, 1984, J. Appl. Phys. **56**, 190.
Muir, T. G., C. R. Culbertson, and J. R. Clynch, 1976, J. Acoust. Soc. Am. **59**, 735.
Murphy, J. C., and L. C. Aamodt, 1977a, Appl. Phys. Lett. **31**, 728.
Murphy, J. C., and L. C. Aamodt, 1977b, J. Appl. Phys. **48**, 3502.
Murphy, J. C., and L. C. Aamodt, 1980, J. Appl. Phys. **51**, 4580.
Murphy, J. C., and L. C. Aamodt, 1981, Appl. Phys. Lett. **38**, 196.
Naugol'nykh, K. A., 1977, Akust. Zh. **23**, 171 [Sov. Phys.—Acoust. **23**, 98 (1977)].
Nechaev, S. Yu., and N. Yu. Ponomarev, 1975, Kvant. Elektron. (Moscow) **2**, 1400 [Sov. J. Quantum Electron. **5**, 752 (1975)].
Nelson, E. T., and C. K. N. Patel, 1981, Opt. Lett. **6**, 354.
Nelson, K. A., and M. D. Fayer, 1980, J. Chem. Phys. **72**, 5202.
Netzelmann, U., and J. Pelzl, 1984, Appl. Phys. Lett. **44**, 854.
Nickolaisen, S. L., and S. E. Bialkowski, 1985, Anal. Chem. **57**, 758.
Nordal, P. E., and S. O. Kanstad, 1977, Opt. Commun. **22**, 185.
Nordal, P. E., and S. O. Kanstad, 1979, Phys. Scr. **20**, 659.
Nordal, P. E., and S. O. Kanstad, 1981, Appl. Phys. Lett. **38**, 486.
Nunes, O. A. C., A. M. M. Monteiro, and K. S. Neto, 1979, Appl. Phys. Lett. **35**, 656.
O'Connor, M. T., and G. J. Diebold, 1983, Nature **301**, 321.
Oda, S., T. Sawada, and H. Kamada, 1978, Anal. Chem. **50**, 865.
Oda, S., T. Sawada, T. Moriguchi, and H. Kamada, 1980, Anal. Chem. **52**, 650.
Olmstead, M. A., and N. M. Amer, 1984, Phys. Rev. Lett. **52**, 1148.
Olmstead, M. A., N. M. Amer, S. E. Kohn, D. Fournier, and A. C. Boccara, 1983, Appl. Phys. A **32**, 141.
Opsal, J., and A. Rosencwaig, 1982, Appl. Phys. **53**, 4240.
Opsal, J., A. Rosencwaig, and D. L. Willenborg, 1983, Appl. Opt. **22**, 3169.
Ort, D. R., and W. W. Parson, 1978, J. Biol. Chem. **253**, 6158.
Ort, D. R., and W. W. Parson, 1979, Biophys. J. **25**, 355.
Palmer, C. H., R. O. Clares, and S. E. Fick, 1977, Appl. Opt. **16**, 1849.
Pao, Y.-H. 1977, Ed., *Opto-acoustic Spectroscopy and Detection* (Academic, New York).
Papadakis, E. P., 1965, J. Acoust. Soc. Am. **37**, 711.
Parker, J. G., 1973, Appl. Opt. **12**, 2974.
Parker, J. G., and D. N. Ritke, 1973, J. Chem. Phys. **59**, 3713.
Patel, C. K. N., 1978, Phys. Rev. Lett. **40**, 535.
Patel, C. K. N., and R. J. Kerl, 1977, Appl. Phys. Lett. **30**, 578.
Patel, C. K. N., and A. C. Tam, 1979a, Appl. Phys. Lett. **34**, 467.
Patel, C. K. N., and A. C. Tam, 1979b, Chem. Phys. Lett. **62**, 511.
Patel, C. K. N., and A. C. Tam, 1979c, Appl. Phys. Lett. **34**, 760.
Patel, C. K. N., and A. C. Tam, 1980, Appl. Phys. Lett. **36**, 7.
Patel, C. K. N., and A. C. Tam, 1981, Rev. Mod. Phys. **53**, 517.
Patel, C. K. N., A. C. Tam, and R. J. Kerl, 1979, J. Chem. Phys. **71**, 1470.
Perkowitz, S., and G. Busse, 1980, Opt. Lett. **5**, 228.
Peterson, R. G., and R. C. Powell, 1978, Chem. Phys. Lett. **53**, 366.
Petts, C. R., and H. K. Wickramasinghe, 1980, in *IEEE 1980 Ultrasonics Symposium Proceedings,* edited by B. R. McAvoy (IEEE, Piscataway, New Jersey), Vol. 1, p. 636.
Pielemeier, W. H., 1943, J. Acoust. Soc. Am. **15**, 22.
Pielemeier, W. H., H. L. Saxon, and D. Telfair, 1940, J. Chem. Phys. **8**, 106.
Pouch, J. J., R. L. Thomas, Y. H. Wong, J. Schuldies, and J.

Srinivansan, 1980, J. Opt. Soc. Am. **70**, 562.
Powell, R. C., D. P. Neikirk, J. M. Flaherty, and J. C. Gualtien, 1980, J. Phys. Chem. Solids **41**, 345.
Powell, R. C., D. P. Neikirk, and D. Sardar, 1980, J. Opt. Soc. Am. **70**, 486.
Quimby, R. S., and W. M. Yen, 1978, Opt. Lett. **3**, 181.
Razumova, T. K., and I. O. Starobogatov, 1977, Opt. Spektrosk. **42**, 489 [Opt. Spectrosc. (USSR) **42**, 274 (1977)].
Robin, M. B., 1976, J. Lumin. **13**, 131.
Robin, M. B., and N. A. Kuebler, 1975, J. Am. Chem. Soc. **97**, 4822.
Robin, M. B., N. A. Kuebler, K. Kaya, and G. J. Diebold, 1980, Chem. Phys. Lett. **70**, 93.
Rockley, M. G., 1979, Chem. Phys. Lett. **68**, 455.
Rockley, M. G., 1980a, Appl. Spectrosc. **34**, 405.
Rockley, M. G., 1980b, Chem. Phys. Lett. **75**, 370.
Rockley, M. G., and J. P. Devlin, 1980, Appl. Spectrosc. **34**, 407.
Rockley, M. G., and K. M. Waugh, 1978, Chem. Phys. Lett. **54**, 597.
Rockley, M. G., D. M. Davis, and H. H. Richardson, 1980, Science **210**, 918.
Rockley, M. G., D. M. Davis, and H. H. Richardson, 1981, Appl. Spectrosc. **35**, 185.
Roessler, D. M., 1982, Appl. Opt. **21**, 4077.
Rohlfing, E. A., J. Gelfand, R. B. Miles, and H. Rabitz, 1981, J. Chem. Phys. **75**, 4893.
Rohlfing, E. A., H. Rabitz, J. Gelfand, R. B. Miles, and A. E. Depristo, 1980, Chem. Phys. **51**, 121.
Rosencwaig, A., 1978, Adv. Electron. Electron Phys. **46**, 207.
Rosencwaig, A., 1979, Am. Lab. **11(4)**, 39.
Rosencwaig, A., 1980a, "Photoacoustics and Photoacoustic Spectroscopy" Chem. Anal. (N.Y.) Vol. 57.
Rosencwaig, A., 1980b, J. Appl. Phys. **51**, 2210.
Rosencwaig, A., and G. Busse, 1980, Appl. Phys. Lett. **36**, 725.
Rosencwaig, A., and A. Gersho, 1976, J. Appl. Phys. **47**, 64.
Rosencwaig, A., J. Opsal, and D. L. Willenborg, 1983, Appl. Phys. Lett. **43**, 166.
Rosencwaig, A., and R. M. White, 1981, Appl. Phys. Lett. **38**, 165.
Rousset, G., F. Charbonnier, and F. Lepoutre, 1983, J. Phys. (Paris) Colloq. **C6**, 39.
Royce, B. S. H., and J. B. Benziger, 1986, IEEE Trans. Ultrasonics, Ferroelectrics, and Frequency Control (in press).
Royce, B. S. H., Y. C. Teng, and J. Enns, 1980, in *IEEE 1980 Ultrasonics Symposium Proceedings,* edited by B. R. McAvoy (IEEE, Piscataway, New Jersey), Vol. 1, p. 652.
Sam, C. L., and M. L. Shand, 1979, Opt. Commun. **31**, 174.
Sawada, T., and S. Oda, 1981, Anal. Chem. **53**, 471.
Schneider, S., U. Möller, and H. Coufal, 1982, Appl. Opt. **21**, 44.
Scruby, C. B., and H. N. G. Wadley, 1978, J. Phys. D **11**, 1487.
Sell, J. A., 1985, Appl. Opt. **24**, 3725.
Sessler, G. M., R. Gerhard-Multhaupt, J. E. West, and H. von Seggern, 1985, J. Appl. Phys. **58**, 119.
Sessler, G. M., J. E. West, and G. Gerhard, 1982, Phys. Rev. Lett. **48**, 563.
Shaw, R. W., 1980, Appl. Phys. Lett. **35**, 253.
Shields, F. D., 1957, J. Acoust. Soc. Am. **29**, 450.
Siebert, D. R., G. A. West, and J. J. Barrett, 1980, Appl. Opt. **19**, 53.
Sigrist, M. K., and F. K. Kneubühl, 1978, J. Acoust. Soc. Am. **64**, 1652.
Silberg, P. A., 1965, Can. J. Phys. **43**, 2078.
Solimini, D., 1966, Appl. Opt. **5**, 1931.
Somasundaram, T., and P. Ganguly, 1983, J. Phys. (Paris) Colloq. **C6**, 239.
Somoano, R. B., 1978, Angew. Chem. Int. Ed. Engl. **17**, 238.
Sontag, H., and A. C. Tam, 1985a, Appl. Phys. Lett. **46**, 725.
Sontag, H., and A. C. Tam, 1985b, Opt. Lett. **10**, 436.
Sontag, H., and A. C. Tam, 1986, Can. J. Phys. (in press).
Stadler, B., J. Billie, P. Blatt, M. Frank, and C. Rensch, 1981, *Technical Digest, Second International Conference on Photoacoustic Spectroscopy, Berkeley* (Optical Society of America, Washington, D.C.), Paper TuB21.
Starobogatov, I. O., 1977, Opt. Spektrosk. **42**, 304 [Opt. Spectrosc. **42**, 172 (1977)].
Stearns, R. G., B. T. Khuri-Yakub, and G. S. Kino, 1983, Appl. Phys. Lett. **43**, 748.
Stearns, R. G., B. T. Khuri-Yakub, and G. S. Kino, 1984, Appl. Phys. Lett. **45**, 1181.
Stearns, R. G., and G. S. Kino, 1985, Appl. Phys. Lett. **47**, 1048.
Stegeman, G. I., 1976, IEEE Trans. Sonics Ultrason. **SU-23**, 33.
Suemune, I., H. Yamamoto, and M. Yamanishi, 1985, J. Appl. Phys. **58**, 615.
Suemune, I., M. Yamanishi, N. Mikoshiba, and T. Kawano, 1980, Jpn. J. Appl. Phys. **20**, L9.
Sullivan, B., and A. C. Tam, 1984, J. Acoust. Soc. Am. **75**, 437.
Sussner, H., D. Michas, A. Asstalg, S. Hunkfinger, and K. Dransfield, 1973, Phys. Lett. A **45**, 475.
Swofford, R. L., M. E. Long, and A. C. Albrecht, 1976, J. Chem. Phys. **65**, 179.
Taine, J., and F. Lepoutre, 1980, Chem. Phys. Lett. **75**, 452.
Tam, A. C., 1980, Appl. Phys. Lett. **37**, 978.
Tam, A. C., 1982, IBM Tech. Discl. Bull. **25**, 1629.
Tam, A. C., 1983, in *Ultrasensitive Laser Spectroscopy,* edited by D. Kliger (Academic, New York), Chap. 1.
Tam, A. C., 1984, Appl. Phys. Lett. **45**, 510.
Tam, A. C., 1985, Infrared Phys. **25**, 305.
Tam, A. C., and H. Coufal, 1983a, Appl. Phys. Lett. **42**, 33.
Tam, A. C., and H. Coufal, 1983b, J. Phys. (Paris) Colloq. **C6**, 9.
Tam, A. C., and W. D. Gill, 1982, Appl. Opt. **21**, 1891.
Tam, A. C., and W. P. Leung, 1984a, Phys. Rev. Lett. **53**, 560.
Tam, A. C., and W. P. Leung, 1984b, Appl. Phys. Lett. **45**, 1040.
Tam, A. C., and C. K. N. Patel, 1979a, Nature (London) **280**, 304.
Tam, A. C., and C. K. N. Patel, 1979b, Appl. Opt. **18**, 3348.
Tam, A. C., and C. K. N. Patel, 1979c, Appl. Phys. Lett. **35**, 843.
Tam, A. C., and C. K. N. Patel, 1980, Opt. Lett. **5**, 27.
Tam, A. C., C. K. N. Patel, and R. J. Kerl, 1979, Opt. Lett. **4**, 81.
Tam, A. C., H. Sontag, and P. Hess, 1985, Chem. Phys. Lett. **120**, 280.
Tam, A. C., and B. Sullivan, 1983, Appl. Phys. Lett. **43**, 333.
Tam, A. C., and Y. H. Wong, 1980, Appl. Phys. Lett. **36**, 471.
Tam, A. C., W. Zapka, K. Chiang, and W. Imaino, 1982, Appl. Opt. **21**, 69.
Taylor, R., 1972, High Temp. High Pressures **4**, 649.
Teng, Y. C., and B. S. H. Royce, 1982, Appl. Opt. **21**, 77.
Tennal, K., G. J. Salamo, and R. Gupta, 1982, Appl. Opt. **21**, 2135.
Terzic, M., and M. W. Sigrist, 1984, J. Appl. Phys. **56**, 93.
Teslenko, V. S., 1977, Kvant. Elektron. (Moscow) **4**, 1732 [Sov. J. Quantum. Electron. **7**, 981 (1977)].

Thielemann, W., and H. Neumann, 1980, Phys. Status Solidi A **61**, K123.
Thomas, R. L., J. J. Pouch, Y. H. Wong, L. D. Favro, P. K. Kuo, and A. Rosencwaig, 1980, J. Appl. Phys. **51**, 1152.
Tilgner, R., 1981, Appl. Opt. **20**, 3780.
Tokumoto, H., M. Tokumoto, and T. Ishiguro, 1981, J. Phys. Soc. Jpn. **50**, 602.
Träger, F., H. Coufal, and T. J. Chuang, 1982, Phys. Rev. Lett. **49**, 1720.
Vansteenkiste, T. H., F. R. Faxvog, and D. M. Roessler, 1981, Appl. Spectrosc. **35**, 194.
Vanzetti, R., and A. C. Traub, 1983, "Automatic Solder Joint Inspection in Depth," in *Proceedings of the Seventh Annual Seminar in Soldering Technology and Product Assurance, China Lake, 1983* (Naval Weapons Center, China Lake, California).
Voigtman, E., A. Jurgensen, and J. Winfordner, 1981, Anal. Chem. **53**, 1921.
von Gutfeld, R. J., and R. L. Melcher, 1977, Appl. Phys. Lett. **30**, 257.
Wang, W., C. Chen, and Y. Liu, 1982, Kexue Tongbao (China) **27**, 400.
Wasa, K., K. Tsubouchi, and N. Mikoshiba, 1980, Jpn. J. Appl. Phys. **19**, L653.
Webb, J. D., K. M. Swift, and E. R. Bernstein, 1980, J. Chem. Phys. **73**, 4891.
Weimer, W. A., and N. J. Dovichi, 1985, Appl. Opt. **24**, 2981.
West, G. A., and J. J. Barrett, 1979, Opt. Lett. **4**, 395.
West, G. A., J. J. Barrett, D. R. Siebert, and K. V. Reddy, 1983, Rev. Sci. Instrum. **54**, 797.
Westervelt, P. J., and R. S. Larson, 1973, J. Acoust. Soc. Am. **54**, 121.
Wetsel, G. C., Jr., and F. A. McDonald, 1977, Appl. Phys. Lett. **30**, 252.
Weulersse, J. M., and R. Genier, 1981, Appl. Phys. **24**, 363.
White, R. M., 1963, J. Appl. Phys. **34**, 3559.
Whitman, R. L., and A, Korpel, 1969, Appl. Opt. **8**, 1567.
Wickramasinghe, H. K., R. C. Bray, V. Jipson, C. F. Quate, and J. R. Salcedo, 1978, Appl. Phys. Lett. **33**, 923.
Williams, C. C., 1984, Appl. Phys. Lett. **44**, 1115.
Wong, Y. H., R. L. Thomas, and G. F. Hawkins, 1978, Appl. Phys. Lett. **32**, 538.
Wong, Y. H., R. L. Thomas, and J. J. Pouch, 1979, Appl. Phys. Lett. **35**, 368.
Wrobel, J., and M. Vala, 1978, Chem. Phys. **33**, 93.
Yariv, A., 1975, *Quantum Electronics,* 2nd ed. (Wiley, New York).
Yasa, Z. A., W. B. Jackson, and N. M. Amer, 1982, Appl. Opt. **21**, 21.
Yeack, C. E., R. L. Melcher, and H. E. Klauser, 1982, Appl. Phys. Lett. **41**, 1043.
Zapka, W., P. Pokrowsky, and A. C. Tam, 1982, Opt. Lett. **7**, 477.
Zapka, W., and A. C. Tam, 1982a, Opt. Lett. **7**, 86.
Zapka, W., and A. C. Tam, 1982b, Appl. Phys. Lett. **40**, 310.
Zapka, W., and A. C. Tam, 1982c, Appl. Phys. Lett. **40**, 1015.

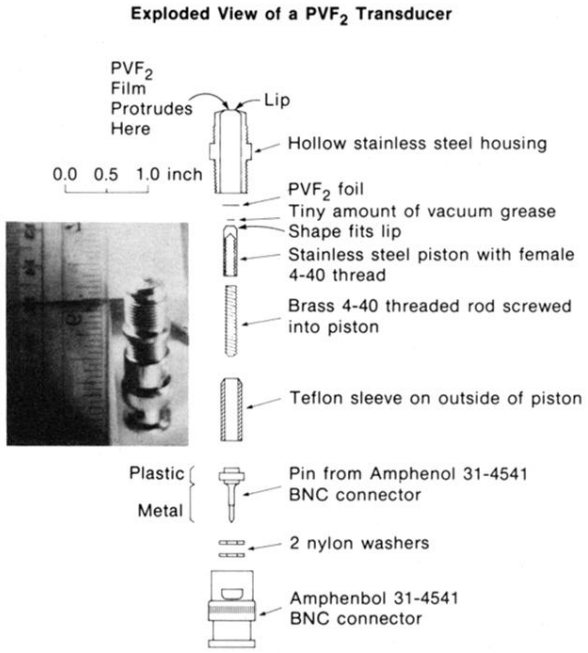

FIG. 16. A new method for mounting a PVF_2 piezoelectric film to produce a fast transducer with rise time $\lesssim 2$ nsec.

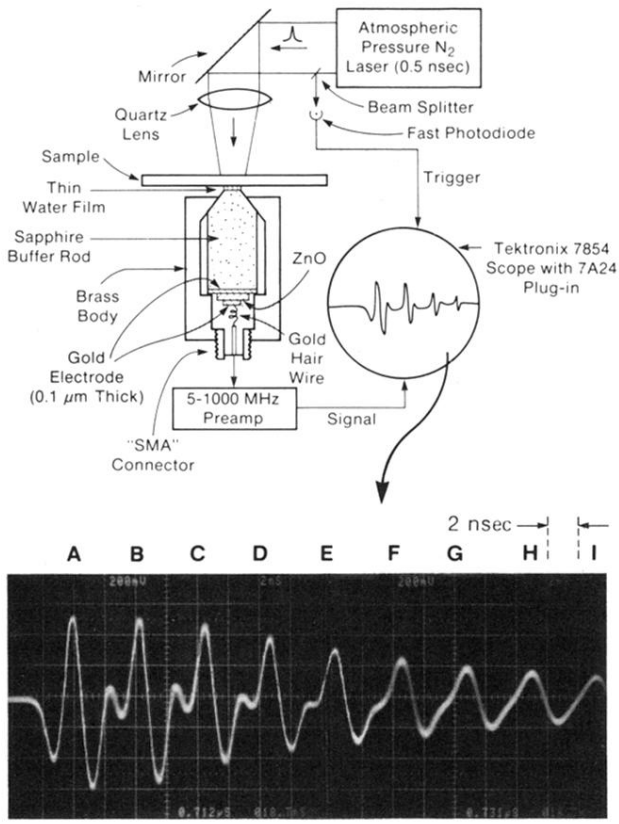

FIG. 26. Top: Experimental arrangement (not to scale) to generate and detect PA pulses of duration $\lesssim 1$ nsec in solids. Bottom: Observed PA pulse and multiple reflections in a type 302 stainless-steel film of thickness 12.6 μm. The first PA pulse labeled *A* is delayed from the laser pulse by 0.892 μsec. The equally-spaced echoes *B* to *I* due to thickness reflections show clearly progressive broadening. Horizontal scale is 2 nsec/division (after Tam, 1984).

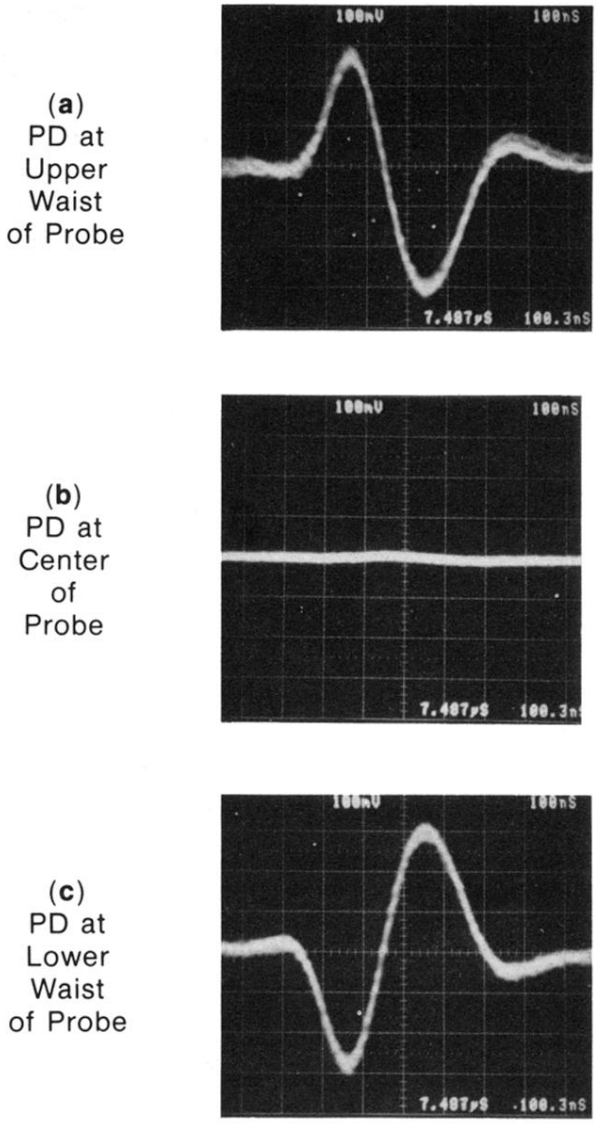

FIG. 32. Observed probe-deflection signal $S(x,t)$ for dry N_2 at 22 °C and $x=2.7$ mm. The photodiode (PD) is located at one wing, at center, and at the other wing of the probe-beam cross section for (a), (b), and (c), respectively (corresponding to the situations in Fig. 17). Each scope picture is delayed by 7.487 μsec from the laser pulse, and the horizontal scale is 100 nsec/division (after Tam and Leung, 1984a).